

---

# Uncertainty Analysis of Minimum Vessel Liquid Inventory During a Small-Break LOCA in a B&W Plant – An Application of the CSAU Methodology Using the RELAP5/MOD3 Computer Code

---

Prepared by  
M. C. Ortiz, L. S. Ghan

Idaho National Engineering Laboratory  
EG&G Idaho, Inc.

Prepared for  
U.S. Nuclear Regulatory Commission

## AVAILABILITY NOTICE

### Availability of Reference Materials Cited in NRC Publications

Most documents cited in NRC publications will be available from one of the following sources:

1. The NRC Public Document Room, 2120 L Street, NW., Lower Level, Washington, DC 20555
2. The Superintendent of Documents, U.S. Government Printing Office, P.O. Box 37082, Washington, DC 20013-7082
3. The National Technical Information Service, Springfield, VA 22161

Although the listing that follows represents the majority of documents cited in NRC publications, it is not intended to be exhaustive.

Referenced documents available for inspection and copying for a fee from the NRC Public Document Room include NRC correspondence and internal NRC memoranda; NRC bulletins, circulars, information notices, inspection and investigation notices; licensee event reports, vendor reports and correspondence; Commission papers; and applicant and licensee documents and correspondence.

The following documents in the NUREG series are available for purchase from the GPO Sales Program: formal NRC staff and contractor reports, NRC-sponsored conference proceedings, international agreement reports, grant publications, and NRC booklets and brochures. Also available are regulatory guides, NRC regulations in the *Code of Federal Regulations*, and *Nuclear Regulatory Commission Issuances*.

Documents available from the National Technical Information Service include NUREG-series reports and technical reports prepared by other Federal agencies and reports prepared by the Atomic Energy Commission, forerunner agency to the Nuclear Regulatory Commission.

Documents available from public and special technical libraries include all open literature items, such as books, journal articles, and transactions. *Federal Register* notices, Federal and State legislation, and congressional reports can usually be obtained from these libraries.

Documents such as theses, dissertations, foreign reports and translations, and non-NRC conference proceedings are available for purchase from the organization sponsoring the publication cited.

Single copies of NRC draft reports are available free, to the extent of supply, upon written request to the Office of Administration, Distribution and Mail Services Section, U.S. Nuclear Regulatory Commission, Washington, DC 20555.

Copies of industry codes and standards used in a substantive manner in the NRC regulatory process are maintained at the NRC Library, 7920 Norfolk Avenue, Bethesda, Maryland, for use by the public. Codes and standards are usually copyrighted and may be purchased from the originating organization or, if they are American National Standards, from the American National Standards Institute, 1430 Broadway, New York, NY 10018.

## DISCLAIMER NOTICE

This report was prepared as an account of work sponsored by an agency of the United States Government. Neither the United States Government nor any agency thereof, or any of their employees, makes any warranty, expressed or implied, or assumes any legal liability of responsibility for any third party's use, or the results of such use, of any information, apparatus, product or process disclosed in this report, or represents that its use by such third party would not infringe privately owned rights.

---

# Uncertainty Analysis of Minimum Vessel Liquid Inventory During a Small-Break LOCA in a B&W Plant – An Application of the CSAU Methodology Using the RELAP5/MOD3 Computer Code

---

Manuscript Completed: December 1992  
Date Published: December 1992

Prepared by  
M. G. Ortiz, L. S. Ghan

Idaho National Engineering Laboratory  
Managed by the U.S. Department of Energy

EG&G Idaho, Inc.  
Idaho Falls, ID 83415

Prepared for  
Division of Systems Research  
Office of Nuclear Regulatory Research  
U.S. Nuclear Regulatory Commission  
Washington, DC 20555  
NRC FIN L1111  
Under DOE Contract No. DE-AC07-76ID01570

## ABSTRACT

The Nuclear Regulatory Commission (NRC) revised the emergency core cooling system licensing rule to allow the use of best estimate computer codes, provided the uncertainty of the calculations are quantified and used in the licensing and regulation process. The NRC developed a generic methodology called Code Scaling, Applicability, and Uncertainty (CSAU) to evaluate best estimate code uncertainties. The objective of this work was to adapt and demonstrate the CSAU methodology for a small-break loss-of-coolant accident (SBLOCA) in a Pressurized Water Reactor of Babcock & Wilcox Company lowered loop design using RELAP5/MOD3 as the simulation tool. The CSAU methodology was successfully demonstrated for the new set of variants defined in this project (scenario, plant design, code). However, the robustness of the reactor design to this SBLOCA scenario limits the applicability of the specific results to other plants or scenarios. Several aspects of the code were not exercised because the conditions of the transient never reached enough severity. The plant operator proved to be a determining factor in the course of the transient scenario, and steps were taken to include the operator in the model, simulation, and analyses.



# CONTENTS

ABSTRACT .....	iii
EXECUTIVE SUMMARY .....	xiii
ACRONYMS .....	xv
1. Introduction .....	1-1
1.1 CSAU Methodology .....	1-2
1.2 Overview of This Report .....	1-2
2. Nuclear Power Plant Description and SELECTED Scenario .....	2-1
2.1 Nuclear Power Plant Description .....	2-1
2.2 Scenario Description .....	2-1
2.3 Results from Scoping Run .....	2-4
2.3.1 Phase 1: Blowdown Phase .....	2-5
2.3.2 Phase 2: Saturation to Natural Circulation .....	2-5
2.3.3 Phase 3: Loss of Loop Natural Circulation .....	2-5
2.3.4 Phase 4: Boiler-Condenser Mode Phase .....	2-6
3. Phenomena Identification and Ranking Table .....	3-1
3.1 Summary of the PIRT Process .....	3-1
3.2 PIRT Results .....	3-1
3.3 Conclusions .....	3-3
4. CODE Applicability .....	4-1
4.1 Global Applicability .....	4-2
4.1.1 Field Equations .....	4-2
4.1.2 Closure Relations .....	4-2
4.1.3 Numerics .....	4-2
4.1.4 Components and Control .....	4-2
4.2 Specific Scenario .....	4-2
4.3 Code Scaling .....	4-2
5. Nodalization .....	5-1
5.1 Pedigree of the Input Deck .....	5-1

5.2	Primary System .....	5-1
5.3	Secondary System .....	5-2
5.4	Integrated Control System .....	5-8
5.5	Initial Conditions .....	5-8
6.	OPERATOR ACTIONS .....	6-1
6.1	Technical Basis for Operator Actions .....	6-1
6.1.1	Monitoring Parameters to Identify Symptoms of Upset in Heat Transfer .....	6-1
6.1.2	Elements of Operator Control .....	6-3
6.1.2	Elements of Operator Control .....	6-2
6.1.3	Overview of Emergency Procedures .....	6-5
6.1.4	Emergency Operating Procedures for Loss of Subcooling Margin .....	6-7
6.2	Implementing Operator Actions in the Model .....	6-11
6.2.1	Philosophy for Selecting Operator Actions .....	6-13
6.2.2	Primary Inventory and Pressure Control .....	6-13
6.2.3	Secondary Inventory and Pressure Control .....	6-13
7.	Ranging of Parameters .....	7-1
7.1	Important Phenomena and Key Code Parameters .....	7-1
7.2	Evaluation of Uncertainty .....	7-2
7.2.1	Break Flow .....	7-2
7.2.2	Interphase Drag .....	7-9
7.2.3	Decay Heat .....	7-10
7.2.4	RCP Performance .....	7-11
7.2.5	ECCS Flow .....	7-11
7.2.6	Steam Generator Heat Transfer .....	7-11
7.2.7	RVVV Performance .....	7-11
8.	Sensitivity Calculations .....	8-1
8.1	Base Calculation (Nominal Case) .....	8-1
8.1.1	Automatic Actions .....	8-1
8.2	Sensitivity Calculations, Results, And Discussion .....	8-3
9.	Total Uncertainty .....	9-1
10.	Conclusions and recommendations .....	10-1
11.	References .....	11-1

Appendix A—RELAP5/MOD3 Assessment Using MIST .....	A-1
Appendix B—The Analytic Hierarchy Process .....	B-1
Appendix C—Probabilistic Analysis of Small-Break LOCA Level in a B&W Reactor .....	C-1

## LIST OF FIGURES

1-1.	Flow chart of CSAU methodology .....	1-3
2-1.	Typical B&W lowered loop plant design .....	2-2
2-2.	Steam generator secondary flow path .....	2-3
2-3.	HPI train lineup in the B&W plant design .....	2-3
2-4.	Pressure history during the scoping calculation, illustrating the occurrence and relative location of the transient phases .....	2-4
2-5.	Schematic description of the interruption-resumption of natural circulation by the intermittent voiding of the top of the U-bend: (a) bubble accumulates at the top; (b) flow is momentarily interrupted due to the bubble; (c) the compressed bubble gives way to a renewed natural circulation path; and (d) natural circulation is permanently interrupted .....	2-5
2-6.	Schematic description of the internal vessel circulation path in the last two phases of the transient .....	2-6
5-1.	RELAP5/MOD3 reactor vessel noding .....	5-2
5-2.	Primary loop showing HPI, makeup, and break locations .....	5-3
5-3.	Pressurizer with PORVs .....	5-4
5-4.	Model of B&W steam generator .....	5-5
5-5.	Feedwater train from condenser to startup and main feed valves .....	5-6
5-6.	EFW train model .....	5-7
5-7.	B&W ICS block diagram .....	5-8
6-1.	Normal P-T trace following a reactor trip .....	6-2
6-2.	Pressure/temperature trace following loss of subcooling margin .....	6-3
6-3.	Pressure temperature relation for nominal case .....	6-4
6-4.	Flow chart for verification of vital systems status .....	6-6
6-5.	Strategy for mitigating a loss-of-subcooling margin .....	6-8
6-6.	Steam generator heat transfer flow chart .....	6-10
6-7.	System pressure history .....	6-12
6-8.	HPI volumetric flow rate per line with one HPI pump running .....	6-14

6-9.	EFW flow control .....	6-15
6-10.	TBV area control .....	6-16
7-1.	Schematic descriptions of the simulated break in the NPP and the Marviken test configuration .....	7-3
7-2.	Comparison of experimental mass flow and RELAP5/MOD3 calculation in the Marviken 22 experiment .....	7-4
7-3.	Comparison of experimental mass flow and RELAP5/MOD3 calculation in the Marviken 24 experiment .....	7-4
7-4.	Comparison of experimental measurements of pressure and RELAP5/MOD3 calculation in the Marviken 22 experiment .....	7-5
7-5.	Experimental measurements of the pressure and density in the Marviken 22 experiment .....	7-5
7-6.	Comparison between the experiment the RELAP5/MOD3 simulation of the relationship between mass flow and pressure for Marviken 22 test .....	7-6
7-7.	Comparison between the experiment and RELAP5/MOD3 simulation of the relationship between mass flow and pressure for Marviken 24 test .....	7-6
7-8.	Error as a function of pressure for single-phase flow in the prediction of the Marviken 22 test .....	7-7
7-9.	Error as a function of pressure for two-phase flow in the prediction of the Marviken 22 test .....	7-7
7-10.	Normality test performed on the single-phase mass flow error data for Marviken 22 .....	7-8
7-11.	Normality test performed on the two-phase mass flow error data for Marviken 22 .....	7-8
7-12.	Bounds of the variation of the interphase drag coefficient FI as a function of void fraction, for bubbly/slug flow .....	7-10
8-1.	Sensitivity calculation results .....	8-5
8-2.	The variations imposed on the important code parameters to run the sensitivity calculations .....	8-6
8-3.	Comparison of the resulting minimum liquid level in the reactor vessel corresponding to variations of the important code parameters .....	8-6
A-1.	MIST nodalization .....	A-8
A-2.	Primary pressure .....	A-10
A-3.	Hot leg collapsed liquid level .....	A-12

A-4.	Feedwater flow rate .....	A-13
A-5.	Steam generator collapsed liquid level .....	A-14
A-6.	Feedwater flow rate .....	A-15
A-7.	Steam flow rate .....	A-16
A-8.	Core collapsed liquid level .....	A-17
A-9.	Steam flow rate .....	A-19
A-10.	Secondary system pressure .....	A-20
A-11.	Steam generator power .....	A-21
A-12.	Primary system mass inventory .....	A-22
A-13.	Core exit temperature .....	A-23
A-14.	Break mass flow rate .....	A-24
A-15.	Integrated break flow .....	A-25
C-1.	B&W SBLOCA minimum vessel, probability distribution function of 200-bin example: best distribution .....	C-5
C-2.	B&W SBLOCA minimum vessel, probability distribution function of 200-bin example: worst distribution .....	C-5
C-3.	B&W SBLOCA minimum vessel, cumulative distribution function of 200-bin example: best distribution .....	C-6
C-4.	B&W SBLOCA minimum vessel, cumulative distribution function of 200-bin example: worst distribution .....	C-6
C-5.	B&W SBLOCA minimum vessel, probability distribution function of 100-bin example: worst distribution .....	C-7
C-6.	B&W SBLOCA minimum vessel, cumulative distribution function of 100-bin example: worst distribution .....	C-8
C-7.	B&W SBLOCA minimum vessel, cumulative distribution function of 100-bin example: best distribution .....	C-9
C-8.	B&W SBLOCA minimum vessel, probability distribution function of 100-bin example: worst distribution .....	C-9
C-9.	B&W SBLOCA minimum vessel, probability distribution function of 100-bin example: best distribution .....	C-10

## LIST OF TABLES

3-1.	Final rankings of phenomena of medium to high importance .....	3-2
------	--	-----



3-2.	NPP breakdown into components per phase .....	3-3
4-1.	List of important phenomena during an SBLOCA, their rank, and the model or code parameter that RELAP5/MOD3 uses to represent them .....	4-1
4-2.	Summary of available experimental assessment for RELAP5/MOD3 relevant to the important phenomena of an SBLOCA in a B&W NPP .....	4-3
5-1.	Comparison of desired and calculated initial conditions .....	5-9
7-1.	List of important phenomena during an SBLOCA, their rank, the code parameter that RELAP5/MOD3 uses to represent them, and the type of model .....	7-2
7-2.	Summary of the ranging of parameters study .....	7-11
8-1.	Sequence of events for nominal case .....	8-1
8-2.	Sensitivity calculations and their results in terms of the PSCs .....	8-4
A-1.	Calculated and measured steady-state conditions .....	A-5
A-2.	Sequence of events comparisons .....	A-5
B-1.	Two-phase natural circulation phase .....	B-3
C-1.	Regression results .....	C-3
C-2.	All uniform parameter distributions preliminary Monte Carlo assessment using 2,000 histories .....	C-4
C-3.	100,000 history Monte Carlo study of Models 3 and 6 .....	C-4
C-4.	All uniform parameter distributions preliminary Monte Carlo assessment using 2,000 histories .....	C-8
C-5.	100,000 history Monte Carlo study of Models 3 and 6 .....	C-10

## EXECUTIVE SUMMARY

### Background and Objective

The Nuclear Regulatory Commission revised the emergency core cooling system licensing rule to allow the use of best estimate computer codes, provided the uncertainty of the calculations are quantified and used in the licensing and regulation process. The Nuclear Regulatory Commission developed a generic methodology called Code Scaling, Applicability, and Uncertainty (CSAU) to evaluate best estimate code uncertainties. The CSAU methodology was demonstrated with a specific application to a Westinghouse Pressurized Water Reactor experiencing a postulated Large-Break Loss-of-Coolant Accident (LBLOCA) using Transient Reactor Analysis Code as the best estimate code. The objective of this work was to adapt and demonstrate the CSAU methodology for a Small-Break LOCA (SBLOCA) in a Pressurized Water Reactor of Babcock & Wilcox Company (B&W) lowered loop design using RELAP5/MOD3 as the best estimate code.

### Overview of the Work

This effort closely followed the guidelines established by the LBLOCA study, with a few important differences.

- A technical program group assisted in defining the specific scenario and the primary safety criteria used and in developing the Phenomena Identification and Ranking Table. For the rest of the study, the consultants provided important reviews.
- Although the experimental database for the type of plant design studied is rather complete (results from Multiloop Integral System Test and University of Maryland of College Park facilities were key in determining the Phenomena Identification and Ranking Table), the assessment data base for the new RELAP5/MOD3 code was small. Special effort was spent making the most use of the available information, and

an independent assessment of an integral facility was conducted (by Prof. Y. Hassan of Texas A&M University) to make our assessment data base more complete.

- This type of nuclear power plant is very sensitive to operator actions. The operator is not modeled by the code; thus it was decided that the operator actions would be introduced in the scenarios they are dictated in the emergency operating procedures. When performing the base case and sensitivity calculations, considerable attention had to be focused on the operator and the operator actions during the transient since they are sometimes the result of subjective decisions and several paths are available to them. This was not a concern for the LBLOCA study, which had no operator participation.
- Two primary safety criteria were defined at the beginning of the study: peak cladding temperature and liquid inventory in the reactor vessel. It was realized early on that this reactor may not exhibit a temperature excursion in the core and a second primary safety criterion was necessary to evaluate the sensitivity of the result to the different contributing uncertainties.

### Results and Conclusions

The CSAU methodology was successfully demonstrated for the new set of variants defined in this project (scenario, plant design, code). However, the robustness of the reactor design to this SBLOCA scenario and the emergency operating procedure actions assumed for the operator limit the applicability of the specific results to other plants or scenarios. Several aspects of the code were not exercised because the conditions of the transient never reached enough severity. Despite these limitations, the following conclusions can be stated:

- For best estimate analysis of SBLOCA scenario, the operator and the operator actions

have to be incorporated into the model and the simulation. The operator actions are not uniquely defined in the emergency operating procedures and can decide the course of the transient. For this reason, the operator is incorporated into the simulation as a sequence of changing boundary conditions, part of the plant scenario.

- The effort carried out in this program suggests one way in which the operator actions can be predicted and incorporated into the analysis, with their own level of uncertainty. Only one of at least three possible paths was simulated because the other paths would significantly change the scenario, from an SBLOCA to an intermediate or even an LBLOCA. However, the adopted operator actions are not necessarily the most likely for the given scenario.
- The B&W design is very robust for this specific SBLOCA. The likelihood of core

uncovery and cladding temperature excursions are very remote in this scenario. The second primary safety criterion, minimum liquid level in the vessel, seems rather insensitive to variations in the key important parameters. It is recommended that subsequent studies of this nature should define a more meaningful measure of accident severity with which to gauge the uncertainty introduced by the important models and input parameters.

- The independent assessment Multiloop Integral System Test of a calculations, conducted by Prof. Hassan, shows that RELAP5/MOD3 captures the main trends and events of the transient with accuracy. It is important to mention that because the benign nature of the scenario, it was beyond our scope to exercise parts of the code that are likely participate in more severe transients and in other plant designs.

## ACRONYMS

B&W	Babcock & Wilcox Company	PCT	peak clad temperature
CE	Combustion Engineering, Inc.	PIRT	Phenomena Identification and Ranking Table
CSAU	Code Scaling, Applicability, and Uncertainty	PORV	power-operated relief valve
CLLV	collapsed liquid level in the vessel	PSC	primary safety criterion
ECCS	emergency core cooling system	PTS	pressurized thermal shock
EFW	emergency feedwater	PWR	Pressurized Water Reactor
EOP	emergency operating procedure	RCP	reactor coolant pump
HPI	high-pressure injection	RELAP5/ MOD3	Reactor Excursion and Leak Analysis Program, Version 5, Mode 3
ICS	Integrated Control System	RVVV	reactor vessel vent valve
IET	integral effect test	SBLOCA	small-break loss-of-coolant accident
INEL	Idaho National Engineering Laboratory	SET	separate effect test
LBLOCA	large-break loss-of-coolant accident	TBV	turbine bypass valve
LPI	low-pressure injection	TPG	technical program group
MIST	Multiloop Integral System Test	TRAC	Transient Reactor Analysis Code
NPP	nuclear power plant	TRG	technical review group
NRC	U.S. Nuclear Regulatory Commission		

# Uncertainty Analysis of Minimum Vessel Liquid Inventory During a Small-Break LOCA in a B&W Plant—An Application of the CSAU Methodology Using the RELAP5/MOD3 Computer Code

## 1. INTRODUCTION

The Nuclear Regulatory Commission (NRC) revised the emergency core cooling system (ECCS) licensing rule to allow the use of best estimate computer codes, provided the uncertainty of the calculations are quantified and used in the licensing and regulation process. The NRC developed a generic methodology called Code Scaling, Applicability, and Uncertainty (CSAU) to evaluate best estimate code uncertainties. The CSAU methodology was demonstrated with a specific application to a Westinghouse Pressurized Water Reactor (PWR) experiencing a postulated large-break loss-of-coolant accident (LBLOCA) using Transient Reactor Analysis Code (TRAC) as the best estimate code.<sup>1,2</sup> The objective of this work was to adapt and demonstrate the CSAU methodology for a small-break LOCA (SBLOCA) in a PWR of Babcock & Wilcox Company (B&W) design, using RELAP5/MOD3 as the simulation tool.<sup>3,a</sup>

This effort followed the guidelines established during the LBLOCA study (see References 1 and 2). However, several important differences were developed:

1. The technical program group (TPG), in part members of the working committee that performed the earlier study (see Reference 2), was used in the beginning of the process to define the scenario, the primary safety criteria, and the Phenomena Identification and Ranking Table (PIRT). Later, the TPG became a technical review (and advisory) group (TRG).
2. Although the experimental data base for the B&W plant design studied is rather complete, the assessment data base for the new RELAP5/MOD3 code is small; special effort was spent making the most use of the available information, and an independent assessment of an integral facility was conducted as part of this work<sup>b</sup> to make our data base complete.
3. While performing the base case and sensitivity calculations, considerable attention had to be focused on the operator and the operator actions during the transient. As opposed to the LBLOCA case, the slow SBLOCA scenario is very sensitive to operator actions, which had to be taken into account in the modeling. A generally applicable result for SBLOCA should include a probabilistic treatment of the operator. For this effort, a best estimate approach to the modeling of the operator was taken by consulting with experienced operator examiners.

The study showed that for the selected scenario, the combined uncertainties of all the important phenomena do not affect the final outcome very much. In fact, the effect of the operator actions is much more significant than any of the important phenomena.

The final answer is not a measure of peak clad temperature uncertainty that can be cited as an expected value for all SBLOCAs. In other words,

a. Babcock & Wilcox Company proprietary information, 1985.

b. Prof. Y. Hassan of Texas A&M University conducted an independent assessment of RELAP5/MOD3 against a Multiloop Integral System Test (MIST) experiment. Results of this effort are included in Appendix A.

the result is not as general as that of the LBLOCA CSAU (see Reference 2).

The program scope was defined within realistic bounds, which should be listed as well. The most important are as follows:

1. The specific scenario was chosen based on the available information and with the criteria that it should be an SBLOCA and of severe consequences. Iterations to find the "worst case" scenario or even fine tune the scenario to make it more severe fell beyond the scope of this demonstration.
2. The frozen code, RELAP5/MOD3, was released during the performance period of this project. Being so new, the available assessment data base was limited almost exclusively to the developmental assessment.
3. The question of code numerics, with respect to the issue of code applicability, could not be adequately addressed in this study. However, a separate study is currently being conducted to examine the numerics of RELAP5/MOD3.
4. The selected nuclear power plant (NPP) design (lowered loop B&W) is very different from other industrial designs [Combustion Engineering, Inc. (CE), and Westinghouse]. The steam generator is not the U-tube type, but a once-through. In general, a B&W plant has a much shorter response time than other plants. Thus the numerical results from this study cannot be directly translated and used for other designs or scenarios.
5. The nodalization step of the CSAU methodology, Step 8 in Figure 1-1, was not pursued in the manner indicated by the flow chart (see References 1 and 2); there was no iteration of the nodalization. An existing RELAP5/MOD2 input deck for a B&W plant, with a well documented history, was used for this work. Thus, iterations to the

nodings were performed outside this CSAU study. The only noding changes made were to upgrade the deck to MOD3 to specifically use MOD3 features and to capture small level changes in the vessel.

## 1.1 CSAU Methodology

Figure 1-1 is a flow chart description of the CSAU methodology as it is considered for this study. Steps 1 through 6 constitute Element 1 of the methodology, "Requirements and Code Capabilities." It includes the selection of the NPP, the specific scenario, the primary safety criteria (PSCs), and the definition of the PIRT. The methodology also establishes the requirements that the code must satisfy in order to be applicable. The documentation of the selected best estimate code is reviewed to determine whether or not these requirements are met (Steps 4, 5, and 6). The second element of CSAU, "Assessment and Ranging of Parameters," encompasses Steps 7 through 11 (Figure 1-1). The available data base is examined to support the nodalization used in the calculations, and the contributions to uncertainty of each important phenomena are investigated and evaluated. Element 3 of the CSAU methodology, "Sensitivity and Uncertainty Analysis," combines all contributing uncertainties and biases to determine the total uncertainty.

## 1.2 Overview of This Report

Using the flow chart (Figure 1-1) as a roadmap, the main body of the report is arranged in the following manner. Section 2 covers the NPP and scenario descriptions; Section 3 describes the PIRT; Section 4 deals with the applicability of the code; Section 5 describes and justifies the nodalization; Section 6 describes the operator actions; Section 7, "Ranging of Parameters," describes the procedures followed to determine the bias and uncertainty contribution associated with the important phenomena; Section 8 describes the sensitivity calculations and their results; and Section 9 describes the completion of the process with the evaluation of total uncertainty. A summary of conclusions and recommendations is given in Section 10.



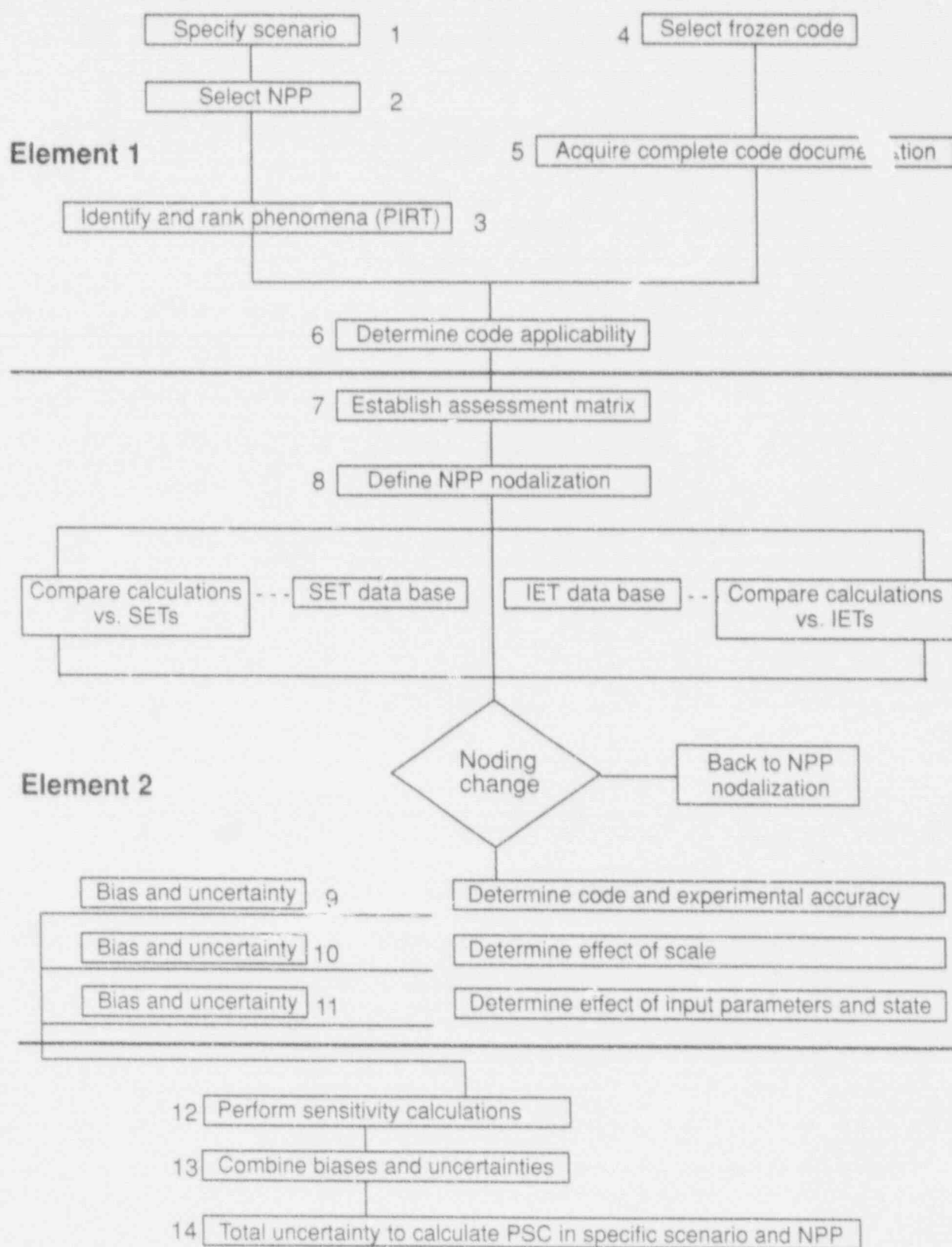


Figure 1-1. Flow chart of CSAU methodology.

## 2. NUCLEAR POWER PLANT DESCRIPTION AND SELECTED SCENARIO

### 2.1 Nuclear Power Plant Description

The selected NPP is a typical B&W lowered loop design as illustrated in Figure 2-1. This design features two hot legs and four cold legs. The elevation of the lowest part of the cold leg is about 6 ft lower than the bottom of the reactor vessel, hence the name "lowered loop." The reactor coolant pumps are mounted such that the centerline of the discharge is 3.5 ft higher than the reactor vessel inlet piping. A section of the cold leg sloped at 45 degrees to make up the elevation difference. One high-pressure injection (HPI) line is connected to each of the cold legs on the side of this sloped section so that gravity will steer the HPI flow toward the reactor vessel.

A unique feature of the B&W vessel internals is the reactor vessel vent valves (RVVVs). These are circular flapper valves, hinged at the top, and are in the closed position held by gravity. Eight of these valves are situated around the perimeter of the upper part of the downcomer and allow flow from the upper plenum to the downcomer. If the pressure in the upper plenum increases 0.1 psi greater than the pressure in the downcomer, the valves start to swing open, allowing mass flow from the upper plenum into the downcomer. The RVVVs are fully open at 0.25 psid. Thus, the RVVVs limit the possibility of pressure building in the upper plenum and depressing core level.

The two steam generators of B&W designs are once-through, counter current flow heat exchangers. The primary coolant flows vertically downwards, between two plenums, through about 15,500 52-ft-long tubes. Since the primary coolant enters the steam generators at the top, the hot leg must rise up past the top of the steam generator and bend down to connect to the upper plenum. The characteristic inverted U-bend shape gives the hot leg a candy cane appearance. The uppermost part of this hot leg U-bend is a potential source of vapor locking in the primary flow

path. If the hot leg should drain such that the level falls below the U-bend, primary coolant flow will be interrupted. The U-bend has a small vent valve that can be opened by the operator to vent any bubbles that may have collected at the top.

In the secondary side of the steam generators, subcooled feedwater, preheated before it enters the steam generator, comes in through several nozzles located around the perimeter of the generator about midway between the bottom and top; the feedwater flows through an annular downcomer to the lower plenum and upward through the center of the steam generator, on the outside of the tubes. As the feedwater enters the downcomer, it mixes with saturated steam, which is pulled from the center of the steam generator through an aspirator. Sufficient steam mixes with the feedwater to produce saturated water at the bottom of the downcomer. Once in its upward path, the water boils and the generated steam superheats. As the water flows through the tube bundle, it is converted to steam, such that at the level of the aspirator all the liquid has been converted to saturated steam. The length of tubes remaining between the aspirator and the upper tube sheet then serve to superheat the steam. Steam superheated to about 33 K (60°F) leaves the generator through the steam annulus and into the steam line. Figure 2-2 shows a schematic description of this flow path.

### 2.2 Scenario Description

The following scenario was selected by the Idaho National Engineering Laboratory (INEL), with the TPG's concurrence. The initiating event is postulated as the break of one of the HPI lines off of its connection to the cold leg (indicated in Figure 2-1). It is assumed that in addition to this initiating event, which disables one of the HPI trains, one of the three HPI pumps is tagged out for service, and one of the remaining pumps fails to start. This amounts to an SBLOCA with reduced HPI capacity.

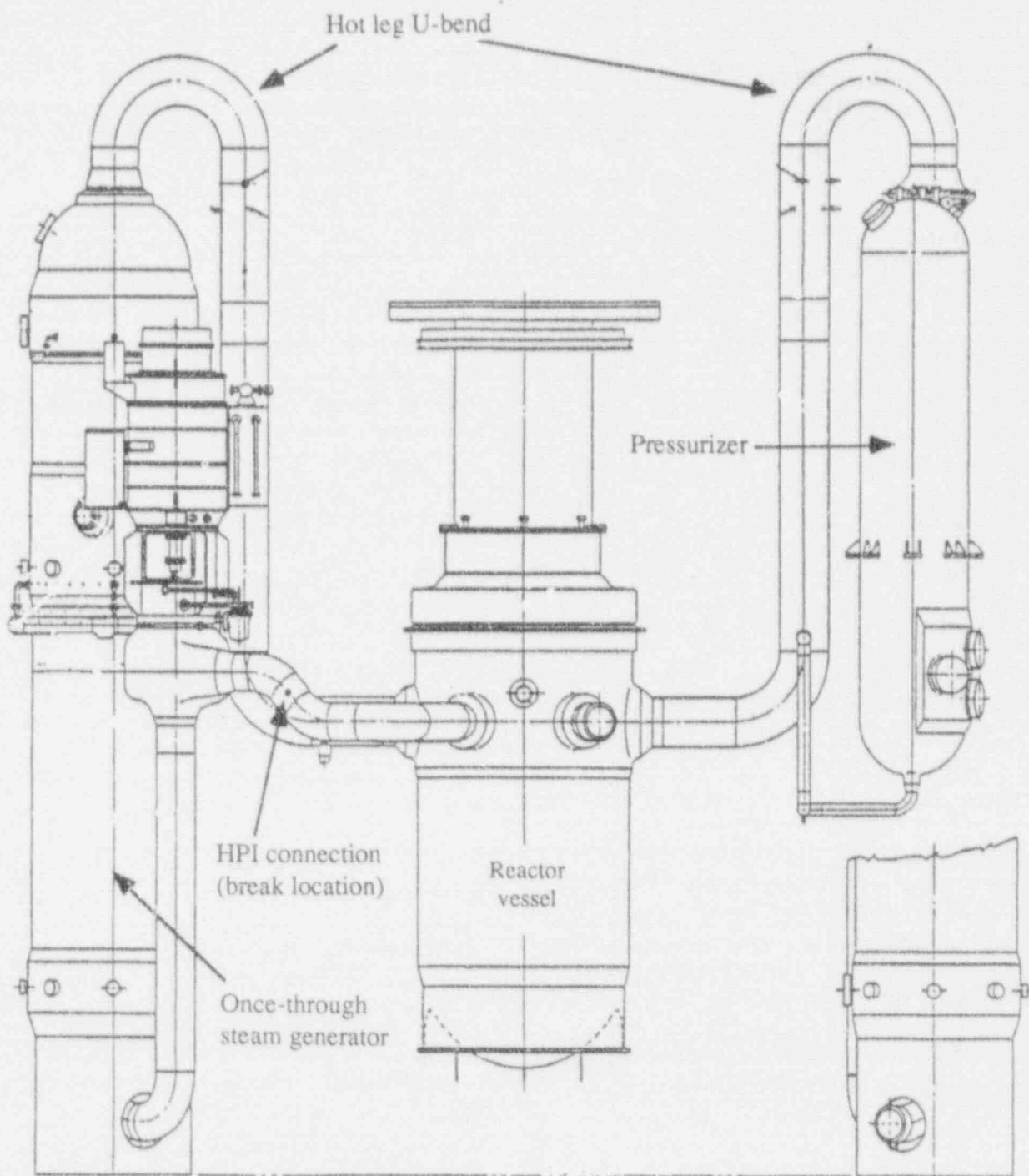
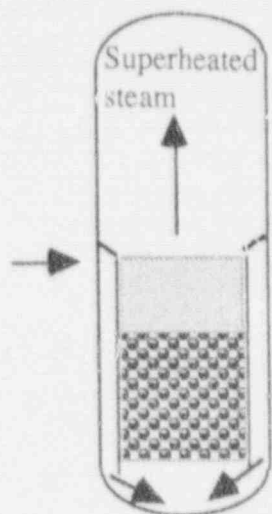


Figure 2-1. Typical B&W lowered loop plant design.



**Figure 2-2.** Steam generator secondary flow path.

Figure 2-3 describes the HPI train for the plant. The break and disabled pump are indicated. The HPI line is severed from the discharge line of reactor coolant Loop A1. This leaves a 5.4-cm (2.125-in.) diameter hole in the side of the 45-degree RCS piping while simultaneously breaking an HPI line. Both of the nonfunctional pumps are located in the broken A HPI train, thus,

the A train is completely unavailable for safety injection. The B HPI train is supplied normally by the only functioning HPI Pump C.

It is also assumed that the operator will act according to emergency operating procedures (EOPs). Since RELAP5/MOD3 is not readily adapted to doing calculations with variable operator actions, specific operator actions are defined as part of the scenario (boundary conditions) and are not treated as a sensitivity code parameter. Including the operator as a part of the scenario's imposed boundary conditions is necessary, because determining the uncertainties due to the operator would require several simulator runs (enough to be statistically significant) with the entire operating crew present. Such a task is well beyond the scope of this demonstration. The results of such a study would likely show that the uncertainties associated with the operator are much greater than the uncertainties due to plant and process mathematical models and would thus mask the results we wish to obtain. For these reasons, the operator was incorporated into the simulation as part of the plant scenario (a time varying boundary condition). The results from this study

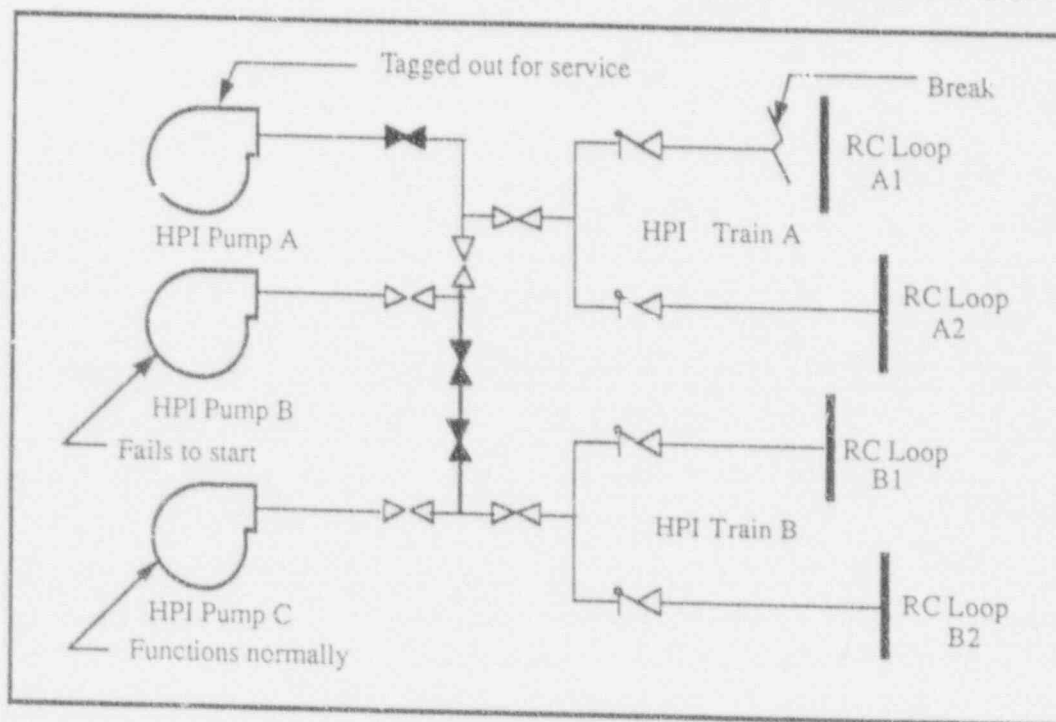


**Figure 2-3.** HPI train lineup in the B&W plant design.

can be applied only to specific sequence of operator actions given in the scenario description.

The operator actions modeled in the simulation were determined from typical EOPs for this plant design.<sup>c</sup> However, the EOPs allow the operator much freedom for subjective judgment. One cannot determine exact timing of actions or the exact setpoints at which an operator decision is made. The EOPs should be thought of as guidelines rather than specific instructions or rules. An SBL OCA scenario with different operator actions than those modeled in this study constitutes a new scenario and requires a separate development of the uncertainty analysis (different PIRT, different sensitivity calculations).

## 2.3 Results from Scoping Run

Once the scenario had been chosen for the NPP and the PIRT was defined, a scoping calculation was conducted to add confidence and give a more specific feel for the scenario. The scoping calculation

was conducted to verify that RELAP5/MOD3 had no gross inadequacies that would preclude its application to this SBLOCA scenario. It was also used to compare the transient phases and governing phenomena with what the PIRT had determined to be important. Furthermore, the scoping calculation results were used to determine the nature and timing of the operator actions modeled in the sensitivity calculations.

The input for the scoping calculation was generated from an input deck for a B&W plant that has been exclusively used at the INEL for previous analyses. The input deck was upgraded so that it would be compatible with RELAP5/MOD3 input requirements. Steady state was then established with the modified input deck and the SBLOCA initiated with the A HPI train disconnected (Figure 2-3). The only operator action required in this scoping simulation was to trip the reactor coolant pumps (RCPs) 60 seconds after loss of subcooling margin.

Figure 2-4 illustrates the phases seen in the pressure trace of this transient. Phase descriptions follow.

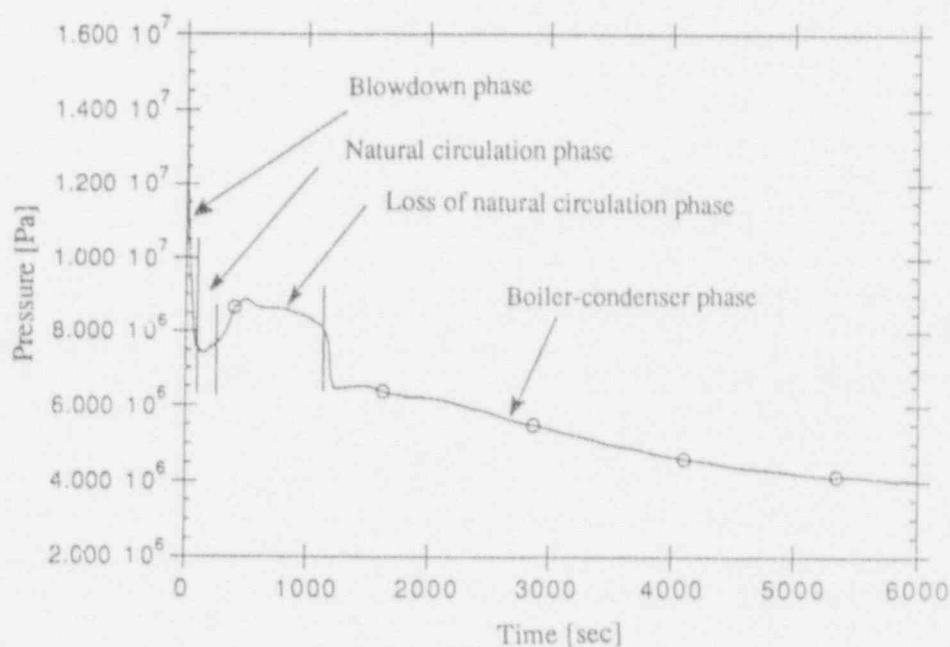


**Figure 2-4.** Pressure history during the scoping calculation, illustrating the occurrence and relative location of the transient phases.



**2.3.1 Phase 1: Blowdown Phase.** This phase begins with the occurrence of the break and ends with the end of the RCP coastdown. Upon occurrence of the break, the reactor begins a fast depressurization, which triggers the reactor trip. It is expected that flashing will start occurring throughout the hot path of the primary, as the primary begins to lose its subcooling margin. The operator becomes aware of the loss of subcooling margin and trips the RCPs, as established by the EOPs for this plant. It is expected that at the end of this phase, most of the primary side is single-phase, primary fluid conditions approach saturation, and the pump coastdown ends.

**2.3.2 Phase 2: Saturation to Natural Circulation.** This phase begins at the end of the pump coastdown and ends with the complete loss of natural circulation. The subcooling margin has been lost at the beginning of this phase, and the pressure has dropped to saturation pressure. The flow is becoming two-phase, and a bubble begins to form at the top of the U-bend. As more and more steam is generated, it becomes increasingly difficult for the natural circulation flow to sweep away the bubbles that accumulate at the top of the

U-bend. A short, intermittent mode is expected (Figure 2-5) as the steam accumulates and the two-phase level recedes downward in the U-bend, thus momentarily interrupting the natural circulation. Once natural circulation is interrupted, the loss of the secondary heat sink results in repressurization of the primary. The pressure increase will compress the bubble on top of the U-bend, reestablishing the natural circulation. After a few cycles, the bubble will become too large to allow the liquid to rise to the inverted U-bend, and the natural circulation will be interrupted permanently, thus ending this phase.

**2.3.3 Phase 3: Loss of Loop Natural Circulation.** This phase begins with the loss of natural circulation through the loops and ends when the vessel steam begins to enter the steam generator tubes. Having lost natural circulation, the pressure begins to increase once again. The main cooling mechanism for the core becomes internal vessel circulation. The RVVVs open a flow path that allows the core outlet fluid into the downcomer, where it can mix with the incoming HPI and recirculate through the core or communicate with the break (Figure 2-6).

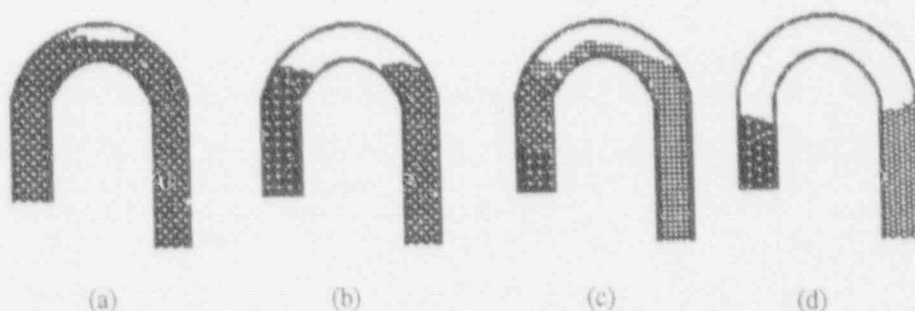


**Figure 2-5.** Schematic description of the interruption-resumption of natural circulation by the intermittent voiding of the top of the U-bend: (a) bubble accumulates at the top; (b) flow is momentarily interrupted due to the bubble; (c) the compressed bubble gives way to a renewed natural circulation path; and (d) natural circulation is permanently interrupted.



During the loss of natural circulation, the operator may decide to run the RCPs for a few seconds (bump the pumps according to EOPs) in an effort to reestablish natural circulation. If the operator does not bump the RCPs, the transient will eventually develop into the next phase, the boiler-condenser mode.

**2.3.4 Phase 4: Boiler-Condenser Mode Phase.** In this phase, the steam generated in the core condenses in the primary side of the steam generator tubes, and a secondary heat sink is reestablished. The pressure will drop as energy is removed by the boiler-condenser mode. This phase ends when the ECCS begins to refill the primary and the plant enters a recovery phase, which is expected some time after 6,000 seconds.

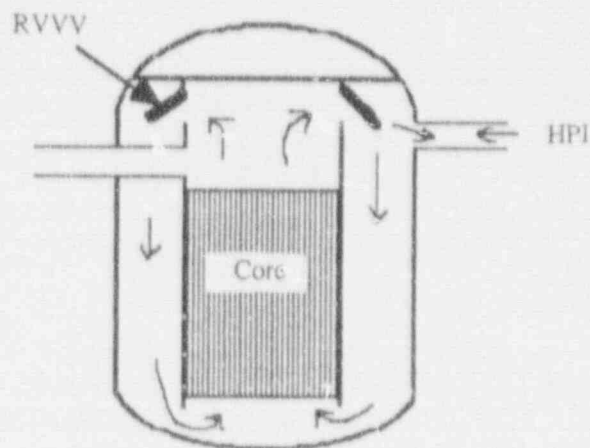


**Figure 2-6.** Schematic description of the internal vessel circulation path in the last two phases of the transient.

### 3. PHENOMENA IDENTIFICATION AND RANKING TABLE

#### 3.1 Summary of the PIRT Process

Step 3 of the CSAU methodology<sup>2</sup> (Figure 1-1) consists of identifying the feasible phenomena that have an important effect on the PSCs and ranking these phenomena according to the importance of their effect. The procedure used two independent panels of experts. Each panel divided the transient into phases, and for each phase the NPP components were evaluated according to their influence during the specific phase being considered. Using the Analytical Hierarchy Process (Appendix B), the components were ranked by the experts. Components were ranked relative to their effect upon the PSCs as judged by the experts. Then, for each component and for each phase, the phenomena pertinent to each component were ranked according to their relative effect on the PSCs. In the end, a system-wide rank of each phenomena is obtained by combining the pair-wise rank of the phenomena within the component and the relative rank of the component. The final rank is normalized and fit into a integer scale of 1 through 9. A rank of 9 implies that the phenomena is of highest importance, and a rank of 1 means the phenomena is of lowest importance in the context of the transient and the PSCs selected.

#### 3.2 PIRT Results

The PSCs chosen in this case were

- The peak clad temperature (PCT)
- The liquid inventory in the core.

Reference 3 discusses in detail the results from each group of experts and the rationale followed to resolve the differences and reach a consensus. The final PIRT, shown in Table 3-1, contains the subset from all phenomena considered that either panel had independently ranked 5 and above (medium and high importance) in their respective PIRTs. The rankings given in this table are the

results of both panels together reranking the previous subset. Thus, a ranking of 1 in this particular table should be interpreted as being of medium importance. This reranking process allowed for a finer differentiation amongst the important phenomena, which otherwise would have all been ranked equally.<sup>d</sup> Table 3-2 describes the components of the NPP that appear in Table 3-1.

It was decided that phenomena ranked 6 and above in the final PIRT would be considered in the NPP sensitivity calculations. These phenomena and their associated components are:

1. The break flow (break)
2. Natural circulation (vessel and steam generator)
3. Decay heat (core)
4. RCP performance (RCP)
5. ECCS flow (HP)
6. Steam generator heat transfer (steam generator)
7. Phase separation in the U-bend (U-bend)
8. RVVV performance (vessel).

The above phenomena are believed to have the most effect on the PSCs. It does not imply that phenomena not listed have no effect. Numerous discussions and Analytical Hierarchy Process calculations led to this result and are documented in Reference 3.

d. Appendix II of Reference 3 contains the preliminary independent PIRTs, which show that because of the complexity of the selected transient and the large number of phenomena considered, many phenomena appear to have equally high importance. Appendix III of Reference 3 lists and defines all the phenomena considered in the context of this work.

# Phenomena Identification and Ranking Table

**Table 3-1.** Final rankings of phenomena of medium to high importance.

Blowdown: Phase 1			Natural circulation: Phase 2		
		Rank <sup>a</sup>			Rank <sup>a</sup>
Break	Break flow	9	Vessel	Natural circulation	9
				Decay heat	8
				RVVV performance	6
				Vessel 2- $\phi$ level	2
Vessel	Decay heat	6	Break	Break flow	7
	Forced convection	2			
	Upper head mixing	1			
	Flashing	2			
	Wall stored heat	1			
RCP	RCP performance	4	U-bend	Phase sep. in U-bend	7
				U-bend voiding	5
				Cold leg void fraction	4
HPI	ECCS flow	4	HPI	ECCS flow	6
Pressurizer	Pressurizer level	2	Upper down- comer	Condensation	5
	Wall stored heat	1	Steam generator	Natural circulation	9
				Primary heat transfer	1
				Steam generator heat	1
				Transfer sec. conditions	1
Loss of natural circulation: Phase 3			Boiler-condenser: Phase 4		
		Rank			Rank
RCP	RCP performance	9	HPI	ECCS	9
HPI	ECCS	7	Break	Break flow	9
Break	Break flow	6	Steam generator	Steam generator heat transfer	8
Vessel	Decay heat	6	Core	Decay heat	6
	Int. vessel circ.	4		Vessel 2- $\phi$ level	3
	Vessel 2- $\phi$ level	3		Int. vessel circ.	1
				Core heat transfer	1
Cold leg	ECCS mix and spill	2			
Steam generator	Primary heat transfer	1			
U-bend	U-bend draining	1			

a. 1 indicates medium importance, 9 indicates very high importance.

**Table 3-2.** NPP breakdown into components per phase.

Blowdown: Phase 1		Natural circulation: Phase 2	
Vessel	Includes the core, vent valves, upper and lower plenum, and lower downcomer	Vessel	Includes the core, vent valves, upper and lower plenum, and lower downcomer
Break	Break itself, not including the cold leg	Break	Break itself, not including the cold leg
HPI	The high-pressure injection connection to the cold leg	HPI	The high-pressure injection connection to the cold leg
RCP	Reactor coolant pumps	Upper downcomer	Upper half of the downcomer
Pressurizer	The pressurizer volume and its connection to the vertical part of the hot leg	U-bend	Inverted U-tube; does not include the horizontal part of the hot leg
		Steam generator	Primary and secondary sides of the steam generator
Loss of natural circulation: Phase 3		Boiler-condenser: Phase 4	
Break	Break itself, not including the cold leg	Break	Break itself, not including the cold leg
HPI	The high-pressure injection connection to the cold leg	HPI	The high-pressure injection connection to the cold leg
Steam generator	Primary and secondary sides of the steam generator	Steam generator	Primary and secondary sides of the steam generator
RCP	Reactor coolant pumps	Core	Core of the reactor
Vessel	Includes the core, vent valves, upper and lower plenum, and lower downcomer		
U-bend	Inverted U-tube; does not include the horizontal part of the hot leg		
Cold leg	Pump discharge to connection to the vessel		

### 3.3 Conclusions

Based on two independent assessments, the thermal-hydraulic behavior of an NPP during a SBLOCA is much more complex than what is expected of a LBLOCA (see Reference 3). The transient can be divided into four distinct phases plus recovery, as opposed to only three for LBLOCA. A large list of phenomena are deemed important throughout the transient. The most important phenomena during the blowdown phase are the break flow and the decay heat of the

core. The most important phenomena during the natural circulation phase are the natural circulation in the vessel and the steam generator, the decay heat of the core, the break flow, the phase separation in the U-bend, the ECCS flow, and the performance of the RVVVs. During the loss of natural circulation phase, the important phenomena are the performance of the RCPs, which may be run momentarily in this phase, the ECCS flow, and the break flow. Finally, during the boiler-condenser mode phase, the ECCS flow, the break flow, the heat transfer in the steam generator, and

the core decay heat are the most important phenomena.

As indicated by the inclusion of RCP performance during the loss of natural circulation phase (momentarily starting the RCPs is an operator action), the operator actions can easily and significantly change the character of the transient in this type of NPP design.

Documentation of the development of separate PIRTs by the two independent panels is shown in

detail in Reference 3. It is important to note that despite the subtle differences in their basic assumptions, a consensus was easily reached, and there were no items of permanent disagreement between any of the two panels.

The Analytical Hierarchy Process (Appendix B) approach proved to be a useful tool not only to determine the final rankings in the PIRT but also to evaluate whether minor disagreements of phenomena rankings had a significant effect on the final ranking.

## 4. CODE APPLICABILITY

Code applicability is Step 6 of the CSAU methodology (Figure 1-1). The specific transient scenario, NPP, and the PIRT establish the requirements that the code must satisfy in order to adequately simulate the transient. The code documentation is then reviewed to determine if these requirements are met.

Table 4-1 summarizes the important phenomena, as determined by the expert panels, and the

models or key parameters used in the code to represent them. These key parameters are not the complete set of parameters used in the representation of each phenomenon; rather they are those thought to provide the uncertainty associated with each phenomenon. For instance, Phenomenon 5, ECCS flow, is characterized in this table with its temperature and not its magnitude as a flow. That is because in our specific scenario the operator is

**Table 4-1.** List of important phenomena during an SBLOCA, their rank, and the model or code parameter that RELAP5/MOD3 uses to represent them.

Phenomena		Model	Key parameters (code)
1	Break flow	Junction with assigned location on pipe (top, side, bottom). Parameters: break area and discharge coefficient.	Subcooled discharge coefficient 2- $\phi$ discharge coefficient
2	Natural circulation	A complete flow loop made of junctions and volumes with angles of inclination. Interfacial drag and heat transfer, wall-fluid heat transfer, flow regime maps.	1- $\phi$ : RCP torsional friction coefficient 2- $\phi$ : Interphase drag coefficient
3	Decay heat	User input into heat structures.	Input table or function
4	RCP performance	User input: homologous curves for head and torque.	RCP torsional friction coefficient
5	ECCS flow	User input: flow versus pressure curves.	Input temperature
6	Steam generator heat transfer	Heat structures attached between primary and secondary sides. Interfacial drag and heat transfer, wall-fluid heat transfer, vertical flow regime map.	Coefficients from heat transfer correlations (area)
7	Phase separation in the U-bend	Geometry defined with suitable volumes. Interface drag and heat transfer. Vertical stratified flow model.	2- $\phi$ : Interphase drag coefficient
8	RVVV performance	Modeled as a valve whose area is controlled by the pressure difference across of it.	Inertia of the valve



instructed to limit the HPI flow to a maximum value of 500 gpm, thus limiting the uncertainty in the magnitude of the flow.

### 4.1 Global Applicability

In terms of global requirements, the following statements can be made based on our review of the code documentation:

**4.1.1 Field Equations.** RELAP5/MOD3 is a one-dimensional, two-fluid, six-equation simulation code. Six equations conserve mass, momentum, and energy for each of two phases. None of the phenomena deemed important calls for a two- or three-dimensional representation in the simulation, which makes the one-dimensional approach sufficient. The two-phase phenomena and two-phase interactions, listed as important phenomena in the PIRT (Table 4-1), are modeled in RELAP5/MOD3, which fulfills this aspect of the requirements.

**4.1.2 Closure Relations.** The code documentation describes closure models, uses, data ranges, accuracy, and ability to scale up. Developmental assessment is available in the documentation to address each of the important phenomena in Table 4-1.

**4.1.3 Numerics.** Although limited to developmental assessment, statements about stability and accuracy of the code are found in the code manuals. An effort is now in progress to evaluate and improve the numerics of this code. Since that study was not complete by the time of this writing, our study could not benefit from that effort.

**4.1.4 Components and Control.** The NPP geometry, flow paths, heat generation, heat transfer, and heat storage can be described by elements available in the code. Suitable control systems and trip logic are also available to model plant controls and operation. Integrated Control System (ICS) actions as well as operator actions were modeled using these tools.

Thus, in terms of the global requirements as set out by the scenario and plant geometry, the code is adequate to perform the simulation. The scop-

ing calculations conducted early on (Section 2.3 of this report) indicated no gross inadequacies of the code and seemed to display all the expected phenomena and behavior.

### 4.2 Specific Scenario

In terms of specific model requirements, one needs to look more closely at each pertinent model, its range of applicability, and its accuracy. To do this within our constraints of time and resources, we had to limit the review to the most important phenomena in the transient (according to Table 4-1). To assist this study, an assessment data base was established with the available information of separate effect and integral effects tests. Table 4-2 summarizes this available data base. The phenomena are indicated in Table 4-2 by their number according to Table 4-1. Decay heat, RCP performance, ECCS flow, and RVVV performance are not represented in this table, for they are user inputs and not phenomena.

Steps 9, 10, and 11 of the CSAU methodology (Figure 1-1), where the bias and uncertainty contributed by each model or parameter is determined, require the same level of documentation review as the applicability study. Therefore, these steps were performed simultaneously. Section 7 describes the results in detail. At this point, the models investigated were appropriate to represent the important phenomena within the ranges expected.

The lack of assessment using experiments in integral facilities (such as MIST) forced us to perform our own assessment of at least one integral experiment. The results of this assessment (conducted by Prof. Yassin Hassan of Texas A&M University) indicate that the code is able to adequately capture the trends and the dominant events of this transient. Appendix A describes the results from this independent assessment.

### 4.3 Code Scaling

Despite the abundant experimental data base that exists for this type of plant design and transient (e.g., MIST, University of Maryland at

**Table 4-2.** Summary of available experimental assessment for RELAP5/MOD3 relevant to the important phenomena of an SBLOCA in a B&W NPP.

Test	Phenomena
SET facilities	
Loft-Wyle test WSBO3R orifice calibration	1
GE, 1-ft level swell test 1004-3	7
GE, 4-ft level swell test 5801-15	7
Dukler-Smith air entrainment test	6, 7
Marviken, critical flow test 24	1, 7
Marviken, critical flow test 22	1, 7
Bennett's heated tube	6, 7
Royal Institute of Technology heated tube	6
ORNL bundle CHF test	6
ORNL void profile test	6
Christensen subcooled boiling test	6, 7
MIT pressurizer insurge tests	6, 7
FLECHT SEASET forced reflood tests	6
UCSB NC tests 101 and 309	6, 7
IET facilities	
LOFT L3-7	1, 2
LOFT L2-5	1
Semiscale	2
LOBI	1
BETHSY	2
ROSA-IV	1, 2
MIST	1, 2, 6, 7

College Park), which was very useful in defining the important phenomena and the specific transient, a definite statement on scaling cannot be made for lack of proper assessment of integral experiments. However, the developmental assessments listed in Table 4-2 conclude that RELAP5/MOD3 reasonably represents the trends, magnitudes, and timing observed in the experiments. The authors of these assessments,

and our own review, do not indicate any obvious reasons why the gap between the experimental results and the RELAP5/MOD3 simulation should increase with the scale of the plant. Furthermore, Prof. Hassan's assessment using MIST data shows good agreement between the RELAP5/MOD3 simulation and the experimental data (Appendix A), which further supports the conclusion that the code is applicable.

## 5. NODALIZATION

### 5.1 Pedigree of the Input Deck

The CSAU process dictates that the nodalization for the input model be defined based on information learned from determining the code's applicability. Thus, the nodalization is to be used to simulate applicable separate effects tests and integral effects tests. Results from the simulations are then analyzed to determine whether the nodalization was adequate. If necessary, the nodalization is changed and the simulations done again. The process is repeated until an adequate nodalization is found. Given the current status of assessment for RELAP5/MOD3, such a procedure is difficult at best. Typically, a code is assessed against separate effects tests with the goal of predicting the phenomena as well as possible rather than as well as is practical. This results in separate effect test models with many more nodes in them than can be practically used in a full plant model.

A previous demonstration of CSAU as applied to an LBLOCA also reports about the general inadequacy of code assessment as it relates to modeling systems rather than separate effects (see Reference 2). Therefore, the nodalization for this simulation was not defined exactly as prescribed by the CSAU methodology. Instead, an input deck was selected that had been used for past analyses. The basic nodalization was used to model similar SBLOCA scenarios for a pressurized thermal shock (PTS) study in 1984<sup>4</sup> and a B&W safety study in 1987.<sup>5</sup> The PTS study used the nodalization to simulate a 2-in.-diameter break in the horizontal portion of the pressurizer surge line. The B&W safety study used the basic nodalization to simulate a hypothetical 0.01-square-ft (1.35-in.-diameter) break in the cold leg. Both of these simulations are similar to this 0.0246-square-ft (2.125-in.-diameter) break at the HPI line. Since the model performed sufficiently well for these simulations, it was assumed it would perform equally well for this application.

To simulate this particular SBLOCA scenario, the input deck used for the B&W safety study<sup>5</sup>

was adapted for RELAP5/MOD3 and some changes were made to the nodalization. This section describes the input model and points out the changes made to the input deck for application to this scenario.

### 5.2 Primary System

The RELAP5/MOD3 vessel model, shown in Figure 5-1, consists of several components describing the various flowpaths through the vessel. The model included an inlet annulus, downcomer, lower plenum, core, core bypass, upper plenum, upper head, vent valves, brazement tubes, and control rod guide tubes. Nozzles are modeled with crossflow junctions as was recommended for RELAP5/MOD2.<sup>6</sup> Since core inventory is a PSC for this analysis, the original three-volume core was changed to 12 volumes to more accurately calculate the liquid level in the core. In addition, rod bundle drag was turned on so that Bestion's correlation would be used for bubbly/slug flow regimes. This improves the excessively high interphase drag calculation for rod bundles in RELAP5/MOD2.<sup>7</sup> The power shape assigned to the fuel rods was changed to a more conservative, top peaked profile representative of the shape after about 400 full-power days of operation. The profile comes from plant data provided by a utility through private communication.

The eight reactor vent valves located between the upper plenum and the inlet annulus were modeled with a single-servo valve component. The servo valve component uses output from a control variable to determine the valve opening. The control variable was designed to calculate the flow area given a pressure difference across the valve.

Also included in the primary system is the low-pressure injection (LPI) system, core flood system, power-operated relief valve (PORV), and the safety valves. The LPI and core flood systems are connected to the vessel inlet annulus. The PORV and safety valves are connected to the top of the

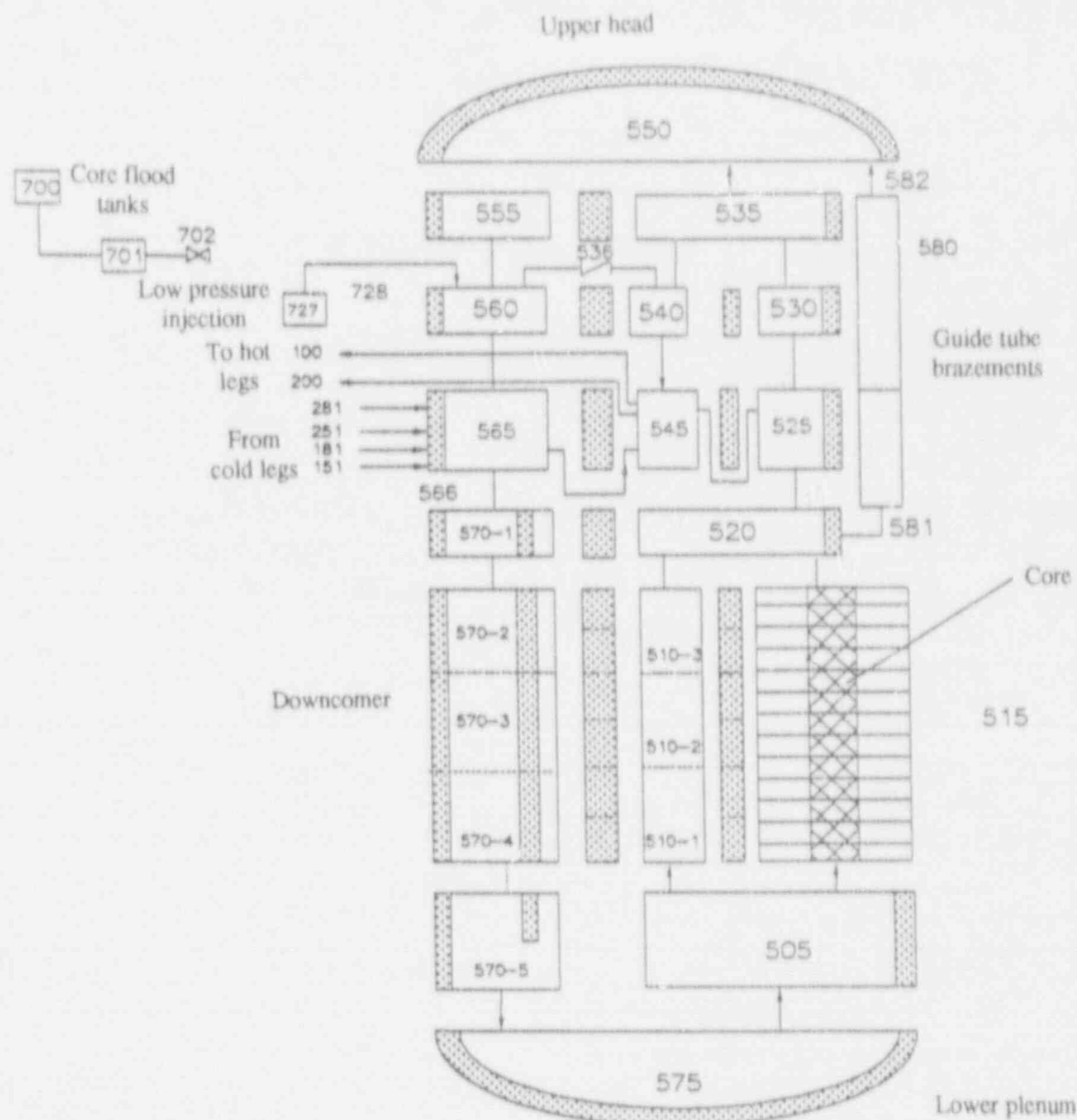


Figure 5-1. RELAP5/MOD3 reactor vessel noding.

pressurizer. The chemical and volume control system is also simulated to provide makeup and letdown for the primary system. Nodalization for these models is shown in Figures 5-2 and 5-3.

Heat structures were used to represent stored energy from fuel rods, steam generator tubes, loop piping, vessel wall, vessel internals, pressurizer wall, pressurizer surge line, and pressurizer heaters.

### 5.3 Secondary System

The RELAP5/MOD3 model of the steam generators is shown in Figure 5-4. As emergency feedwater (EFW) is injected into the generator, it will wet only a portion of the tube bundle as it flows downward and towards the center of the bundle. To capture this behavior, the tube bundle was modeled by splitting the tube bundle into two regions. The first region represents the outer 10% of the tubes, and the second region represents the

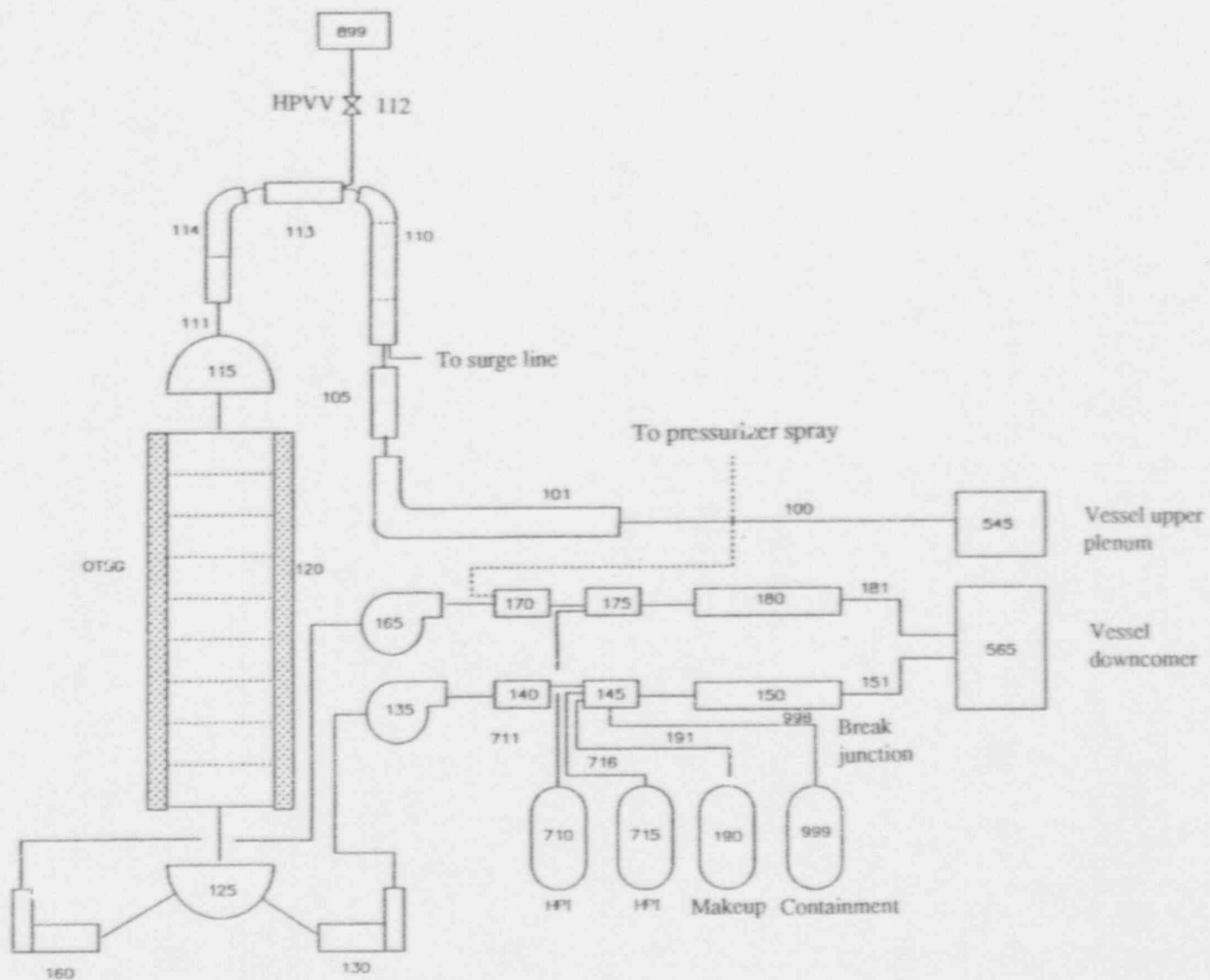


Figure 5-2. Primary loop showing HPI, makeup, and break locations.

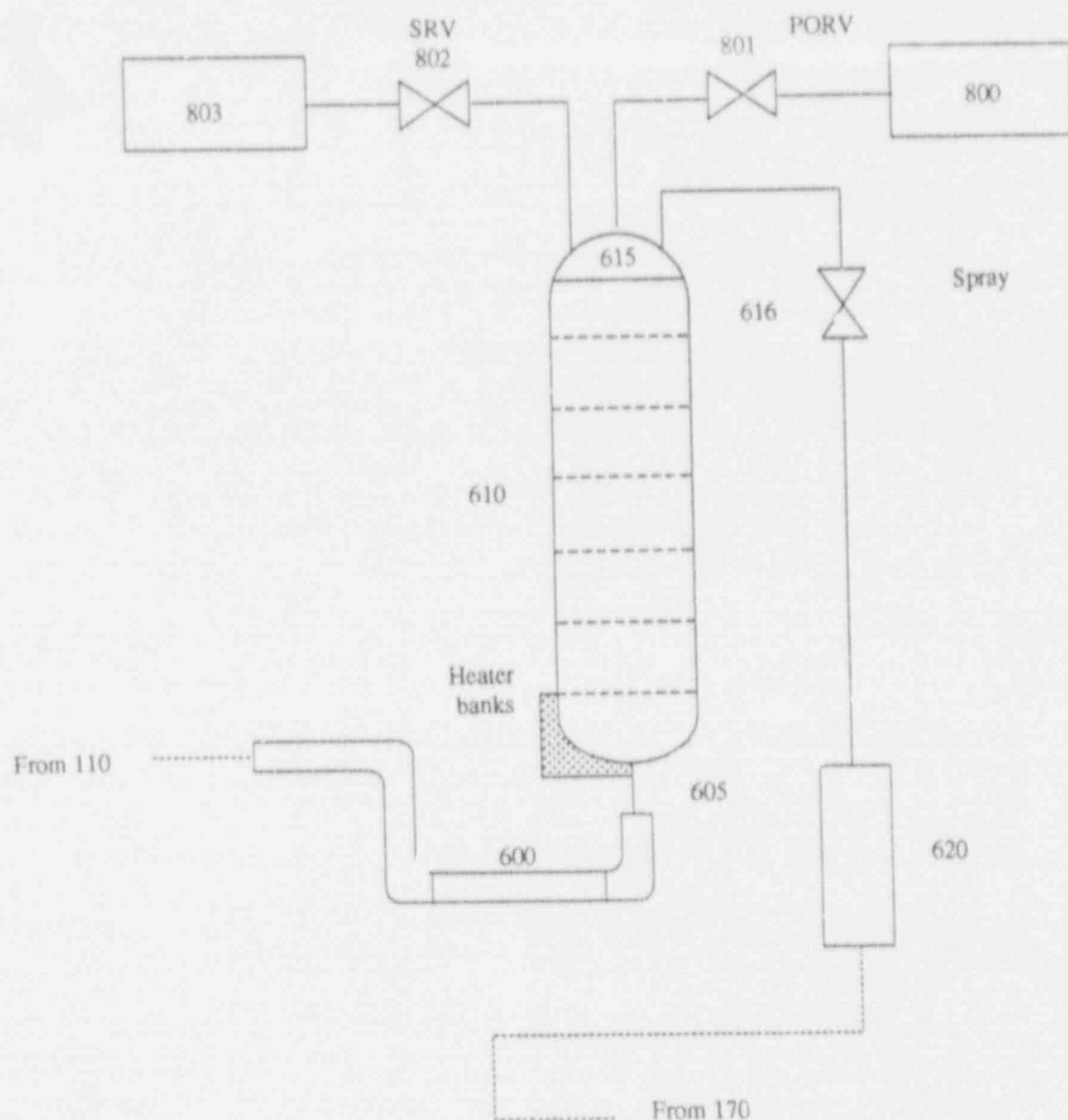


Figure 5-3. Pressurizer with PORVs.

inner 90% of the tubes. Both regions were connected with crossflow junctions so there is a flow path between the two regions, as shown in Figure 5-4. The EFW injection port was connected to the 10% region. Thus, during EFW injection, only 10% of the tubes will be wetted at the top of the generator. As EFW flows downward, it is free to flow radially inward via the crossflow junctions. The choice of splitting the secondary side into 10 and 90% wetted/unwetted regions is somewhat arbitrary. However, experiments per-

formed at the INEL, with one section of a full-scale, once-through steam generator, show that for upward steam flow comparable to those seen in scoping runs for this SBLOCA scenario, anywhere from 3–10% of the tubes will be wetted.<sup>8</sup> In addition, RELAP5/MOD3 contains a new counter current flow limiting model, which limits downward liquid flow in the presence of upward steam flow. The user is allowed the choice of the Wallis, Kutateladze, or no counter current flow limiting model. For this simulation, the Wallis



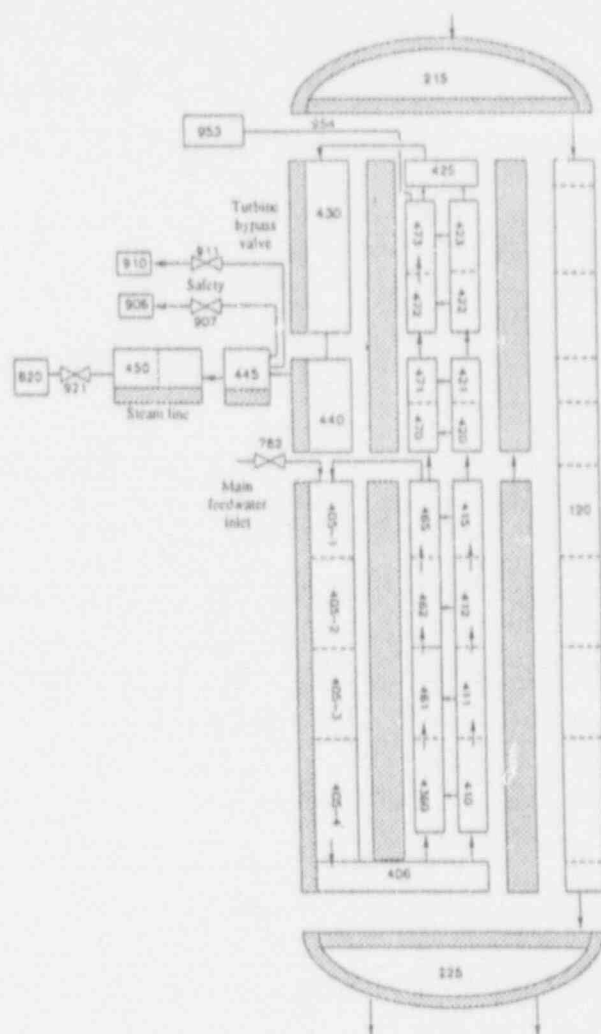


Figure 5-4. Model of B&W steam generator.

form was used with the gas intercept set at 2.06 and the slope set at 1.09 as recommended by McCreery et al. (see Reference 8). Also, the flag for rod bundle drag was turned on so that Bestion's correlation for interphase drag would be used on the secondary side of the generators.

The RELAP5 model of the main steam lines represents the region from the outlet of the steam generator to the turbine stop valves. The model represents the flow restrictors located in the steam lines, the safety relief valves and the turbine bypass valves (TBVs). The 16 safety relief valves in the plant are represented by one valve in the model. Likewise, the two TBVs are also repre-

sented by one valve in the model. Heat structures are used to simulate the steam line piping.

The various components of the feedwater model are shown in Figures 5-5 and 5-6. The water is heated and pressurized from 90°F and 1.5 psia to 460°F and 950 psia. The crossover between the main and emergency feed trains, which is accomplished in the plant by appropriately aligning three different valves, is simplified and modeled with a single valve. The main feedwater pumps are modeled with the mechanistic model in RELAP5. In the NPP, EFW is supplied by two motor-driven pumps and one turbine-driven pump. Each of the motor-driven pumps

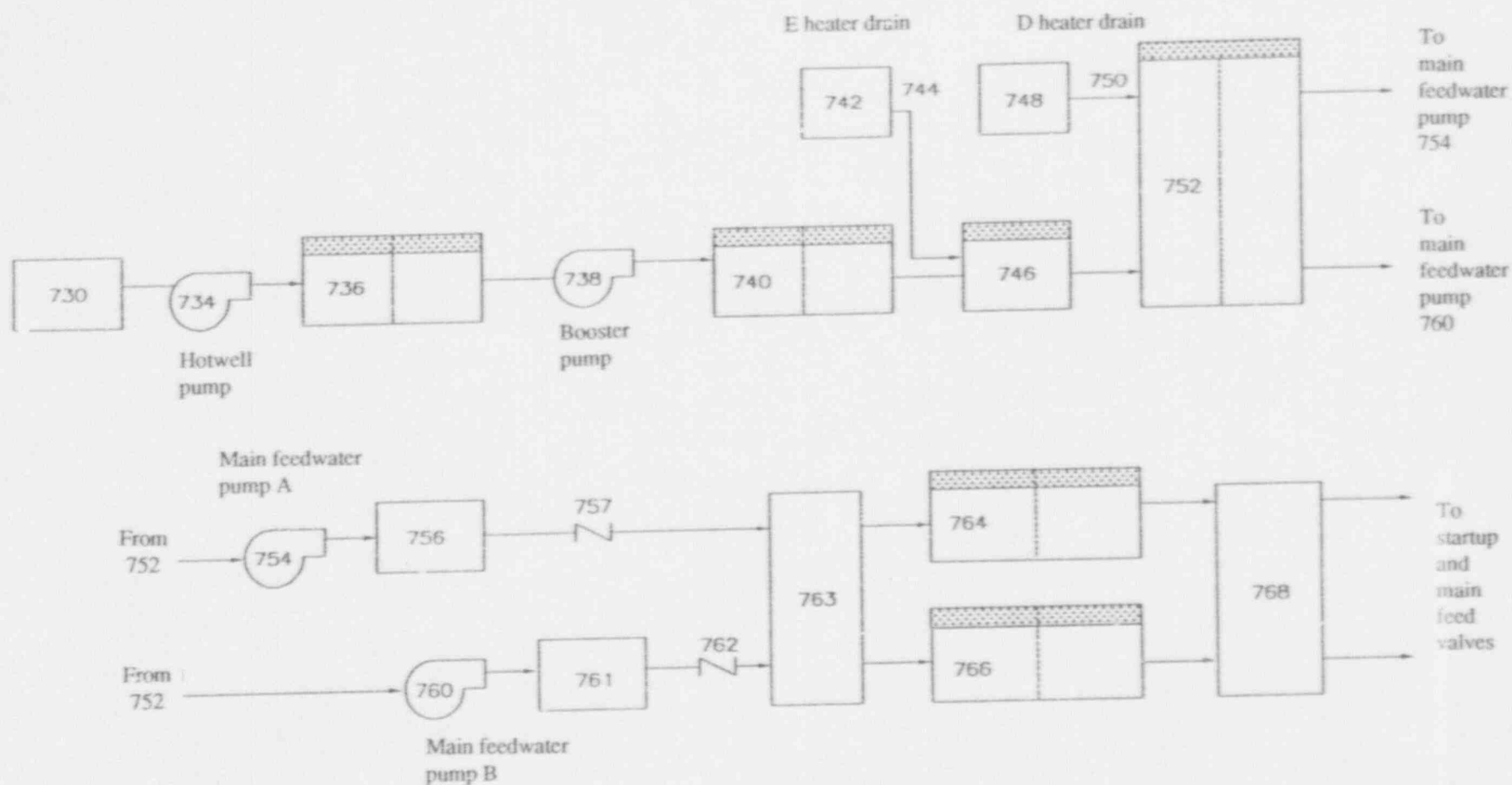


Figure 5-5. Feedwater train from condenser to startup and main feed valves.

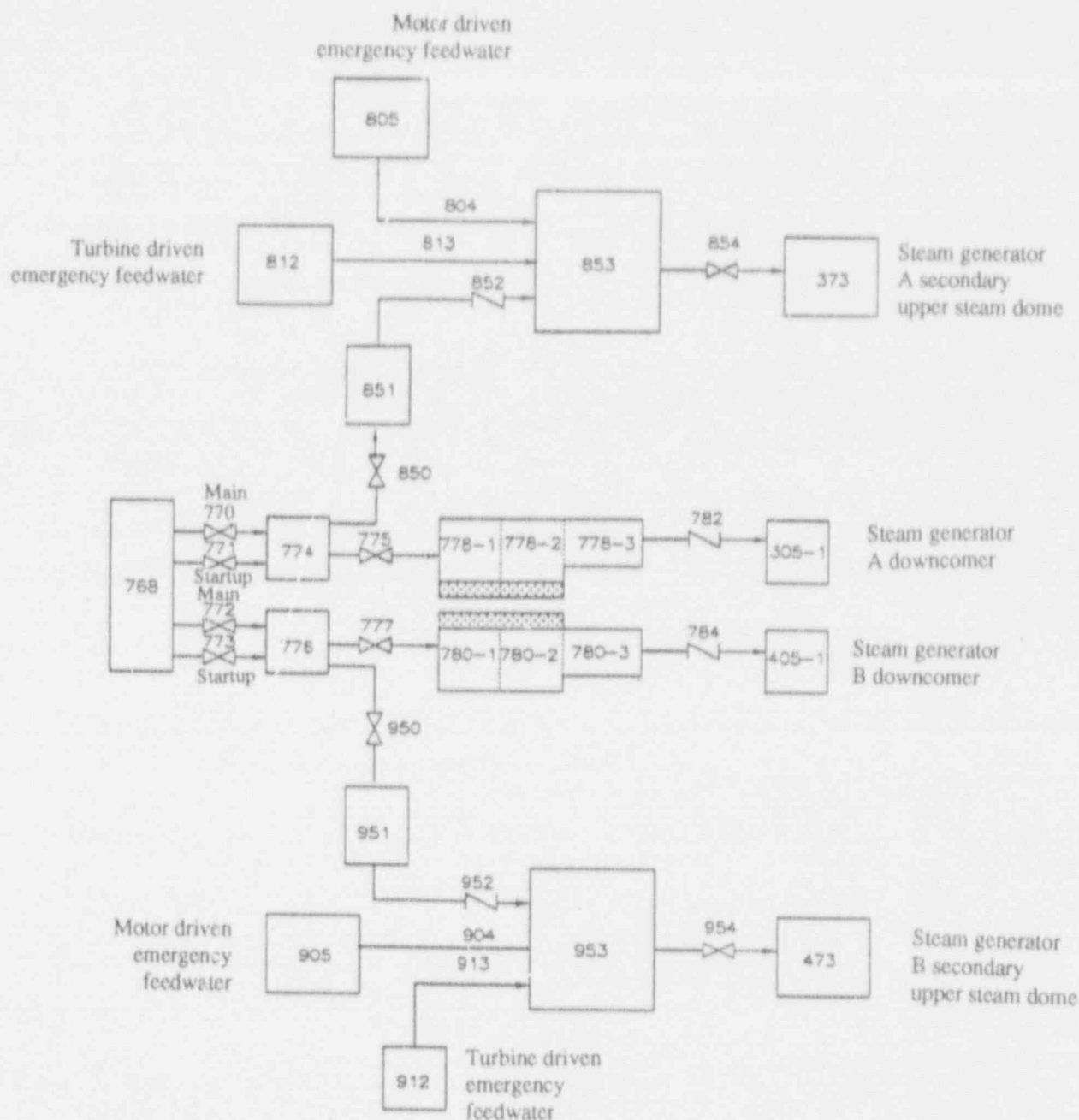


Figure 5-6. EFW train model.

supplies one steam generator while the turbine-driven pump supplies both steam generators. Figure 5-6 shows how the EFW train is modeled. EFW piping for each steam generator is represented by a single volume. This volume is supplied by two time-dependent junctions, one of which represents the motor-driven EFW pump, the other representing one-half of the capacity of the turbine-driven EFW pump. Pump performance

is represented by flow tables, which depend upon EFW piping pressure. Between the EFW piping and the steam generator a valve can be throttled to regulate overall EFW flow into the generator.

Heat structures are used to represent the high- and low-pressure heaters and piping metal masses. The feedwater heaters are modeled using

the appropriate tube bundle surface areas. The energy contributed to the feedwater from the heater secondaries is modeled using the heat structure energy source option. The piping was modeled by first calculating the applicable metal volume and then adding the equivalent metal thickness to the appropriate heat structure. Heat structures representing several components were combined and added to selected components in order to reduce computer storage requirements.

## 5.4 Integrated Control System

The B&W ICS controls all major portions of the NPP. A block diagram of the system is shown in Figure 5-7. The models used for this study were used for the pressurized thermal shock study

(Reference 4) and by B&W.<sup>e</sup> The modeled ICS consists of three parts: turbine bypass control, feedwater control, and EFW control.

The unit load demand and reactor control subsystems have not been modeled except to provide the demand signal for the feedwater control subsystem. The integrated master was not modeled except for the TBV control. All other portions of the feedwater control and turbine bypass control were representative of the ICS logic.

## 5.5 Initial Conditions

A steady-state calculation established consistent initial conditions representing full-power

e. Babcock & Wilcox Company proprietary information, 1985.

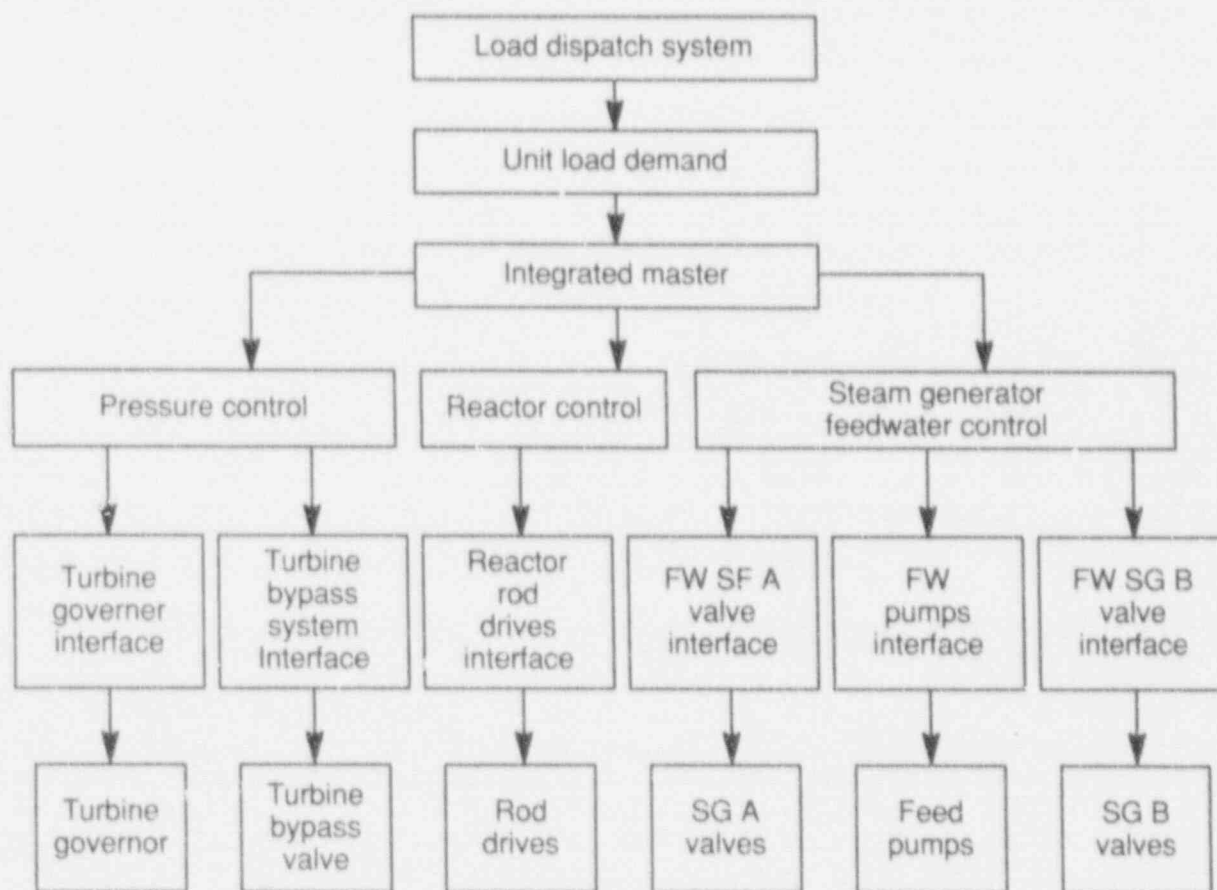


Figure 5-7. B&W ICS block diagram.

plant operation. The calculated steady-state conditions are shown in Table 5-1 compared with desired conditions. The desired conditions come from Reference 4. As indicated, the agreement is good. However, the code unrealistically calculated a small amount of liquid being entrained in the steam line. The liquid then evaporated in the steam line, thereby reducing the superheat. Because the calculated equilibrium steam super-

heat was too low, the calculated feedwater flow rate was about 4% larger than the actual flow. These steady-state conditions were used as the starting point for almost all the sensitivity runs. In two cases, the sensitivity parameter being studied affected the steady-state solution: interphase drag and steam generator heat transfer area. New steady-state solutions were calculated for these sensitivity runs.

**Table 5-1.** Comparison of desired and calculated initial conditions.

Parameter	Desired value	Calculated value
Primary:		
Core power (MW)	2,568	2,568
Average of hot and cold leg temperatures (°F)	578	581
Hot leg pressure (psia)	2,161	2,170
Pressurizer level (in.)	220	229
Hot leg mass flow rate (lbm/s)	19,404	19,216
Secondary:		
Steam generator secondary pressure (psia)	925	917.4
Liquid mass per steam generator secondary (lbm)	38,940	38,265
Feedwater temperature (°F)	460	460.5
Steam exit superheat (°F)	60	28.8
Feedwater flow per steam generator (lbm/s)	1,497	1,561

## 6. OPERATOR ACTIONS

For long-term accident scenarios such as this SBLOCA, the operator has many interactions with the system. From the first operator action at 107 seconds until the plant is in a stable HPI/break cooling mode 6,000 seconds later, the operator is interacting with the system as directed by the EOPs. Because there is human interaction with the system, a significant source of uncertainty is associated with these actions: which actions the operator will take and how long it takes the operator to perform them. A CSAU study requires that all major sources of uncertainty be accounted for; therefore, the effect of operator actions on the safety criteria must be considered. It is necessary then to have a basic understanding of the EOPs and to understand the technical basis behind them. The purpose of this section is to develop a basic understanding of the EOPs and their technical basis so that we can view the uncertainty associated with the operator's actions relative to uncertainties associated with other important parameters listed in Section 3, "Phenomena Identification and Ranking Table."

Section 6.1, "Technical Basis for Operator Actions," discusses the reasoning used to develop the EOPs. Sections 6.1.1 and 6.1.2 discuss the parameters the operator monitors and the elements of control that are available to the operator to recover from an abnormal plant condition. Section 6.1.3 gives a broad overview of the EOPs, showing the plant condition that causes the operator to enter the EOPs. Section 6.1.4 then elaborates on those procedures specific to this scenario. Thus, with the technical basis established and the operator actions selected, Section 6.2, "Implementing Operator Actions in the Model," discusses both the philosophy of selecting the appropriate operator action and how those actions were modeled with RELAP5/MOD3. Section 6.2.1 discusses the philosophy used to select the specific operator actions. Sections 6.2.2 and 6.2.3 then discuss how the model regulates the main plant parameters as discussed in Section 6.1.2.

### 6.1 Technical Basis for Operator Actions

EOPs for B&W NPPs are based on the symptom approach. Operators continually monitor plant parameters for signs of upset in heat transfer from the core. If an upset in heat transfer is suspected, the operator treats the symptom as EOPs direct. The following sections discuss how the operator uses monitored parameters to identify symptoms and how the EOPs direct the operator to treat the symptom once identified. Section 6.1.1 shows how parameters monitored by the operator are used to identify symptoms. The elements of control available for the operator to restore an upset in heat transfer are listed in Section 6.1.2. Finally, Sections 6.1.3 and 6.1.4 discuss how the EOPs direct the operator in treating the symptoms.

**6.1.1 Monitoring Parameters to Identify Symptoms of Upset in Heat Transfer.** Five key plant parameters are continually monitored by the operator for symptoms of upset in heat transfer from the core. The monitored parameters are

- Hot leg temperature
- Primary pressure
- Cold leg temperature
- In-core thermocouple temperature
- Steam generator pressure.

The symptoms of upsets in heat transfer are

- Lack of adequate subcooling margin
- Inadequate primary to secondary heat transfer
- Excessive primary to secondary heat transfer.



An important tool for identifying a symptom is a pressure/temperature trace, similar to the one shown in Figure 6-1, which is continually displayed in the control room on a cathode-ray tube. Hot leg and cold leg temperatures are plotted against primary pressure. To identify a symptom, the operator compares the current primary pressure and hot leg and cold leg temperatures to limits that are superimposed on the screen. These limits are

- Saturation line
- Subcooling margin limit
- Post trip window.

Primary temperature would not normally exceed the high temperature setpoint for reactor trip, thus the high temperature setpoint determines the maximum temperature boundary. The minimum temperature boundary is determined by the saturation temperature corresponding to the normal operating pressure of the steam generator

secondary side. Normally, primary pressure would not exceed the setpoint of the PORV. Therefore, the upper pressure boundary is determined by the setpoint of the PORV. The lower pressure boundary is determined by calculations and reviews of actual plant trips. The subcooling margin limit also describes a boundary for the posttrip window as shown in the figure.

Figure 6-1 shows the pressure/temperature traces following a normal reactor trip. Upon reactor trip, the hot leg temperature cools as core power is reduced and eventually reaches cold leg temperature. As the primary liquid cools, it shrinks, causing a depressurization. Pressurizer heaters will turn on to compensate for the pressure reduction, and the makeup pumps will compensate for the reduction in pressurizer level by supplying more flow. Eventually, pressure returns to its pretrip value, but the hot leg and cold leg temperatures stabilize near the saturation temperature of the secondary. Notice that the pressure/temperature trace remains entirely within the posttrip window.

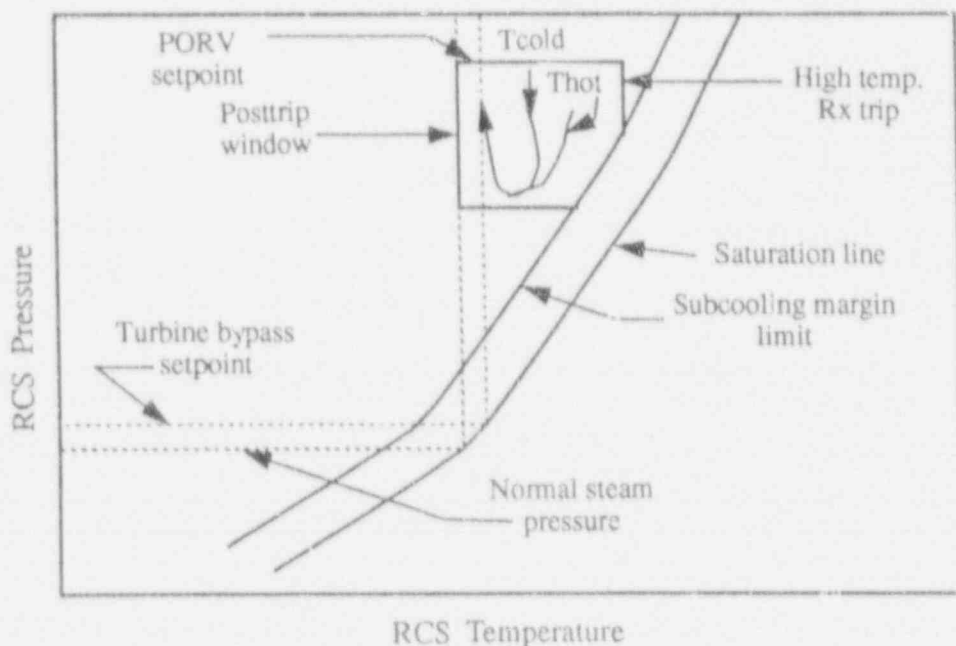


Figure 6-1. Normal P-T trace following a reactor trip.

The pressure/temperature trace of the hot leg for a loss of subcooling margin is shown in Figure 6-2. (The pressure/temperature trace of the cold leg is not included as it is of lesser importance in a SBLOCA.) It is readily apparent that subcooling is lost as primary pressure falls outside the posttrip window to the saturation line without the temperature dropping significantly. The primary pressure/temperature trace will continue to follow the saturation line unless subcooling margin is restored by the HPI system or the operator. Eventually, primary temperature will fall below that of the steam generator secondary. Unless the operator interacts to lower secondary saturation temperature, heat transfer to the generators will be lost. Operator actions specific to a loss of subcooling margin incident are discussed further in Section 6.1.4, "Emergency Operating Procedures for Loss of Subcooling Margin."

Figure 6-3 shows the pressure/temperature trace from the simulated SBLOCA, nominal case. Also shown in the figure is the posttrip window, the saturation line, and the subcooling margin

limit. Notice that in the posttrip window in this case, the pressure/temperature relation for reactor trip is more conservative than the subcooling margin limit. We see in the figure the pressure/temperature trace falling to the saturation line, rising as if subcooling margin were about to be regained, and then falling to the saturation line. To the operator, this is a clear indication of a loss of subcooling, and he or she will follow appropriate procedures to remedy that symptom.

**6.1.2 Elements of Operator Control.** Section 6.1.1 discussed how certain parameters are monitored and used by the operator to identify symptoms of upset in heat transfer from the core to the steam generators. Now we need to understand how EOPs direct the operator in remedying a symptom. Basically, heat transfer from the core to the steam generators is governed by controlling five parameters:<sup>f</sup>

f. Babcock & Wilcox Company proprietary information, 1985.

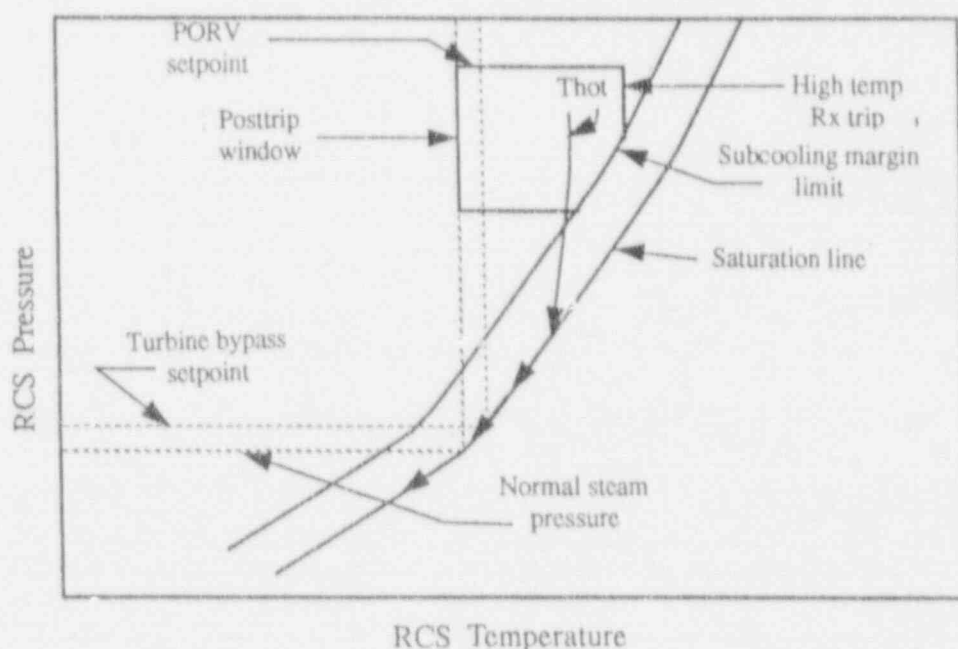


Figure 6-2. Pressure/temperature trace following loss of subcooling margin.

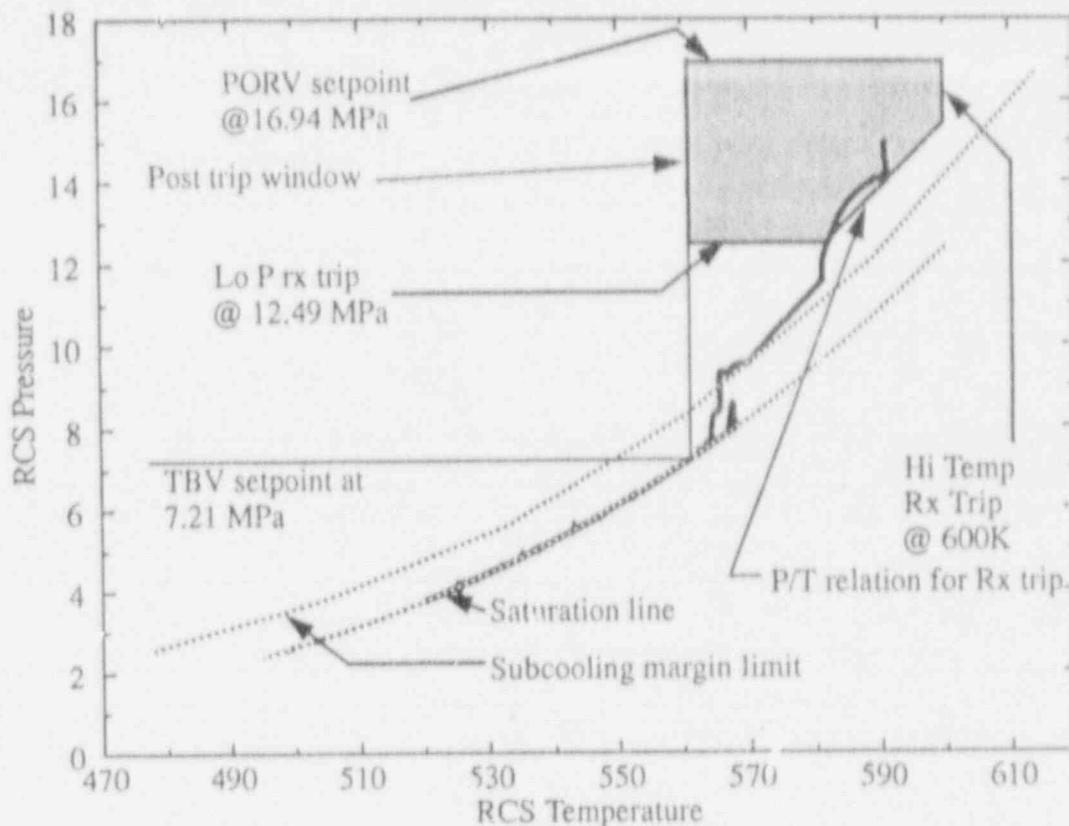


Figure 6-3. Pressure temperature relation for nominal case.

- Reactivity
- Reactor coolant inventory
- Reactor coolant pressure
- Steam generator pressure
- Steam generator inventory.

Each of these parameters can be controlled by the operator to some degree. The remainder of this section will briefly discuss how the operator controls these parameters for an SBLOCA.

Reactivity control is achieved by the shutdown rods, which is an automatic action. If this action fails, boron injection is available. However, this scenario postulates the shutdown rods insert as designed when the reactor trips; thus, no operator action is required.

It is essential to have enough reactor coolant in the primary system to maintain a flow path from the core to the steam generators. If sufficient reactor coolant is lost from the primary system, the liquid flow path to the steam generators will be interrupted as the hot leg level falls below the U-bend. Reactor coolant will not be able to communicate energy to the steam generators, and the potential exists for a core heatup. The operator has two means of controlling reactor coolant inventory: RCPs and ECCS. The operator must trip the RCPs. If the RCPs continue to run long after the break opens, there is a potential for uncovering the core if they are turned off later because the two-phase froth may collapse. Also, depending on location of the break, a running RCP may force inventory out the break. The operator can influence the rate that lost coolant is replaced by the ECCS. For this particular scenario, LPI does not actuate. Makeup/HPI pumps will automatically actuate, but soon thereafter the operator limits the flow, as directed by the EOPs, to prevent pump runout.

Maintaining a subcooling margin, hence high pressure, in the reactor is important, for if the subcooling is lost, a great possibility exists of forming voids in the primary system. These voids may collect in the U-bends of the hot legs and inhibit liquid flow through the loops as discussed in the previous paragraph. Also, performance of the RCPs is impeded as coolant cavitates in low pressure regions around the impellers. In short, losing the subcooling threatens the ability to cool the core. Therefore, the EOPs place a high priority on regaining the subcooling margin. For very small breaks, subcooling may be restored by repressurizing the primary system with HPI. However, this break is too large for HPI to repressurize, so actions must be taken to remove core energy from a saturated primary system. Section 6.2 discusses these actions.

Of all the plant parameters influenced by the operator, secondary pressure and inventory are the most affected. Secondary temperature is kept below that of the primary by maintaining secondary pressure lower than primary pressure. Since there are no automatic controls to do this, the operator must regulate TBVs to depressurize the secondary. EFW injection is used to increase secondary inventory above that of normal operation. This puts the thermal center of cooling at the highest point possible, thus maximizing the potential for natural circulation in the primary system. However, EFW cannot be injected too rapidly or it cause an excessive cooldown rate in the primary. EFW injection is not controlled by any automatic system and the EOPs do not specify the rate of EFW injection. Thus, its rate is left to the discretion of the operator. Also, since it supplies cold water into a steam space at the top of the generator, EFW injection serves to depressurize the secondary. Thus, EFW injection and secondary pressure relief via TBVs act together to control secondary pressure and inventory.

**6.1.3 Overview of Emergency Procedures.** Sections 6.1.1 and 6.1.2 discussed how an operator identifies a symptom of upset in heat transfer and the elements of control the operator uses recovering from a symptom. Now we can look at the procedures that direct the operator once he or she has identified a symptom. This

section will discuss the general strategy taken by the EOPs to treat the loss of subcooling margin. Section 6.1.4 will go into more detail about procedures specific to this SBLOCA scenario. Figure 6-4 is a flow chart that lays out the general strategy taken by the controlled EOPs.<sup>8</sup> Blocks that apply to this SBLOCA are denoted with bold lines. First, for this SBLOCA, the pressure/temperature relationship falls outside the posttrip window (Figure 6-3); therefore, the operator enters the flow chart from "Conditions exist for reactor trip." The first concern addressed by the EOPs is the reactivity of the core. EOPs direct the operator to verify that all shutdown rods are fully inserted after the reactor trip signal is generated. If they are not, the operator must take action to manually shut down the reactor. However, this SBLOCA does not require manual action from the operator to control reactivity.

Second, the operator must determine whether the secondary inventory and pressure are controlled. If the operator takes no action, main feedwater will run back and eventually shut off, turbine stop valves will automatically close, and TBVs will control secondary pressure to about 6.9 MPa. EFW injection will actuate and deliver maximum flow. These conditions are not ideal for an SBLOCA. Unthrottled EFW injection could cause overcooling problems in the primary. Also, TBVs automatically keep secondary pressure high. If primary pressure falls below secondary pressure, the steam generators can no longer remove heat from the primary system. To prevent these problems, secondary pressure and inventory must be manually controlled by the operator. EOPs direct the operator to throttle EFW and depressurize the generators so that a heat sink is always available as long as primary loop flow exists.

Third, if primary pressure and inventory are not controlled, as is the case for this SBLOCA, the operator must act. The operator will verify emergency safeguard actuation of the HPI pumps,

g. Babcock & Wilcox Company proprietary information.

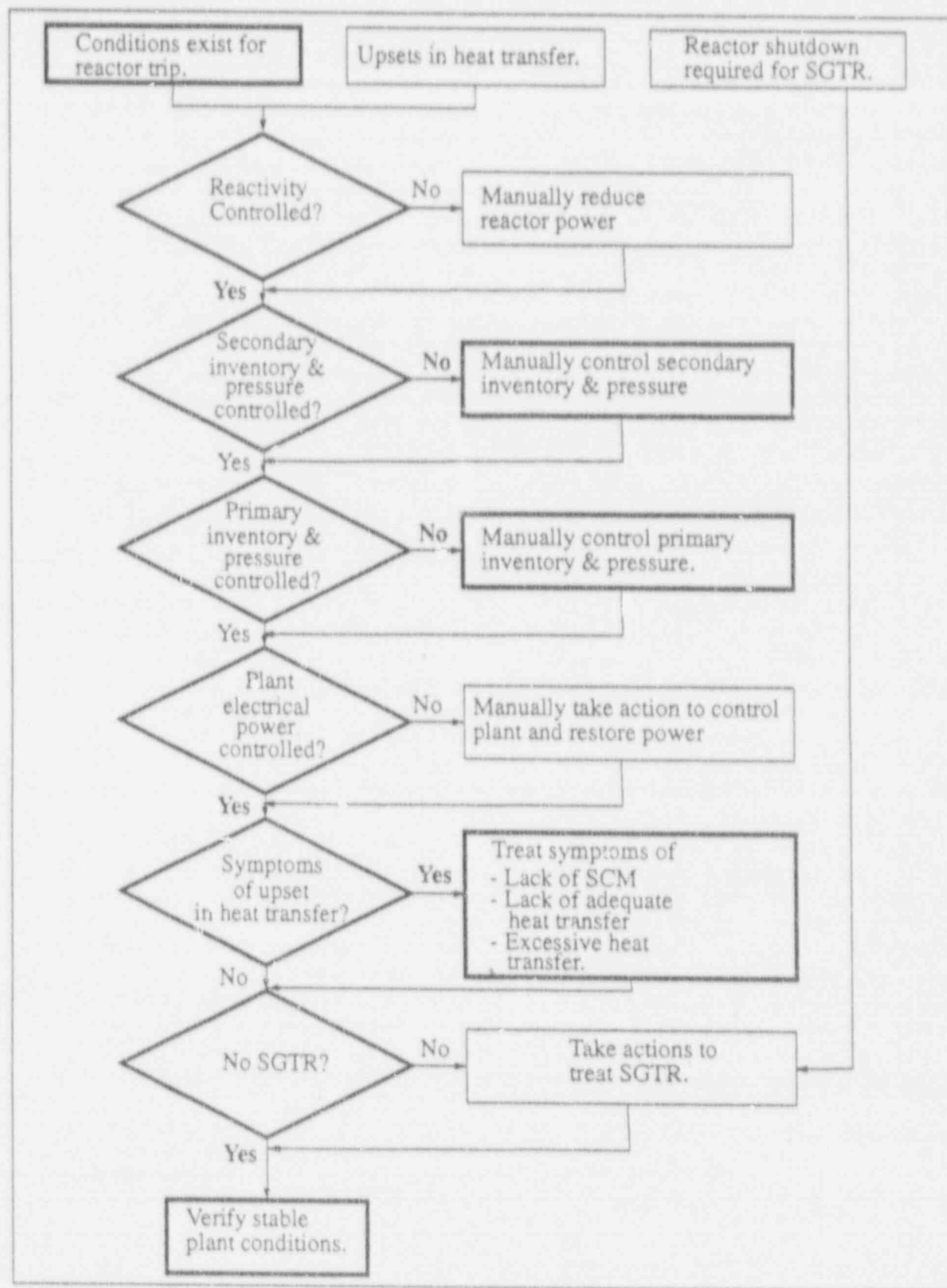


Figure 6-4. Flow chart for verification of vital systems status.



manually throttle them to prevent pump runout, and balance the flow in each HPI train to ensure that each reactor coolant loop receives the maximum HPI flow. To reduce the potential for core uncover, the operator will trip the RCPs immediately (within one minute) after subcooling margin is lost.

Fourth, electrical power output must be controlled. For this SBLOCA, electrical power is controlled automatically. Reactor trip automatically initiates a turbine/generator trip, which is postulated to operate as designed. Therefore, no operator intervention is required.

Identifying the symptom of upset in heat transfer is the fifth block. As mentioned in Section 6.1.2, loss of subcooling margin is easily identified as the pressure/temperature trace falls to the saturation line. Also mentioned in Section 6.1.2, the EOPs give top priority to treating the loss of subcooling margin. However, subcooling margin is lost early in the transient, so the operator has little time to respond to it. Automatic actions (letdown isolation, HPI actuation, and pressurizer heater actuation) occur quickly to try to regain the subcooling margin. There is not much more the operator can do but verify proper emergency safeguard actuations. However, later in the transient, symptoms of inadequate heat transfer will appear as voids accumulate in the U-bends of the hot legs, causing primary loop flow to be lost. The operator will respond to this as EOPs direct.

The last decision block is to determine whether a steam generator tube rupture exists. Since we are not postulating a tube rupture, we need not consider operator actions associated with it. Finally, the postulated scenario ends shortly after the core flood tanks begin to flow significantly into the downcomer of the reactor vessel. This inevitably depressurizes the primary system to the point where LPI can make up lost inventory and leads to a transfer to the residual heat removal system. Thus, when primary pressure reaches the pressure of the core flood tanks, we assume stable plant conditions are shortly ahead and end the calculation.

**6.1.4 Emergency Operating Procedures for Loss of Subcooling Margin.** This section will describe the operator actions chosen for this scenario. Explanations will be given for the actions and justification given for the choice of actions.

The operator will enter the EOPs immediately upon reactor trip (at 11.8 seconds on pressure/temperature relation) and begin verification procedures to ensure that all safety systems are actuated. The operator will then perform a series of manual actions and verification procedures to limit the primary inventory loss and to ensure that all appropriate safety systems have actuated. At about 47 seconds, the subcooling margin is lost, and the operator identifies this on the pressure/temperature display on the cathode-ray tube.

Once into the procedures for the loss of adequate subcooling margin, the operator will follow the pattern outlined in Figure 6-5. First, the operator will trip the RCPs. The reasons for this are twofold. First, loss of subcooling margin is a symptom of overcooling, which in turn may be a symptom of a break. If a break exists, the RCPs may be pumping water out the break. Therefore, it is best to shut them off. However, past analyses have shown that if the RCPs are not turned off within two minutes after the loss of subcooling margin, it is necessary to leave one RCP in each loop running to limit the chance of level depression in the core as the two-phase mixture in the loops settle. Documented simulator runs show that the operators are very likely to trip the RCPs within one minute after the loss of subcooling margin. Therefore, we assume in this model the operator trips the RCPs one minute after adequate subcooling margin is lost. Thus, it is not necessary to leave any RCPs running. Second, if subcooling margin is lost, the RCPs may cavitate as pressure is reduced around the tips of the rotor blades, causing voiding to occur. Therefore, one must trip the RCPs to prevent damage.

Next, the operator will take actions to control primary inventory. Tripping the RCPs is one aspect of this and has already been discussed.



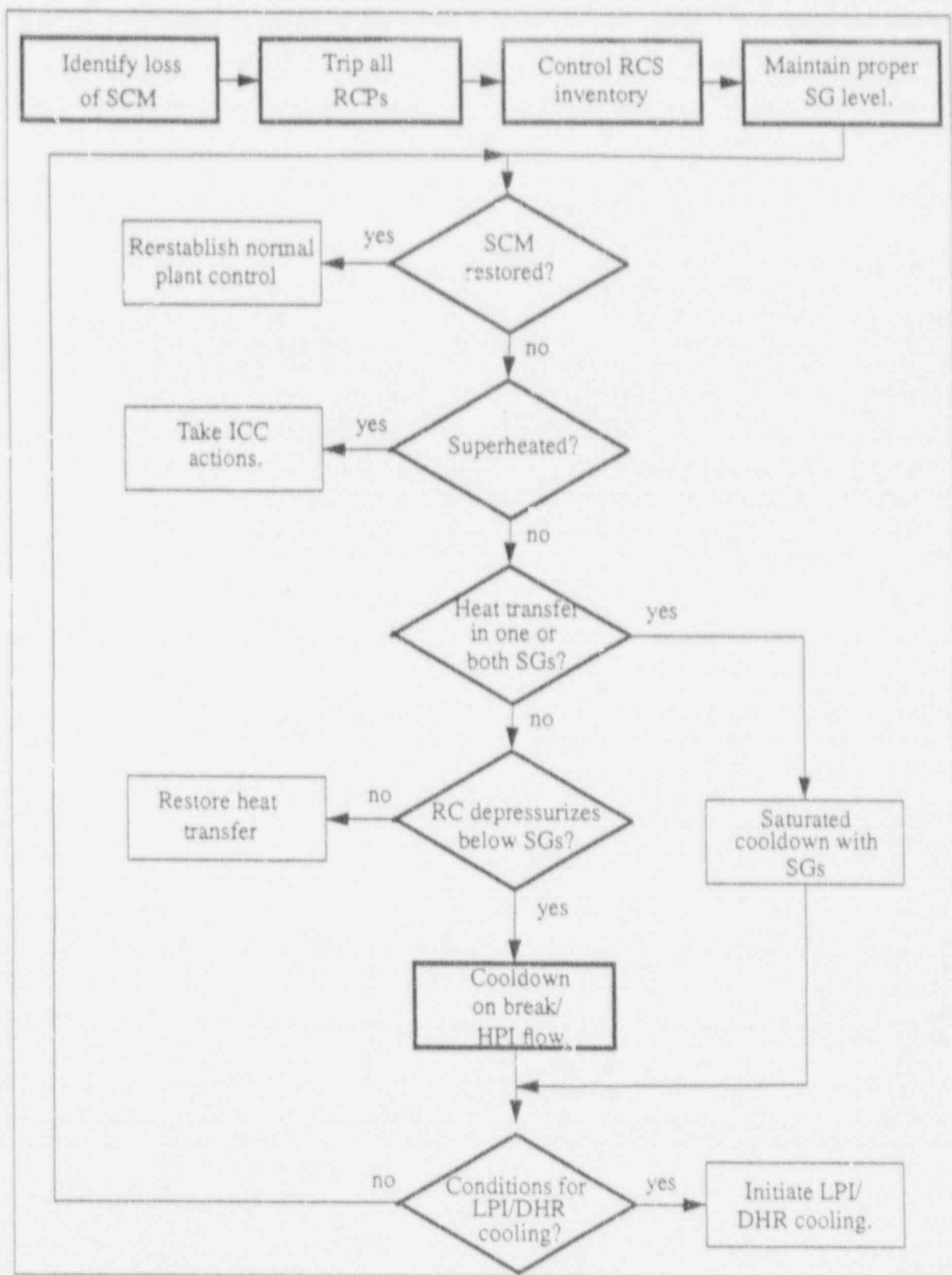


Figure 6-5. Strategy for mitigating a loss-of-subcooling margin.

Further actions to control inventory include isolating letdown lines and verifying that the HPI system actuated. Since we assume no failures except for one HPI pump in our scenario, these procedures require only that the operator verify that automatic actions have occurred. HPI automatically actuates and injects at full capacity. The operator will take manual control of the HPI system and throttle the flow to prevent pump runoff.

The next step is to increase the potential for natural circulation by raising the thermal center of the steam generators. This is accomplished by filling the secondary sides of the generators to just below the aspirators (95% operating range). In order to do this, the operator must manually reset the level setpoint from 50% operating range to 95% operating range. We assume the operator performs this task at the same time he or she trips the recirculation pumps. The basis for this is that the only means for loop flow after the RCPs are tripped is natural circulation. The operator realizes this and simultaneously increases the level setpoint for the steam generators as he or she trips the RCPs.

Next on the flow chart (Figure 6-5) is a decision block for determining whether the subcooling margin has been restored. Note that the operator does not pass through this diagram only once; rather, he or she continually monitors the plant condition, ready to initiate another set of procedures if the situation dictates. If the break is small enough, HPI could restore the subcooling margin. However, the break for this scenario releases more water from the system than the HPI is able to replace. Thus, pressure continues to decrease, and subcooling margin is not ever restored for this transient. Thus, the operator cannot reestablish normal plant control and must continue through the procedure.

The next decision block is to determine whether the core exit is superheated. For this particular scenario, the core exit never dries out such that superheated steam is produced. Therefore, it is never necessary to initiate actions for inadequate core cooling. The operator proceeds to determine whether heat transfer is lost in the

steam generators. This decision is not nearly so straightforward as the previous decisions were. Determining whether or not the steam generators are transferring heat is a largely subjective process on the part of the operator. This decision will depend upon the operator's experience and simulator training. There are no rules for determining whether steam generator heat transfer is lost; the EOPs leave the decision up to the operator.

From discussions with operator examiners at the INEL who were formerly senior reactor operators at B&W type nuclear power plants, Figure 6-6 was developed. Figure 6-6 indicates a typical sequence an operator might perform to determine whether steam generator heat transfer is lost or not. Notice that all of the decision blocks contain subjective decisions (shown underlined). The operator will make judgements based on the trends of these parameters. Because determining steam generator heat transfer is so subjective in nature, a control model cannot easily be developed for RELAP or any code. So rather than try to model the logic within the confines of RELAP, we ran the simulation up to the point where a decision was required concerning steam generator heat transfer. We then showed the operators plots of the variables indicated in Figure 6-5 and asked each of them independently to make a judgement as to whether they would determine that steam generator heat transfer is lost. Each of them stated that they would conclude that heat transfer is probably lost based on the subcooling margin not being regained and the primary pressure increasing. However, it was difficult to make a concrete decision because many of the trends the operator would look at require operator action to be established. For example, the last decision block looks at the trend of the difference in primary to secondary temperature difference as the operator lowers secondary pressure. However, the simulation had not proceeded to the point where the operator had done anything on the secondary side to reduce the pressure. Therefore, it was impossible to determine whether the primary to secondary temperatures diverged or not. However, the operators noted that even if steam generator heat transfer were lost, they would not likely make any attempts to restore it if the core exit

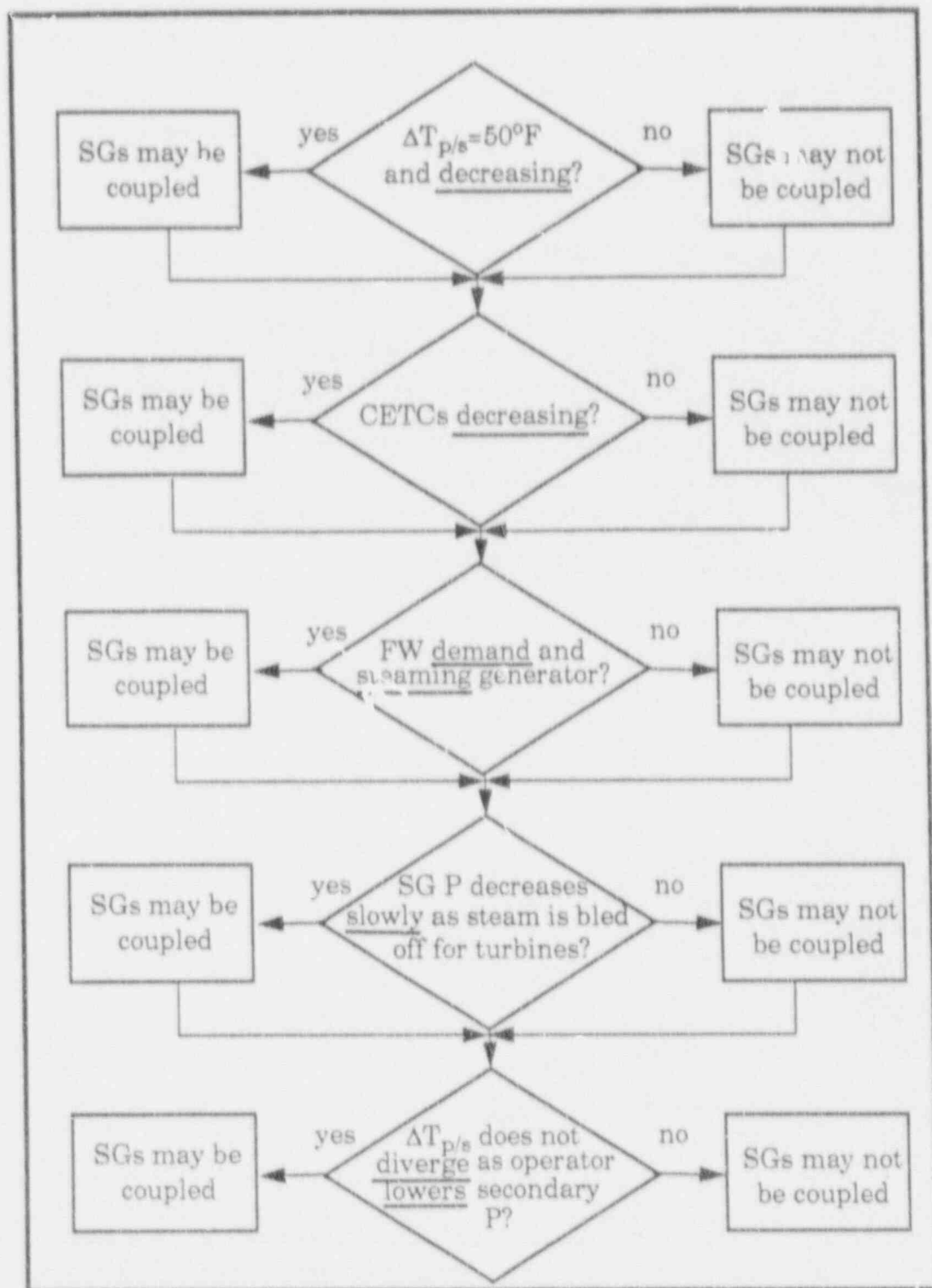


Figure 6-6. Steam generator heat transfer flow chart.

thermocouples indicated decreasing temperature and the subcooling margin were not restored. The reason for this is that in order to restore heat transfer, the first step is to restore circulation via the RCPs.

As mentioned earlier, the RCPs could be damaged if started with no subcooling margin. Therefore, they are prohibited from starting by the equipment protection system. To restart them would require the operator to manually disable the RCP protection system. So, if the plant does not appear to be in danger, the operator will not likely override the RCP protection circuits.

In this simulation, the plant is apparently in no danger since the core exit thermocouples indicate decreasing temperature and the primary pressure is also decreasing. As the simulation proceeded through the procedures, assuming loss of steam generator heat transfer, the operator's suspicions of loss of steam generator heat transfer were confirmed. As the TBVs opened, secondary pressure fell rapidly while primary pressure remained unchanged. In a design review where the modeled actions and the plant response to them were presented for acceptance by operators, they agreed that the operator would indeed have determined that steam generator heat transfer was lost.

To determine the next path to take through the operator actions, the operator must determine whether the primary coolant is depressurizing below the normal operating pressure of the secondary. If the answer is yes, this would indicate that the RCS is cooling even though steam generator heat transfer is lost. Thus, there is no need to restore heat transfer in the steam generators. This supports the idea mentioned above that even if heat transfer is lost in the steam generators, the operator will not try to restore heat transfer so long as subcooling margin is not regained and the RCS pressure does not increase.

For the nominal case, one can see in Figure 6-7 that primary pressure increases after the initial depressurization. However, the pressure maximizes and begins coming down soon after the break opens (about 6 minutes after break initia-

tion). After consulting with the operators, we concluded that this was too soon for the operator to realize and act upon the repressurization. It is likely that by the time the operator realized RCS pressure was increasing, RCS pressure would have already been headed steadily downward.

Now that the operator has established that the RCS is cooling even without the steam generators, he or she is instructed to proceed with cooling the plant on HPI and break flow. These procedures call for maintaining RCS liquid inventory with HPI and reducing pressure via venting if necessary. For this scenario, venting is not necessary because the high quality break flow is adequate to depressurize the RCS.

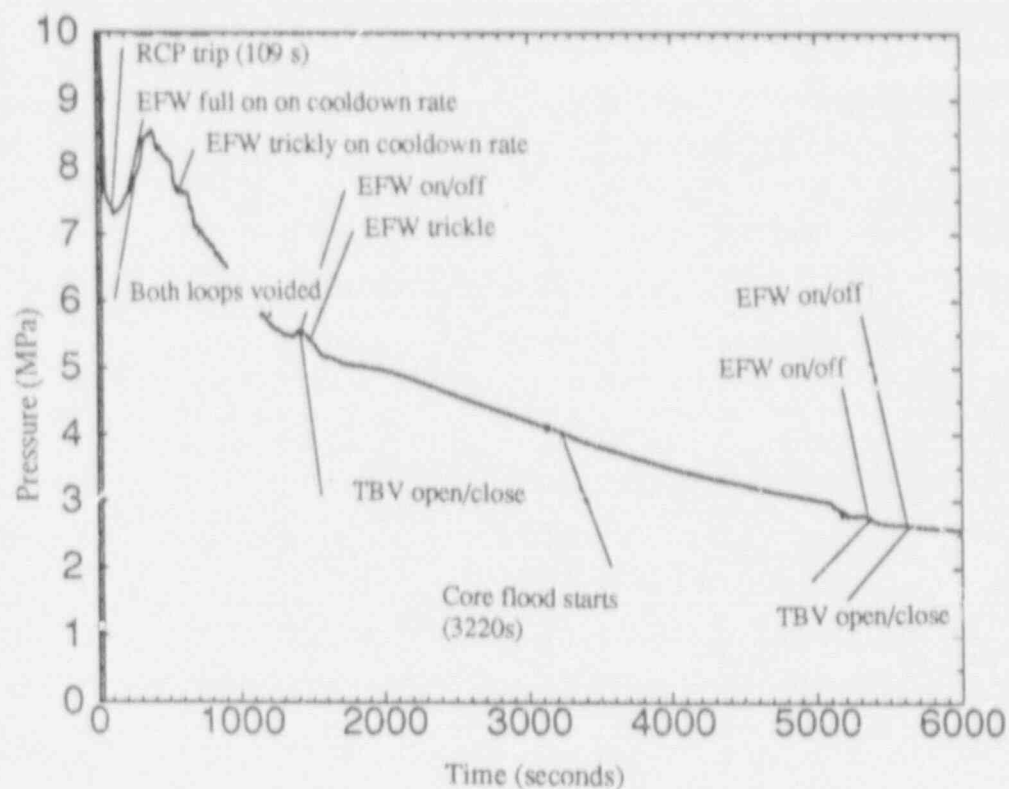
The simulation ends as accumulator flow supplies the core with liquid and begins to set the RCS up for cooling via HPI or the decay heat removal system. At 6,000 seconds, the accumulator has depressurized the RCS via condensation of the steam in the upper part of the downcomer and in the upper plenum as steam is drawn through the RVV to be condensed by the accumulator liquid flow. Thus, system pressure is decreasing at the same time liquid inventory is increasing, and the plant is on its way to a controlled cooldown with LPI and or decayed heat removal.

## 6.2 Implementing Operator Actions in the Model

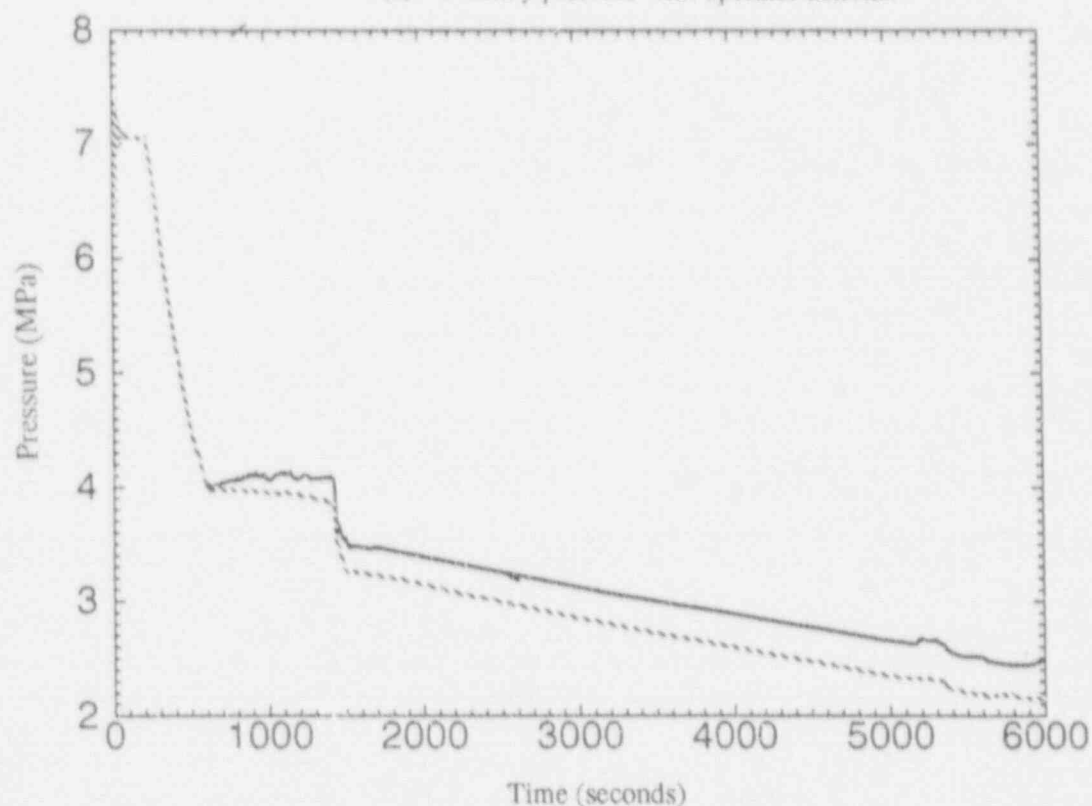
The input deck for the SBLOCA was modified in a way that the operator actions would be simulated in the model. The modeled operator actions were selected based on the EOPs and numerous consultations with operators. The following sections describe how each operator action was implemented into the model. For this scenario, we are concerned with only two aspects of the operator control as listed in Figure 6-4: secondary inventory and pressure control, and primary inventory and pressure control.

As stated before, reactivity is controlled automatically via SCRAM. Likewise, plant electrical

# Operator Actions



(a) Primary pressure with operator actions.



(b) Secondary pressure for nominal case.

Figure 6-7. System pressure history.



power is automatically controlled via turbine trip. This scenario assumes that these systems function as designed, therefore the operator does not intervene but merely verifies the automatic actuations. The verification procedures need not be modeled. The symptom of lack of subcooling margin will be treated by manually interacting with the plant to control primary and secondary inventory and pressure and secondary inventory and pressure. This manual interaction from the operator is modeled and is discussed below.

### 6.2.1 Philosophy for Selecting Operator Actions.

The operator actions for this scenario were selected based on close communication between thermal-hydraulic analysts and personnel at the INEL who have been operators at B&W-designed NPPs. The analysts prepared the simulation based on EOPs (which are subject to interpretation), and presented the results to the operators for their opinion as to whether the simulated action would indeed be performed by an operator given this scenario.

For actions in question, operators and analysts discussed and agreed that the questionable actions simulated are technically sound with respect to the EOPs, but some simulated actions may not be taken given the operator's training and subjective decisionmaking. (The EOPs are subject to interpretation and are written to allow the operator some freedom for subjective judgement. One cannot acquire hard numbers for the timing of actions or the setpoints at which an action should occur. Thus, EOPs should be thought of as guidelines and not requirements.) These differences are pointed out in greater detail in later subsections. This CSAU demonstration project relies on a best estimate approach to simulating the SBLOCA. Because the role of the operator is very significant in the way the transient progresses, the operator must be modeled. However, we are not treating the operator actions as an uncertainty parameter, as mentioned already in Section 1. Rather, we are modeling the operator as best as we can estimate and including those actions as part of the scenario definition. So, the operator actions are just as much an integral part of the scenario as the break size. Altering the operator

actions in any way from those presented here would constitute another scenario and require a separate CSAU analysis.

### 6.2.2 Primary Inventory and Pressure Control.

The first thing the operator will do after identifying the loss of subcooling margin is trip the RCPs. As previously discussed, the operator must trip the RCPs within two minutes of loss of subcooling margin to avoid possible core damage that may result from excessive voiding of the core during a LOCA after the RCPs are tripped. Thus, tripping the RCPs is the first action in the procedures. This simulation assumes that the operator trips the RCPs one minute after the loss of subcooling margin. This assumption is based on responses from several simulator runs in which adequate subcooling margin was simulated. Every operator responded within one minute.

The next concern the operator will have is to control the net inventory loss as much as possible. Automatic isolation of the letdown lines will prevent avoidable losses from the RCS. The HPI system will automatically actuate on low pressure. However, the HPI will deliver flow to the RCS at the maximum rate possible, thus running the risk of damaging the HPI pumps by pump run-out. Therefore, the operator is instructed by the EOPs to throttle the flow to a maximum of 1.9 cubic meters per minute (500 gpm). The pressure versus flow curve that was in the model was very similar to the one given in the EOPs and was left unchanged (see Figure 6-8). Figure 6-8 shows the 1.09 m<sup>3</sup> per second limit as compared to the curve input to the model. This limit was not changed because we did not expect the RCS pressure to fall below approximately 3.6 MPa for this transient, although it did for the last approximately 1,000 seconds. There is no effect on the final conclusion of uncertainty because the minimum reactor vessel level occurred at 1,375 seconds, far before the RCS reached 3.6 MPa at 5,000 seconds.

### 6.2.3 Secondary Inventory and Pressure Control.

Secondary inventory and pressure is controlled by three means: resetting the



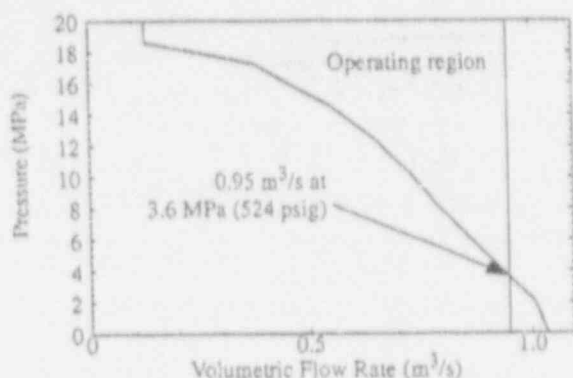


**Figure 6-8.** HPI volumetric flow rate per line with one HPI pump running.

secondary level setpoint, regulating EFW flow, and regulating turbine bypass flow. Each of these three elements is discussed below.

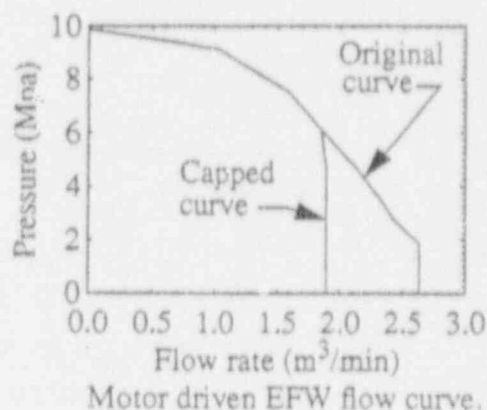
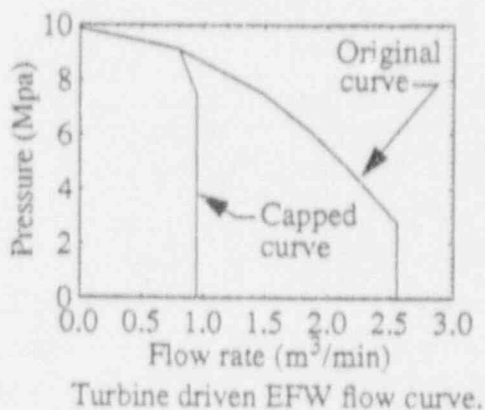
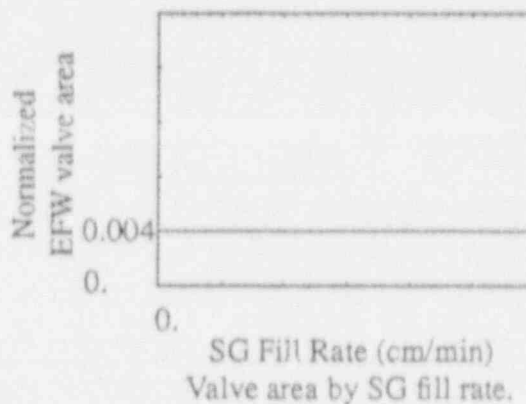
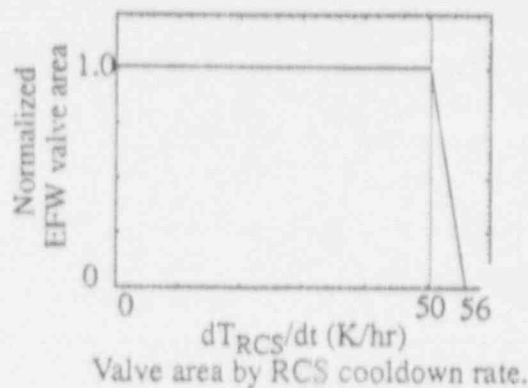
EOPs instruct the operator to raise the level setpoint for the steam generator secondaries to 95% on the operating range. This is to increase the thermal center of cooling for the loop in order to establish the greatest possible natural circulation after the RCPs are tripped. Resetting the setpoint is a simple matter for the operator and is assumed to happen immediately upon RCP trip. The operator would supposedly realize as soon as he or she tripped the RCPs that in order to maintain the maximum possible loop flow with no RCPs, he or she must maximize natural circulation, thus raising the level setpoint to 95%. In the model, the setpoint was changed from 50 to 95%. There was no need to link the time for resetting the setpoint to the operator tripping the RCPs because in scoping runs we found that the steam generator level is far below the 50% setpoint when the operator trips the RCPs and supposedly resets the setpoint. Thus, there is no period in the transient when the steam generator would fill to 50% and remain at that level until the operator reset the setpoint to 95%. That is to say, when the steam generator fills, it continues to fill continuously until it reaches 95%. EFW is automatically actuated on RCP trip and will flow at the maximum rate until the operator takes manual control of it. The model allows the EFW to come on at maximum flow, but the operator immediately throttles the flow

knowing that excess EFW will aggravate the overcooling situation. According to the EOPs, the operator must control the EFW flow to three limits:

1. The RCS cooldown rate: less than 56 K/hr (100°F/hr)
2. Maximum flow: 1.9 m³/s (500 gpm), to prevent pump runout
3. Minimum flow: what is necessary to maintain a filling rate in the steam generators of at least 5.1 cm/min (2 in./min).

EFW flow is controlled by two means in the model: (a) by limiting the maximum flow allowed through the time-dependent junctions representing EFW pumps and (b) by throttling the EFW valve (Valves 854 and 954).

The limit on RCS cooldown rate was satisfied by calculating a normalized valve area that would ramp EFW flow off as the cooldown rate approached the 56 K/hr limit. The slope of the ramp chosen was arbitrary, selected such that the model performed reasonably well—that is, the secondary behavior was stable with few oscillations in EFW flow rate as RCS cooldown rate approached 56 K/hr. The maximum flow limitation was imposed by simply capping the pressure versus flow curves at the appropriate flow rate. The two motor-driven EFW pumps are modeled with two time-dependent junctions. The pressure versus flow curves for these junctions was simply capped at the maximum flow rate. The turbine-driven EFW pump is modeled with two time-dependent junctions, each of which supplies one steam generator with half the capacity of the turbine-driven EFW pump. Thus, the pressure versus flow curves for these two junctions is capped at half the maximum flow allowed for the turbine-driven EFW pump. The minimum flow requirement was met by not allowing the valve to completely close. With trial runs, it was found that a normalized valve opening of 0.004 would allow enough EFW to maintain the required filling rate of 5.1 cm/min. Figure 6-9 illustrates how the normalized valve area was calculated and how



$$\text{EFW normalized valve area} = \max (A_{\text{cooldown}}, A_{\text{fill rate}})$$

Figure 6-9. EFW flow control.

the pump flow was limited. The EOPs instruct the operator to regulate turbine bypass flow to satisfy three limits:

- Maintain the cooldown rate of the RCS at less than 56 K/hr (100°F/hr).
- Maintain tube-to-shell temperature difference at less than 56 K (100°F).

- Maintain the primary to secondary saturation temperature difference between 22–33 K (40–60°F). To achieve these limits, a normalized valve area was calculated for each of the limits. The minimum area calculated was then selected for the TBV area.

Figure 6-10 shows in more detail how the TBV area was calculated. Section 8 discusses the response of the system due to these actions.

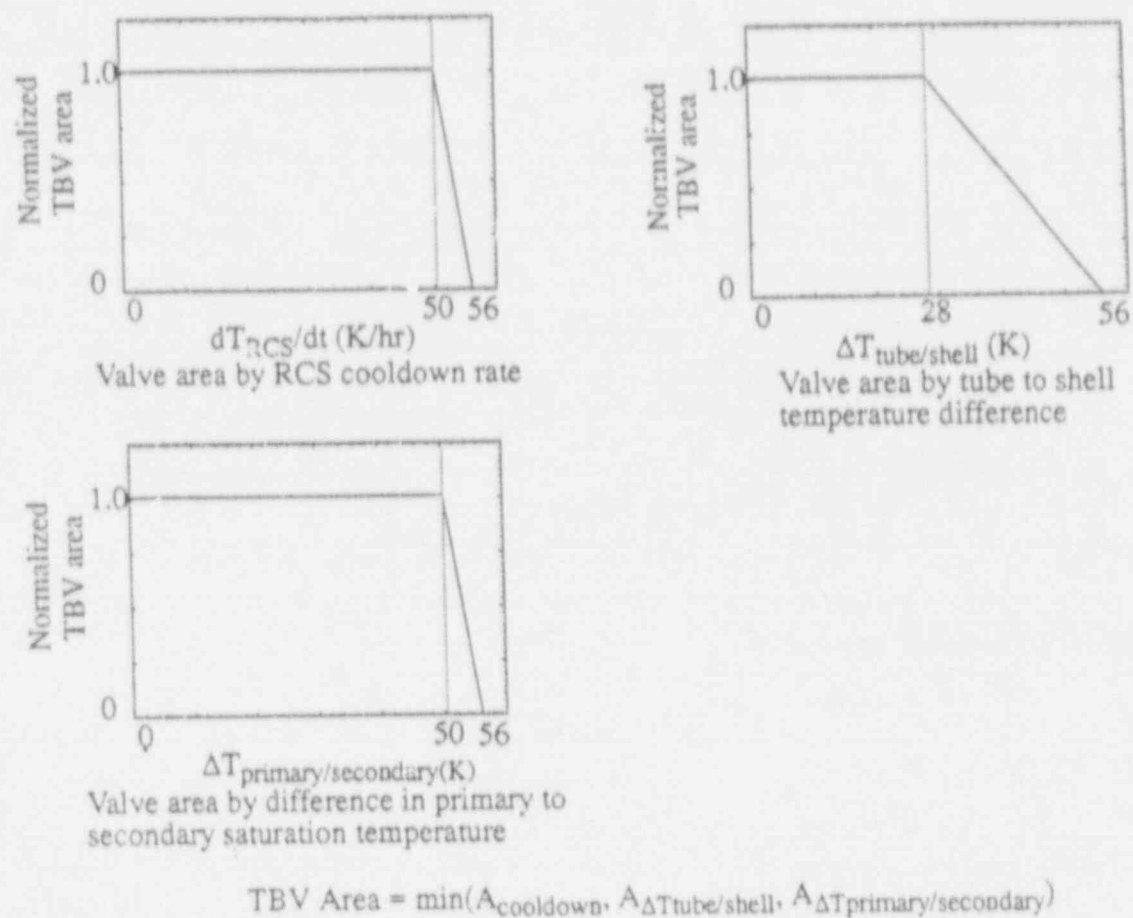


Figure 6-10. TBV area control.

## 7. RANGING OF PARAMETERS

In Steps 9-11 of the CSAU process (see Figure 1-1), the uncertainty with which phenomena contributes to the simulation is evaluated. The PIRT lists in order of importance the phenomena that are believed to participate in the transient (Reference 3) and allows us to choose the phenomena believed to most strongly affect the PSC (the minimum liquid level in the reactor vessel). The eight phenomena from this PIRT regarded as highly important are

- Break flow
- Natural circulation
- Decay power
- RCP performance
- HPI temperature
- Steam generator heat transfer
- Phase separation in the U-bend
- RVVV performance.

### 7.1 Important Phenomena and Key Code Parameters

The phenomena as such do not appear in the code (e.g., there is no natural circulation model). However, there are parameters, models, and inputs that are used to represent those phenomena. Section 4 of this document identifies the key code parameters or models associated with each phenomenon and the aspects of models that contribute the most to uncertainty (Table 4-1).

The models can be of three different kinds: (a) first principles or mechanistic models, (b) empirical correlations, and (c) input parameters or tables (some may be combinations of these). Table 7-1 lists the important phenomena, the key code parameters, and the type of model used to represent each phenomenon. Later, these

classifications will be used in evaluating uncertainty.

Break flow, the most important of the phenomena, is modeled in the code from first principles (Reference 4). The uncertainty of the break flow representation can be traced to the uncertainty about the exact geometry of the flow at the break. To allow for this uncertainty, RELAP5/MOD3 allows the user to modify the flow with break discharge coefficients. Natural circulation depends on the interactions between the liquid and vapor phases. This interaction is modeled using an empirical correlation (Reference 6) to produce an interphase drag coefficient  $F_I$  as a function of void fraction, flow regime, and relative velocities between the phases.<sup>9</sup>

This is also the way in which Phenomenon 7, "Phase separation in the U-bend," is represented. Decay heat is given by the user as tables of power versus time. Heat structures representing fuel rods use these tables to determine how much energy to deposit into the system. The uncertainty of decay power depends on the fuel burnup history and power distribution. The RCP performance is a mechanistic model for which the user inputs several coefficients to capture pump coast-down characteristics. The primary source of uncertainty was estimated to be the coefficient of torsional friction. The ECCS flow is reduced to an input value, temperature. HPI flow is limited by the operator to prevent pump runout. Thus, the real uncertainty is in the temperature of the water in the makeup tank. This variable depends on the weather, and its variation is bounded by technical specifications between 275 K (35°F) and 316.5 K (110°F). The steam generator heat transfer is calculated according to several empirical heat transfer correlations. The uncertainty of this model is then evaluated according to the uncertainty of the correlations. The RVVV is also a mechanistic model for which the user must input all the parameters. It was estimated that the inertia of the valve is the major contributor to the uncertainty of its performance; thus, it is the key parameter chosen for the sensitivity studies.

**Table 7-1.** List of important phenomena during an SBLOCA, their rank, the code parameter that RELAP5/MOD3 uses to represent them, and the type of model.

Phenomena	Key (code) parameters	Type
Break flow	Subcooled discharge coefficient 2- $\phi$ : Discharge coefficient	First principles
Natural circulation	1-f: RCP torsional friction coefficient 2- $\phi$ : Interphase drag coefficient	Empirical
Decay heat	Input table or function	User input
RCP performance	RCP torsional friction coefficient	Mechanistic-user input
ECCS flow	Input temperature	User input
Steam generator heat transfer	Coefficients from heat transfer correlations (area)	Empirical
Phase separation in the U-bend	2- $\phi$ : Interphase drag coefficient	Empirical
RVVV performance	Inertia of the valve	Mechanistic-user input

Table 4-2 lists the available assessments that may be used to evaluate the accuracy of the code in representing these phenomena. However, in many cases the usefulness of the assessment is limited to the comparison of trends and the prediction of important events during the experiment. One concludes from these assessments that RELAP5/MOD3 adequately describes the phenomena, but a quantitative measure of accuracy cannot be readily obtained from them. The following sections state the uncertainty for each phenomenon and describes the processes followed.

## 7.2 Evaluation of Uncertainty

This classification is important because it determines the way in which the uncertainty can be evaluated. It would be ideal if assessment against separate experiments existed for all important phenomena, thus yielding a measurement of accuracy of the code for each phenomenon. However, this is not the case for any of the

phenomena except break flow. Therefore, a different strategy must be developed.

**7.2.1 Break Flow.** RELAP5/MOD3 has two critical flow models that are used in simulating the break flow: single-phase flow and two-phase flow. These models are described in detail in the code documentation.<sup>10</sup> Both models are derived analytically from first principles. These models are assessed against two separate effect tests, of Marviken 22, and Marviken 24. The experimental data and results from the assessment calculations were obtained from the RELAP5/MOD3 code developers to be used in support of this CSAU effort. Therefore, we did not need to re-perform the calculations. However, this is not a repetition of the assessment shown in the code documentation (see Reference 10), for we processed the data to arrive at a bias and uncertainty of the critical flow models in RELAP5/MOD3. The diagrams in Figure 7-1 are schematic descriptions of the break configuration and the Marviken test vessel.



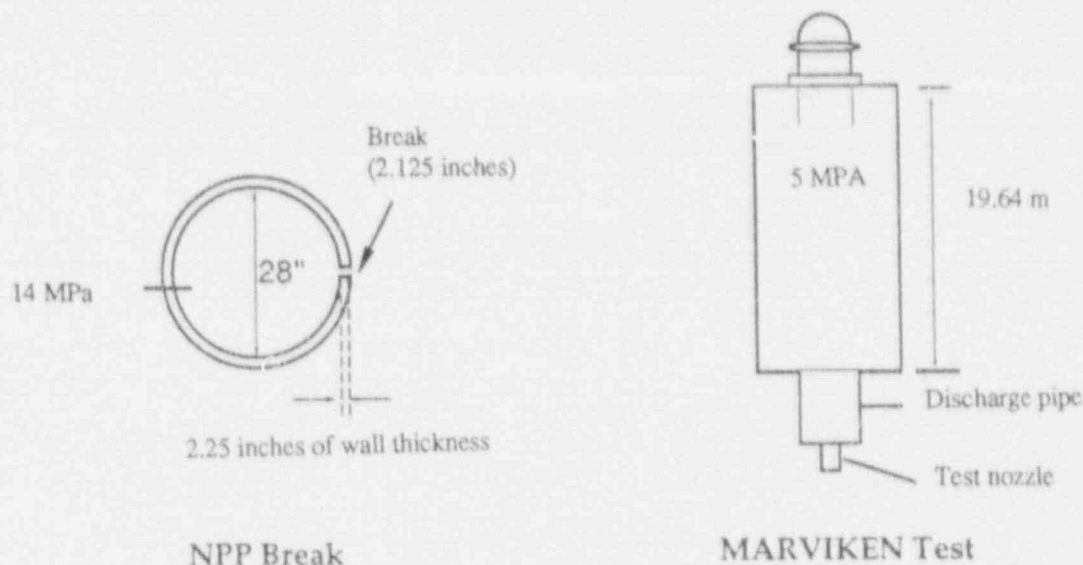


**Figure 7-1.** Schematic descriptions of the simulated break in the NPP and the Marviken test configuration.

The most relevant differences between the test configuration and the simulated break geometry are the size of the break openings and the fact that the nozzle in Marviken is aligned with the main flow direction (downward), while the break flow in the NPP is perpendicular to the main flow direction (sideways). The length to nozzle diameter ratio for the tests and for the assumed break compare as follows.

Figures 7-2 through 7-4 show the comparisons between the test results and the corresponding RELAP5/MOD3 simulations. The usual statement that the code captures the trends and the main events of the transient can be made here based on these comparisons (that statement is in fact made in Reference 10). However, to evaluate the uncertainty of the model, this is not sufficient. The inadequacy of direct comparisons can be deduced from Figures 7-2 and 7-3. These figures imply that RELAP5 underpredicts the flow. By simply looking at the plots, the error seems small. However, when measured, the predicted mass flow is more than 60% lower than the test value. Further inspection shows that the simulated pressure initially decreases faster than experimental pressures (Figure 7-4) and later remains at a higher level.

Figure 7-5 shows the Marviken 24 test histories of pressure and density, indicating a much smaller

variation in density than in pressure throughout the transient. This observation is used to support the assumption that the pressure is dominating the behavior of the flow. It is expected that other variables, such as temperature, also have an effect in the mass flow. However, given the limited information available and the trend suggested by Figure 7-5, the assumption that pressure is dominant is reasonable. Figures 7-6 and 7-7 show the comparison of mass flow versus pressure for both test cases. The figures reveal that at high pressure, when the fluid is subcooled, RELAP overpredicts the mass flow; while at low pressures, during two-phase flow, the simulation underpredicts the actual flow. The accuracy of the code representing critical flow and therefore the break flow can then be measured from these plots. The error is defined as

$$\text{Error} = (\text{prediction} - \text{measurement}) / \text{measurement}$$

and is measured in each of the flow regimes. Figures 7-8 and 7-9 are plots of the error versus pressure for 1- $\phi$  and 2- $\phi$  flow. It is clear from Figures 7-8 and 7-9 that the error can be characterized with a bias and some statistical distribution. It was assumed that the error had a normal distribution. The assumption was verified with a normality test.<sup>11</sup> Figures 7-10 and 7-11 show the normality test performed on the error data



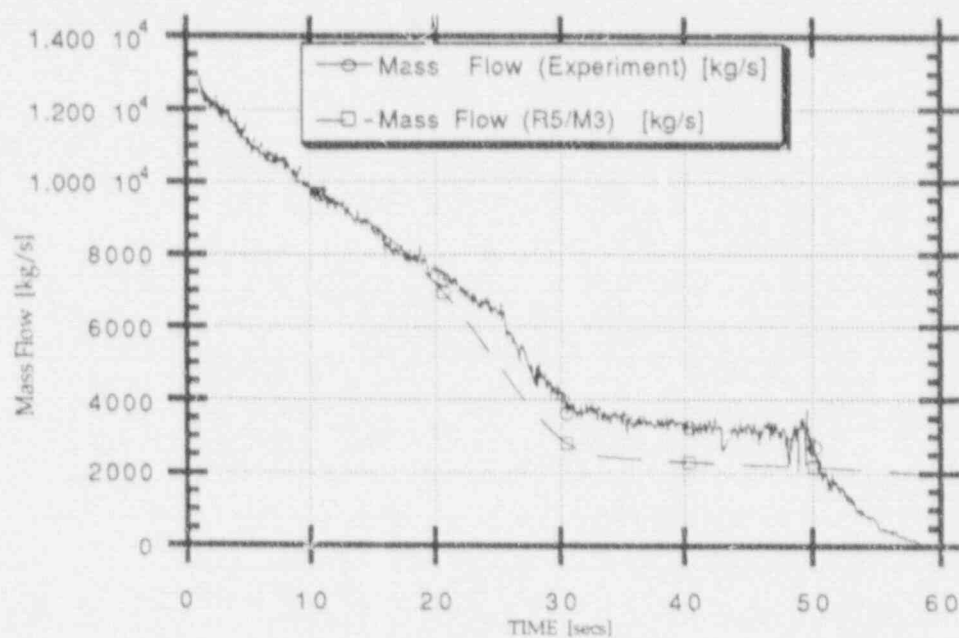


**Figure 7-2.** Comparison of experimental mass flow and RELAP5/MOD3 calculation in the Marviken 22 experiment.

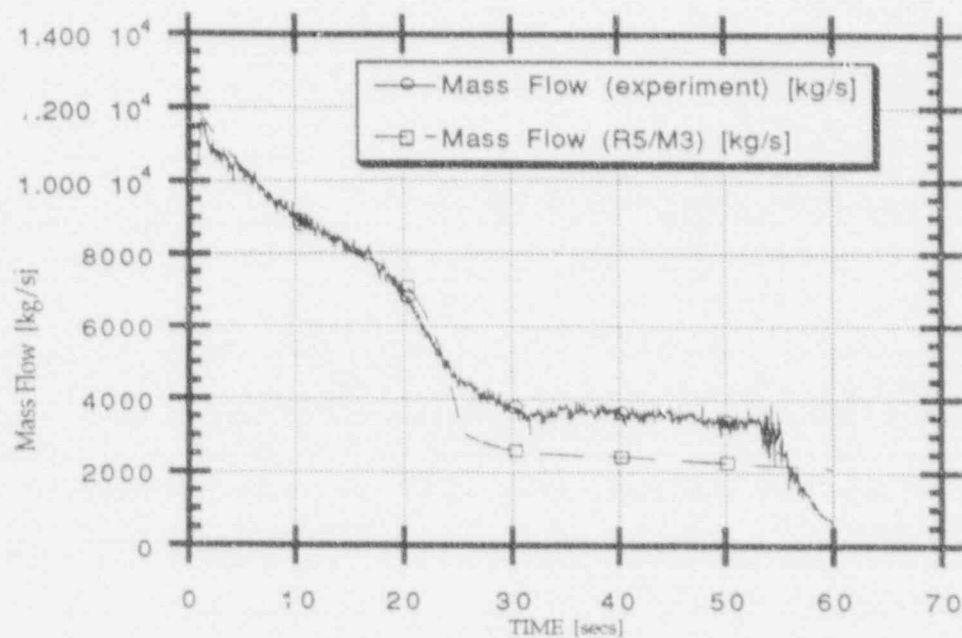


**Figure 7-3.** Comparison of experimental mass flow and RELAP5/MOD3 calculation in the Marviken 24 experiment.

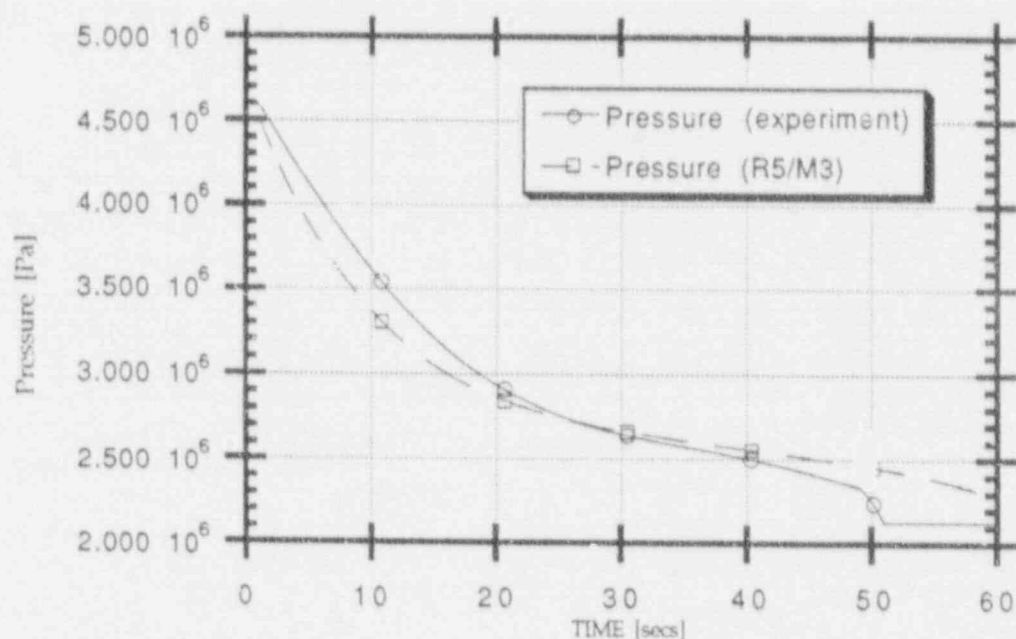


Figure 7-4. Comparison of experimental measurements of pressure and RELAP5/MOD3 calculation in the Marviken 22 experiment.

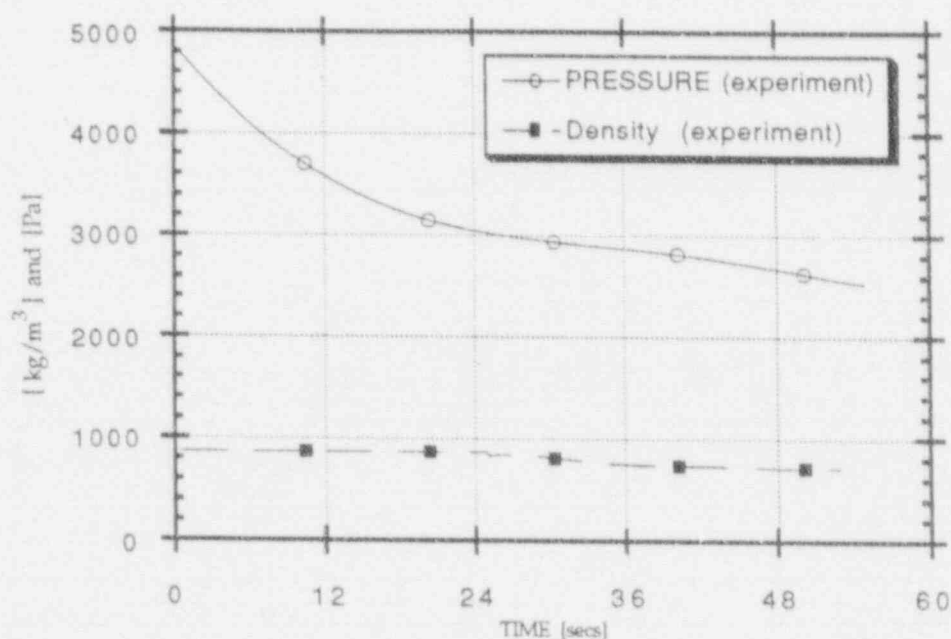
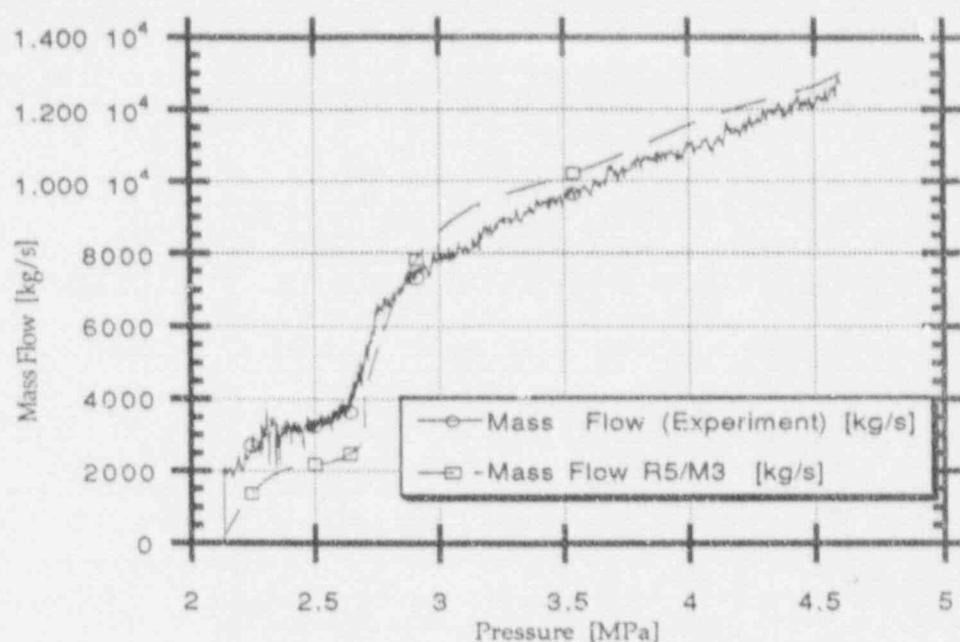
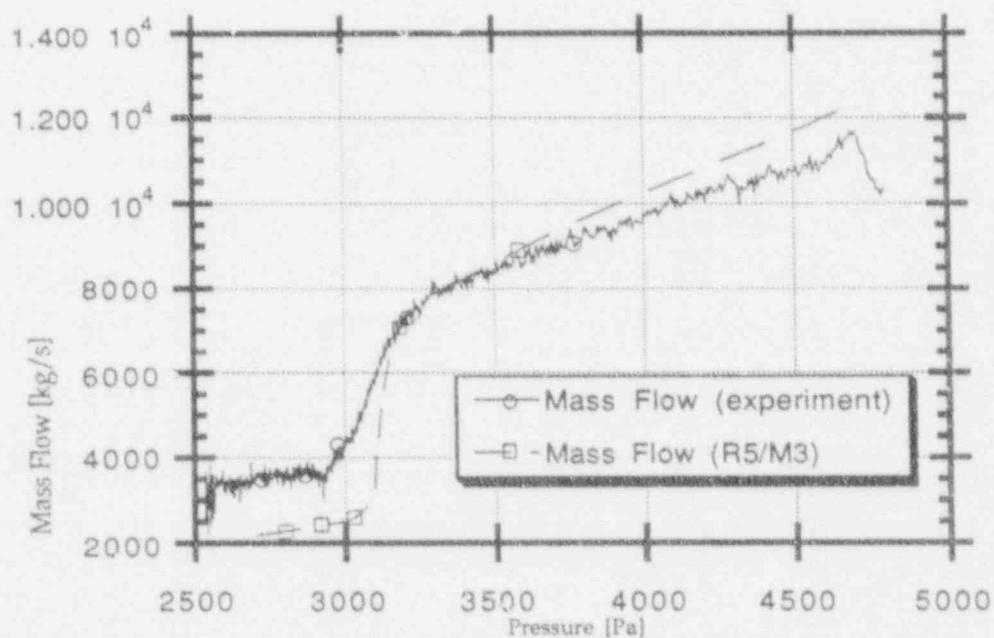


Figure 7-5. Experimental measurements of the pressure and density in the Marviken 22 experiment.



**Figure 7-6.** Comparison between the experiment the RELAP5/MOD3 simulation of the relationship between mass flow and pressure for Marviken 22 test.



**Figure 7-7.** Comparison between the experiment and RELAP5/MOD3 simulation of the relationship between mass flow and pressure for Marviken 24 test.

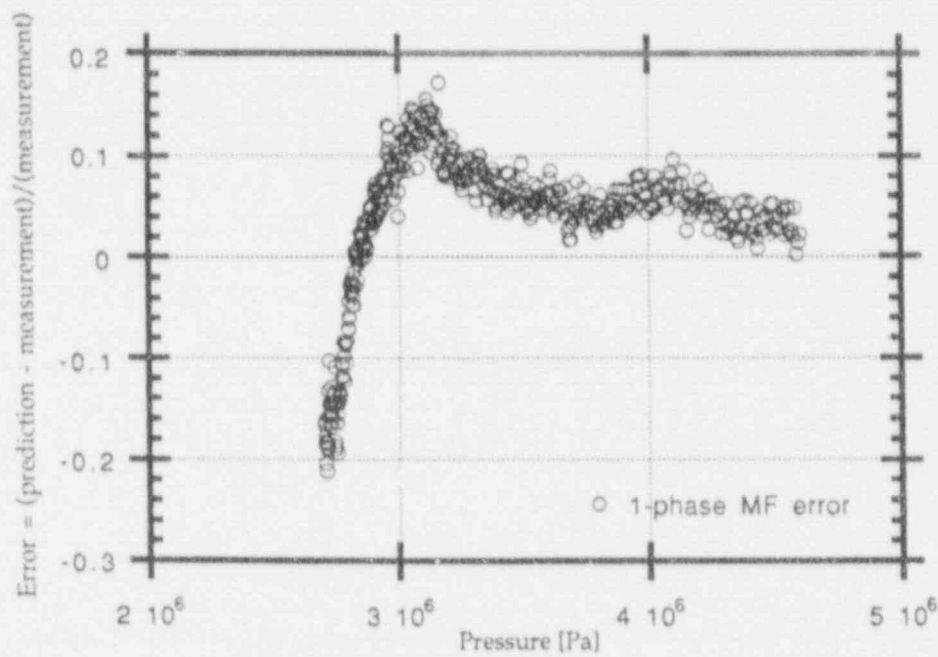


Figure 7-8. Error as a function of pressure for single-phase flow in the prediction of the Marviken 22 test.

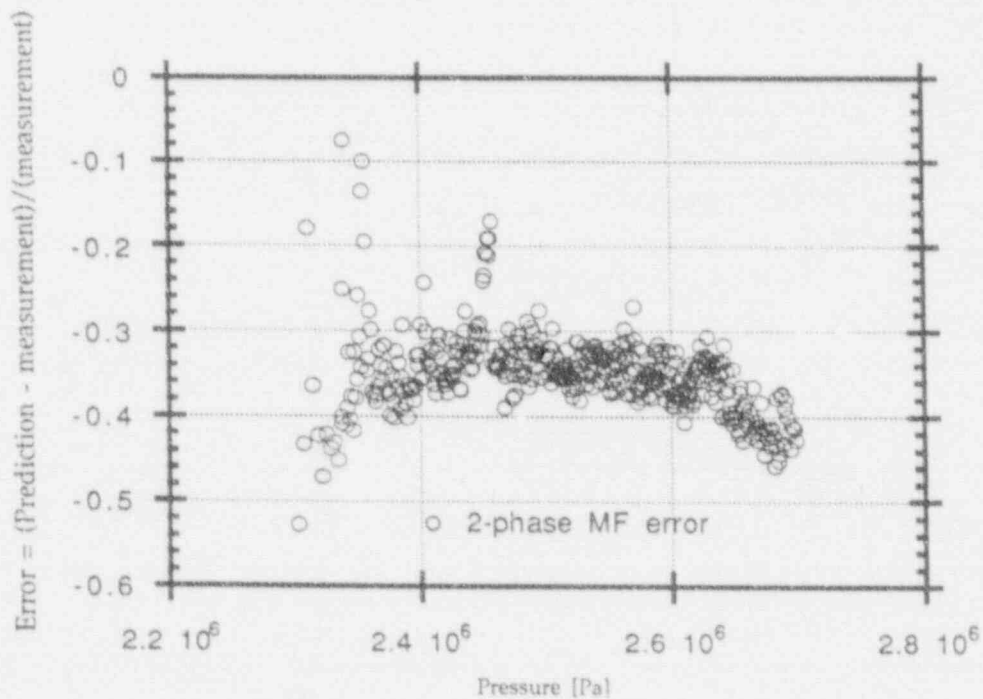


Figure 7-9. Error as a function of pressure for two-phase flow in the prediction of the Marviken 22 test.

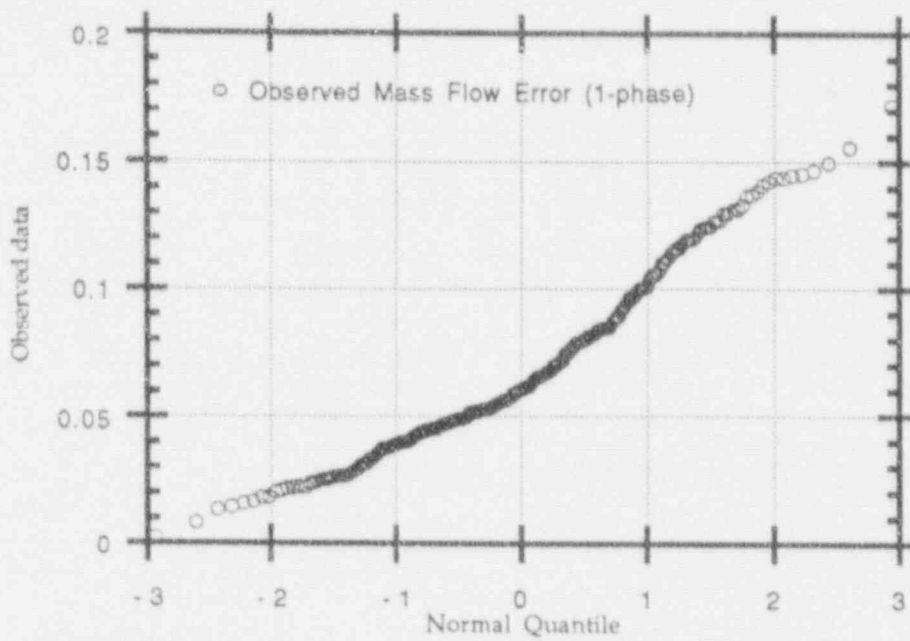


Figure 7-10. Normality test performed on the single-phase mass flow error data for Marviken 22.

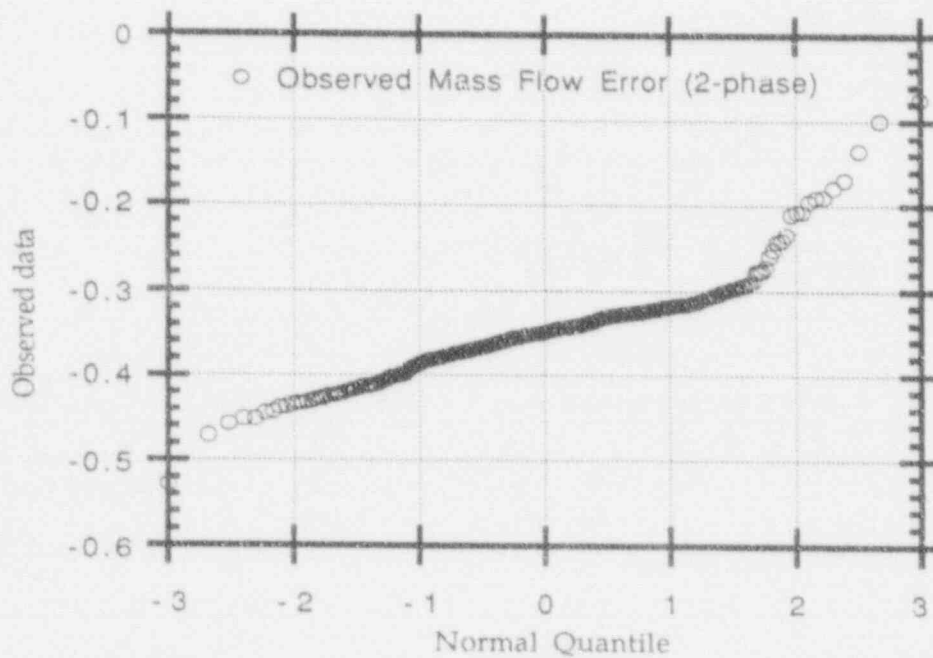


Figure 7-11. Normality test performed on the two-phase mass flow error data for Marviken 22.



obtained from test Marviken 22. Marviken 24 results (not included in this report) are quite similar.

The bias and standard deviation were determined for both tests. The expected error for the actual NPP break was estimated by interpolating between the length and diameter that characterized the geometries of the nozzles. These parameters are tabulated as follows.

**7.2.2 Interphase Drag.** It was determined that the interphase drag model is most responsible for the uncertainty in the representation of two-phase natural circulation (Phenomenon 2) and phase separation in the U-bend (Phenomenon 7). RELAP5/MOD3 uses an empirical correlation (see Reference 9) to evaluate an interphase drag coefficient  $FI$ . Since there are no interphase drag tests or natural circulation separate effect tests against which to assess the code accuracy, one must evaluate the accuracy of the model against the body of data used to generate it.

Equation (6.1-1) of the models and correlations document (Volume IV) of Reference 10 is the momentum equation that contains the interphase drag term. The term appears as

$$(\rho FI) \frac{d}{dz} (C_1 V_g^{n+1} - C_0 V_f^{n+1})$$

From Equation (6.1-2) of Reference 10 and the above expression, the interphase drag force term per unit volume and the term  $FI$  can be related as follows:

$$\alpha(1-\alpha)\rho_g \rho_f FI = f_{gf} f |C_1 V_g - C_0 V_f|$$

For bubbly and slug flow regimes in vertical flow, the drift flux was adapted. The coefficient  $f_{gf}$  is, from Equation (6.1-8) of Reference 10:

$$f_{gf} = \frac{\alpha(1-\alpha)^3(\rho_f - \rho_g)g \cdot \sin \phi}{|V_g|V_{gf}}$$

$C_0$  and  $V_{gf}$  are calculated using the Chexal-Lellouche correlation<sup>9</sup> as indicated by Equations (6.1-25) and (6.1-26) on pages 6.1-10 through 6.1-12 of Reference 10. Manipulation of

these equations yields the following expression for the term  $FI$ :

$$FI = \frac{(1-\alpha)^2(\rho_f - \rho_g)g \cdot \sin \phi |C_1 V_g - C_0 V_f|}{|V_g|V_{gf}\rho_g \rho_f}$$

The Chexal-Lellouche correlation is based on 13 sets of data. The statistical behavior of the error for each of the 13 sets of data is tabulated in Reference 9. The table assumes that the distribution of each data set is normal; thus the distribution of the uncertainty of this model is also normal. To obtain the uncertainty of the entire (not having the specific values of the points) data set the following procedure was performed:

$$\text{Average error} = \frac{\sum_{i=1}^{13} (\text{number of points})_i (\text{mean error})_i}{\text{Total number of points}}$$

which is a weighted average of the mean errors published in the table. This average error is -0.000298 and indicates the bias. This small bias is then considered negligible in this study.

The standard deviation  $S$  of the combination of all points was obtained as follows: for each data set  $i$  with  $n_i$  points

$$S_i = \sqrt{\frac{\sum_{j=1}^{n_i} (x_j - \bar{x})^2}{n_i - 1}}$$

Squaring this expression and adding all of the data sets, we obtain

$$\sum_{i=1}^{n_{\text{total}}} (x_i - \bar{x})^2 = \sum_{i=1}^{13} (n_i - 1) S_i^2$$

which yields the standard deviation for the entire data set:

$$S_{\text{total}} = \sqrt{\frac{\sum_{i=1}^{13} (n_i - 1) S_i^2}{n_{\text{total}} - 1}}$$

The result is  $S = 0.0413$ .

To include this uncertainty (and 97.7% of all points;  $2S = 2s$ ) in the sensitivity calculations, the following logic modifies  $FI$ .

Case 1:

IF FLOW REGIME IS BUBBLY OR SLUG FLOW

$$b = a - 0.0826.$$

If  $a < 0.0826$  then  $b = 0$ .

$$FI = FI \frac{(1 - \beta)^2}{(1 - \alpha)^2}$$

Case 2:

IF FLOW REGIME IS BUBBLY OR SLUG FLOW

$$b = a + 0.0826.$$

If  $a > 0.9174$  then  $b = 1$ .

$$FI = FI \frac{(1 - \beta)^2}{(1 - \alpha)^2}$$

We have assumed no bias and  $2s$  to include 97.7% of the data.

Figure 7-12 shows the variation of the correction factor for  $FI$  as a function of  $\alpha$ .

**7.2.3 Decay Heat.** The decay power is modeled as a table that is part of the user's input. The decay power depends on the burnup history of the fuel prior to this event. It has been suggested, by Tran and Schrock,<sup>12</sup> that if we know the core burnup history in some detail, we can estimate the decay power uncertainty more accurately than by using the American Nuclear Society standard.<sup>13</sup> For this analysis, the information needed to evaluate the uncertainty in the fashion suggested by Tran and Schrock was not available. Therefore, a bounding uncertainty range of 20% ( $\pm 10\%$  about the nominal) was assumed based on the American Nuclear Society standard; this is large enough to include the spatial contribution to uncertainty. To implement this, the bounding decay power curves originate at the same power level as the nominal and their values for a given time are 10% higher or lower than the corresponding nominal value. To prevent an initial power overshoot, the power was limited to the lesser of 100% full power and 110% (American Nuclear Society standard curve).

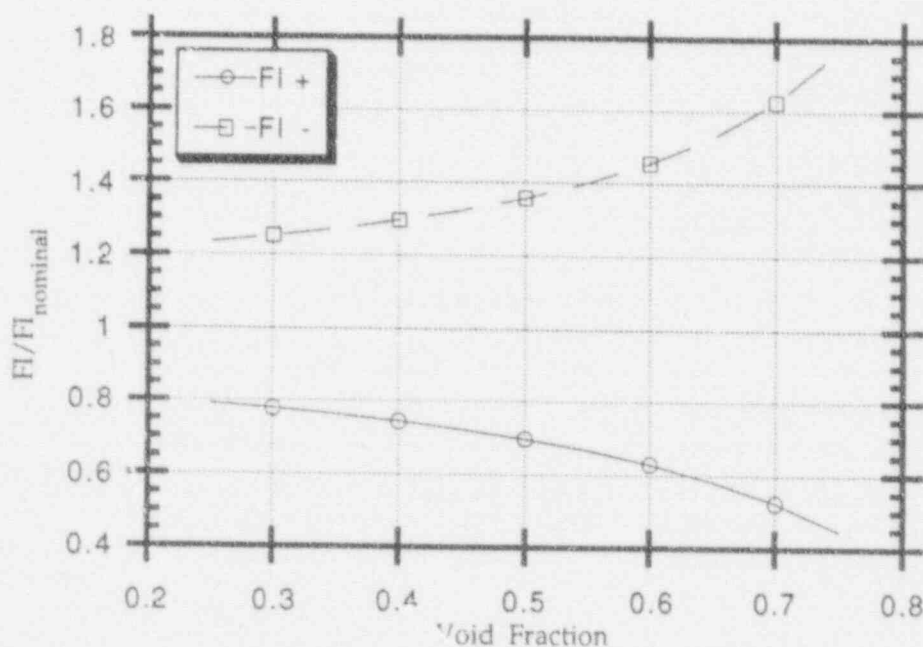


**Figure 7-12.** Bounds of the variation of the interphase drag coefficient  $FI$  as a function of void fraction, for bubbly/slug flow.

**7.2.4 RCP Performance.** RELAP5/MOD3 models the pumps in a mechanistic fashion. The user must enter parameters that characterize the pump. The pumps are of concern in three instances: (a) coastdown, (b) as a resistance to the natural circulation around the primary loops, and (c) in the case where pumps are bumped. In this scenario only the first two instances occur. The torsional friction coefficient of the pump affects both its coastdown performance and its effect as a resistance to natural circulation flow. Thus the frictional torque coefficient can be used to allocate all of the uncertainty regarding the pump and its performance. Based on the information available regarding the pumps,<sup>3</sup> it was estimated that bounding values of +100% and -50% of the nominal torsional friction coefficient were appropriate for the sensitivity calculations.

**7.2.5 ECCS Flow.** Originally, this phenomena was intended to include both flow magnitude and fluid temperature uncertainties.<sup>3</sup> We learned in the process that in case of an accident that requires HPI, the operator will monitor and throttle the flow to no more than a prescribed maximum of 500 gpm per pump.<sup>h</sup> Therefore, the magnitude of the HPI flow is no longer as uncertain as fluid temperature. Thus, for this study the

h. Babcock & Wilcox Company proprietary information.

HPI flow uncertainty refers to its inlet temperature. This temperature is limited by technical specifications and it is not allowed to go above 316.5 K (110°F) or below 275 K (35°F).

**7.2.6 Steam Generator Heat Transfer.** The steam generator heat transfer is perhaps the most complex of the phenomena modeled. The flow in a once-through steam generator experiences many flow regimes and a multiplicity of heat transfer modes. Many heat transfer correlations are invoked by the code to evaluate the heat transfer along the steam generator. In total, there are more than 50 empirical coefficients that may contribute to the uncertainty of this model. The approach used in this case was to bond the uncertainty according to the accuracy reported for the several correlations, taking the largest ones.<sup>10</sup> The result was an uncertainty of +30% -25% and was represented by changing the heat transfer area of the table.

**7.2.7 RVVV Performance.** The NPP has eight RVVVs that in the input deck are modeled as one. The model is a mechanistic model for which the user must enter the physical parameters. It is estimated that the largest source of uncertainty is the inertia of the valve and is +/-10%.

The following table (Table 7-2) summarizes all of the findings of this parameter ranging study.

**Table 7-2.** Summary of the ranging of parameters study.

Parameter	Bias	Distribution type	$\sigma$	Lower bound	Upper bound
1- $\phi$ discharge coefficient	0.083	Normal	0.042	0.833	1.001
2- $\phi$ discharge coefficient	-0.435	Normal	0.062	1.311	1.559
RCP torsional friction coefficient	0.0	Uniform	—	0.5	2.0
2- $\phi$ interphase drag coefficient ( $\alpha$ )	0.0	Normal	0.0413	0.9174	1.0826
Decay heat	0.0	Uniform	—	0.9	1.1
ECCS temperature	0.0	Uniform	—	0.9	1.036
SG heat transfer	0.0	Uniform	—	0.75	1.25
Inertia of the valve	0.0	Uniform	—	0.9	1.1

## 8. SENSITIVITY CALCULATIONS

### 8.1 Base Calculation (Nominal Case)

Table 8-1 presents the sequence of events for the base calculation.

**8.1.1 Automatic Actions.** Several automatic actions occur as the primary depressurizes due to the break. As hot leg pressure drops below 2150 psia, the pressurizer heaters will actuate in order to try to reestablish system pressure. As mass exits the break, pressurizer level will drop and the heaters will turn off as pressurizer level falls below the heater cutoff setpoint of 26.13%. While hot leg pressure remains above 1515 psia, makeup flow will increase above letdown flow in an effort to restore pressurizer level. As pressure continues to fall, the pressure/temperature relationship falls outside the range for operation, and the reactor trips with subsequent turbine/

generator trip. Upon reactor trip, the steam generator level setpoint is automatically set to 25 in. on the startup range. As a result, the main feedwater pumps must run back to allow steam generator level to drop from its normal operating level of 50% on the operating range to 25 in. on the startup range.

As a result of the turbine/generator trip, the turbine stop valves will close as the turbine bypass valves open in response to the increase in secondary pressure. However, due to a lag in instrument response, the turbine bypass valves do not begin to open until about 2 seconds after the secondary pressure reaches 1,050 psia. Subsequently, with the secondary momentarily bottled up, secondary pressure rises to 1,050 psia before the setpoint for the TBVs is reached. Approximately 2 seconds later, the TBVs begin to open, but, by this time, pressure has risen to 1,065 psia and Safety Bank 1

**Table 8-1.** Sequence of events for nominal case.

Event description	Time (s)	Automatic action	Operator action
Break initiated in HPI line	0.0		
Reactor scrams on pressure/temperature relation	11.8	X	
Main feedwater pumps begin to run back	12.2	X	
Turbine stop valves close	12.8	X	
TBVs open on high steam generator pressure	13.7	X	
Safety relief valves begin opening on high steam generator pressure	14.2	X	
Pressurizer heaters turn off on low pressurizer liquid level	26.0	X	
HPI begins on low primary pressure	27.9	X	
Main feedwater pumps trip on high discharge pressure	39.6	X	
Safety relief valves close as steam generator pressure falls	41.0	X	
Adequate subcooling margin lost	46.9		

Table 8-1. (continued).

Event description	Time (s)	Automatic action	Operator action
Upper head begins to void	48.2		
Bubble begins forming in U-bends	74.0		
Reactor coolant pumps tripped 60 seconds after loss of subcooling margin. Subsequently, EFW starts on reactor coolant pump trip. Operator immediately throttles the EFW flow, realizing he or she are in an overcooling situation	107		X
Primary pressure begins increasing due to reduced circulation	120		
Upper head volume completely voided	168		
Operator allows full EFW flow because RCS cooldown rate is less than 100°F/hr	210		
TBVs close as steam generator pressure falls	229	X	
RVVVs open	255		
Loop circulation stops as U-bend is completely blocked by bubble	275		
Primary pressure begins decreasing again	389		
Operator throttles EFW flow as RCS cooldown rate exceeds 100°F/hr	580		X
HPI flow equals break flow	1,327		
Operator allows full EFW flow because RCS cooldown rate is less than 100°F/hr	1,410		X
Operator throttles EFW flow as RCSA cooldown rate exceeds 100°F/hr	1,450		X
Core flood tanks begin injection as primary pressure falls	3,215		
Operator opens then closes EFW and TBVs because RCS cooldown rate is less than 100°F/hr	5,350		X
Operator opens then closes EFW and TBVs because RCS cooldown rate is less than 100°F/hr	5,600		X
Calculation terminated	6,000		



opens. Now one safety bank and the TBVs are open, but pressure continues to rise to 1,075 psia and the second safety bank opens. This is enough to relieve secondary pressure, and Safety Bank 2 closes as pressure falls to 1,020 psia. A short time later, Safety Bank 1 closes as pressure falls to 1,010 psia.

With the safety valves closed, secondary pressure begins to rise again, but now the TBVs modulate to control secondary pressure to 1,020 psia. Returning to the primary side, as hot leg pressure drops below 1,515 psia, letdown will isolate, and a safety injection signal will tell the HPI/makeup pumps to start and/or switch over from makeup mode to HPI mode. Very shortly afterwards, adequate subcooling margin is lost and the timer begins the countdown to two minutes, within which time the operator must trip the RCPs or else leave them running. On the secondary side, the main feedwater pumps have tripped on high discharge pressure due to the main feedwater valves closing on RCP trip. Whether or not the main feedwater pumps will trip on high discharge pressure is an issue.

Since the model has no recirculation lines, it is likely that the modeled pump will see a higher discharge pressure than the real pump when the main feedwater valves are closed. However, even if the main feedwater pumps do not automatically trip, the operator will trip them at about the same time he or she trips the RCPs because an RCP trip automatically initiates EFW. If the operator did not trip the main feedwater pumps, the pumps would be running along with the EFW pumps. So much feedwater capacity would further increase the overcooling potential of the steam generators. Thus, if the main feedwater pumps did not automatically trip, the operator would have tripped them some short time after (about 50 seconds) the predicted automatic trip.

At about 41 seconds into the transient, all automatic actions have happened. The remainder of the transient is largely controlled by the operator. The operators actions will be discussed later. At about 47 seconds, adequate subcooling margin is lost and the timer starts, indicating that the opera-

tor has a maximum of two minutes to trip the reactor coolant pumps. Shortly after the subcooling margin is lost, the upper head begins to void. The upper head voids first, as it is the hottest part of the system. Some time later, bubbles begin rising in the hot legs and start blocking the flow path over the U-bend. By the time the operator trips the RCPs at 107 seconds, the hot leg is significantly voided. RCP trip allows the two-phase mixture in the hot legs to stratify, gradually reducing loop flow. This results in reduced loop flow and gradually decouples the steam generators. As a result, primary pressure begins increasing. As power in the core decays, the break is eventually capable of removing most of the energy being generated in the core, thus pressure begins decreasing steadily with the steam generators essentially decoupled. The primary system cools and depressurizes due to break flow and HPI. At about 3,215 seconds, primary pressure falls below the pressure in the core flood tanks, and the core flood tanks begin delivering flow to the primary system in addition to the HPI.

## 8.2 Sensitivity Calculations, Results, And Discussion

Table 7-2 summarizes the findings of the bias and uncertainty study. It tabulates the type of probabilistic distribution of each uncertainty and the limits recommended for the sensitivity studies. The two discharge coefficients are the only parameters that show a measurable bias. Because of this, two sets of sensitivity calculations were performed. In the first set, the nominal run takes into account these biases of the discharge coefficients; while in the second set, the discharge coefficients are assumed unity. The base calculation for the entire study is the aforementioned first nominal case, in which the biases of the discharge coefficients are incorporated in the calculation.

Table 8-2 lists all the sensitivity cases and their results in terms of the PSCs. All parameters listed are normalized with respect to the base calculation (Run 0). Figure 8-1 is a graphic representation of these results in order from lowest to highest collapsed liquid level in the vessel

# Sensitivity Calculations

**Table 8-2.** Sensitivity calculations and their results in terms of the PSCs

Run	1- $\phi$ d.c.	2- $\phi$ d.c.	hpiT	SGHTA	DKP	IDC	RCP	RVVV	CLLV <sub>f</sub>	CLLV (in.)
0	1	1	1	1	1	1	1	1	1.0	139.8
1	0.908	1	1	1	1	1	1	1	0.9964	139.3
2	1.091	1	1	1	1	1	1	1	1.0193	142.5
3	1	0.6894	1	1	1	1	1	1	1.0544	147.4
4	1	0.904	1	1	1	1	1	1	1.0186	142.4
5	1	1.075	1	1	1	1	1	1	0.9664	135.1
6	1	1	0.9054	1	1	1	1	1	1.9778	136.7
7	1	1	1.0344	1	1	1	1	1	1.0143	141.8
8	1	1	1	0.75	1	1	1	1	0.9871	138.0
9	1	1	1	1.25	1	1	1	1	1.0136	141.7
10	1	1	1	1	0.9	1	1	1	0.9721	135.9
11	1	1	1	1	1.1	1	1	1	1.0351	144.7
12	1	1	1	1	1	0.9174	1	1	1.0265	143.5
13	1	1	1	1	1	1.0826	1	1	1.0129	141.6
14	1	1	1	1	1	1	0.5	1	1.0007	139.9
15	1	1	1	1	1	1	2	1	0.9715	135.82
16	1	1	1	1	1	1	1	0.9	1.0033	140.26
17	1	1	1	1	1	1	1	1.1	1.0053	140.54
18	1.0905	0.6894	1	1	1	1	1	1	1.0572	147.8
19	0.908	0.6894	1	1	1	1	1	1	1.0594	148.1
20	1.0905	0.904	1	1	1	1	1	1	1.015	141.9
21	1.0905	1.075	1	1	1	1	1	1	0.9843	137.6
22	1.0905	0.6894	0.9054	1	1	1	1	1	1.0036	140.3
23	1.0905	0.6894	1.0344	1	1	1	1	1	1.0565	147.7
24	1.0905	0.6894	1	0.75	1	1	1	1	1.0486	146.6
25	1.0905	0.6894	1	1.25	1	1	1	1	1.0622	148.5
26	1.0905	0.6894	1	1	1.1	1	1	1	1.0665	149.1
27	1.0905	0.6894	1	1	1	0.9174	1	1	1.0465	146.3
28	1.0905	0.6894	1	1	1	1.0826	1	1	1.0701	149.6
29	1.0905	0.6894	1	1	1	1	0.5	1	1.0544	147.4
30	1.0905	0.6894	1	1	1	1	2	1	1.0622	148.5
31	1.0905	0.6894	1	1	1	1	1	0.9	1.0558	147.6
32	1.0905	0.6894	1	1	1	1	1	1.05	1.0615	148.4
33	1.0905	0.6894	1	1	1	1	1	1.1	1.0558	147.6

1- $\phi$  d.c. single phase discharge coefficient; 2- $\phi$  d.c. two-phase discharge coefficient

hpiT: HPI temperature; SGHTA: steam generator heat transfer

DKP: decay power; IDC: interphase drag coefficient; RCP: reactor coolant pump

CLLV<sub>f</sub>: collapsed liquid level in the vessel (normalized)

(CLLV). The numbers in the horizontal axis correspond to the calculation number in Table 8-2. The base calculation is Run 0; the minimum calculated CLLV (96.64% of nominal) occurred in Run 5; and the maximum CLLV (107.01% of nominal) corresponds to Run 28. The effects of individual parameter changes on the CLLV were well behaved (monotonic variations) for most parameters. Only the RVVV and the interphase drag coefficient suggested the existence of extremes of CLLV within the uncertainty ranges of those parameters. However, these variations were relatively small (~1 to 9 cms) compared to oscillations of the CLLV within the same run.

Figures 8-2 and 8-3 are graphical illustrations of the results tabulated in Table 8-2. Figure 8-2 shows side by side how the different code parameters were varied (only maximum and minimum values shown), one at a time; Figure 8-3 shows the corresponding collapsed liquid level in the vessel resulting from each of these variations. It is easy to see that despite large variations of the important parameters, the minimum collapsed liquid level in the vessel only varied slightly.

The results of the sensitivity calculations indicate that this system is very robust with respect to uncertainties of the important phenomena and the selected PSC. Changes of the PSC are very small, even for large variations in some parameters. This also leads to the conclusion that a different choice of PSC might have been more appropriate to evaluate the "severity of the accident" and its sensitivity to the uncertainties involved. During our analysis, we explored other options. One of the alternative PSCs suggested was a parameter defined as

$$S = \int_0^{t_{rec}} \frac{\alpha_{core} H \cdot P}{P_0} dt$$

in which  $P$  is the reactor power;  $P_0$ , initial power;  $H$ , core height; and  $t_r$ , time to recovery (to be defined). In this fashion, the lack of liquid water in the core, integrated over time and scaled according to the core power, would be a measure of severity. Time constraints did not allow us to pursue this route to a successful conclusion; it is mentioned here as a recommendation based on the experience gained during this exercise.

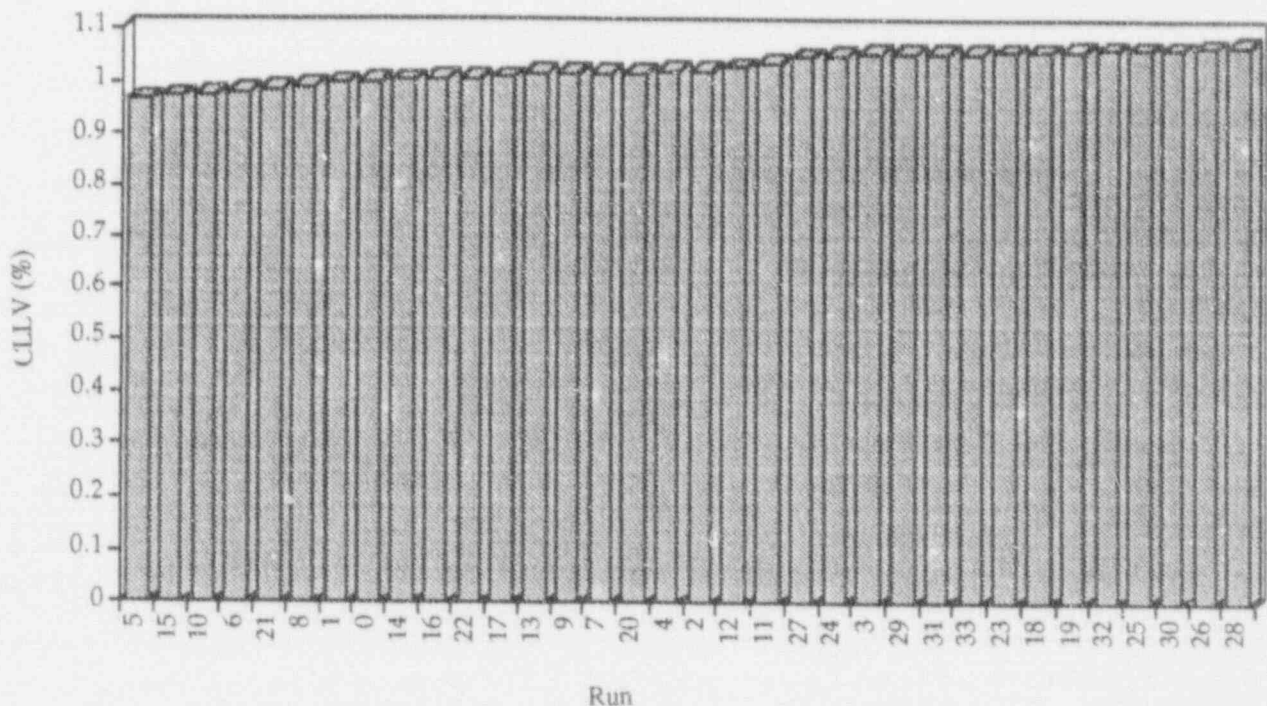
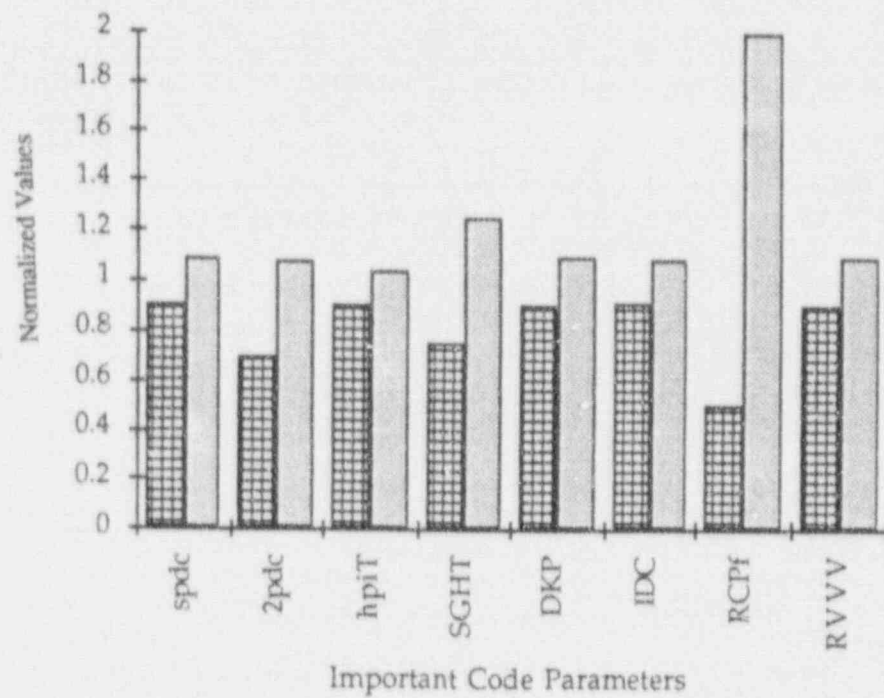
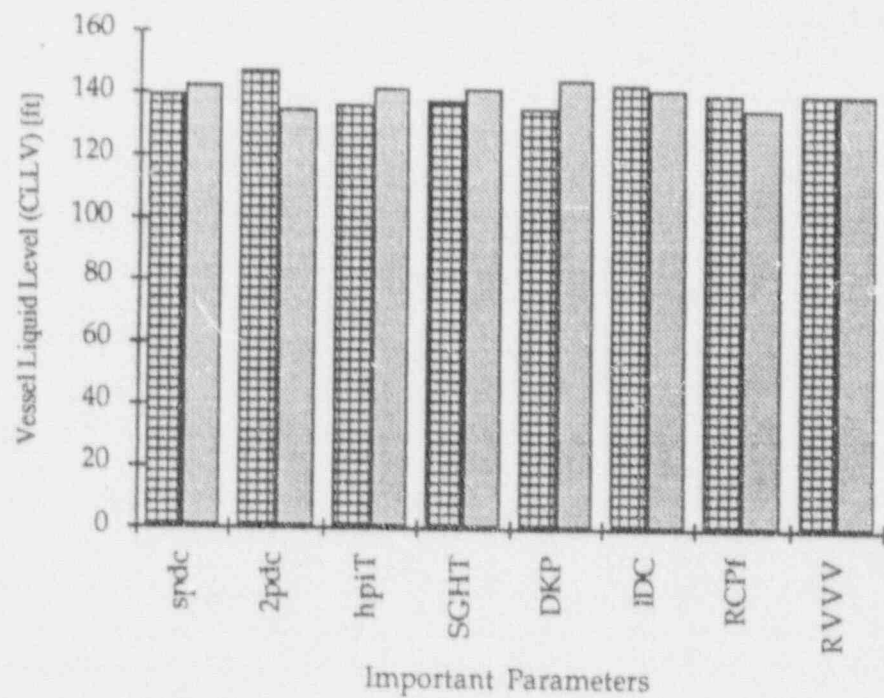


Figure 8-1. Sensitivity calculation results.



**Figure 8-2.** The variations imposed on the important code parameters to run the sensitivity calculations.



**Figure 8-3.** Comparison of the resulting minimum liquid level in the reactor vessel corresponding to variations of the important code parameters.

## 9. TOTAL UNCERTAINTY

The sensitivity calculations results, discussed in the previous section, were used to build a response surface (Appendix C). The response surface then was used to simulate several thousands of cases in which the sensitivity parameters vary randomly according to their respective uncertainty range and distribution (Section 7 of this report). The results indicate the probability that the primary safety criteria is less than 85% of the nominal value is  $4.5 \times 10^{-4}$ . Thus, in this SBLOCA scenario, there is no meaningful likelihood of core uncover.

The MIST calculation performed by Prof. Hassan (Appendix A) shows that the difference between the calculated and the experimental core collapsed liquid level is less than seven percent for most of the range of the simulation, and in fact, RELAP5/MOD3 conservatively underpredicts the level. This difference of less than 7% is well within the range limits of 15% indicated by the statistical analysis mentioned above.



## 10. CONCLUSIONS AND RECOMMENDATIONS

Based on our experience during this work, we can make the following concluding remarks.

We were able to apply the CSAU methodology to a different NPP, scenario, and best estimate code than had previously been demonstrated.

Faced with the limited availability of assessment data, we were able to devise procedures to optimize our utilization of the available information and evaluate the accuracy of the code when representing the important phenomena.

Although CSAU is a method to quantify code uncertainty and the code does not model operator decisions, we learned that for best estimate calculations of operator intensive transients such as this one, the operator actions need to be considered and included in the simulation. The uncertainty of the operator actions fall beyond the

scope of this work. However, we recommend that this be also considered in any subsequent study.

This particular plant design, B&W lowered loop, is rather robust to the specific SBLOCA studied. The likelihood of core uncover and cladding temperature excursion in this scenario with the given operator actions is very remote. It is recommended that subsequent studies should define a more indicative measure of accident severity, for the purpose of sensitivity studies, in addition to the two PSCs defined here.

Our information with respect to code numerics and scaling was very limited. Thus, our conclusions are not as complete as we would like. The MIST calculation conducted for this work helps to fill some of the void with respect to scaling. Also, an independent code numerics study is currently under way.

## 11. REFERENCES

1. R. A. Shaw, S. Z. Rouhani, T. K. Larson, R. A. Dimenna, *Development of a Phenomena Identification and Ranking Table (PIRT) for Thermal-Hydraulic Phenomena During a PWR Large-Break LOCA*, NUREG/CR-5074, EGG-2527, October 1988.
2. Technical Program Group, *Quantifying Reactor Safety Margins*, NUREG/CR-5249, EGG-2552, December 1989.
3. M. G. Ortiz, L. S. Ghan, G. E. Wilson, *Development of a Phenomena Identification and Ranking Table (PIRT) for Thermal-Hydraulic Phenomena During a PWR Small Break LOCA*, EGG-EAST-9080, May 1990.
4. C. Don Fletcher, Mark A. Bolander, Benjamin D. Stitt, Michael E. Waterman, *RELAP5 Thermal-Hydraulic Analyses of Pressurized Thermal Shock Sequences for the Oconee-1 Pressurized Water Reactor*, NUREG/CR-3761, June 1984.
5. P. D. Wheatley et al., *Evaluation of Operational Safety at Babcock and Wilcox Plants, Volume 2, Thermal Hydraulic Results*, NUREG/CR-4966, July 1987.
6. P. D. Wheatley, et al., *RELAP5/MOD2 Code Assessment at the Idaho National Engineering Laboratory*, NUREG/CR-4454, EGG-2428, March 1986.
7. R. A. Riemke, *Report on CCFL and Interphase Drag Models for RELAP5/MOD3*, EGG-TFM-8012, February 1988.
8. K. G. Condie, T. K. Larson, G. E. McCreery, "Flooding, AFW Penetrations, and Visual Investigations in Scaled Once-Through Steam Generator Facilities," *25th ASME/AIChE National Heat Transfer Conference, Houston, Texas, July 1988*.
9. Nuclear Safety Analysis Center of EPRI, *The Chexal-Lellouche Void Fraction Correlation for Generalized Applications*, NSAC/139, April 1991.
10. K. E. Carlson, R. A. Riemke, S. Z. Rouhani, R. W. Shumway, W. L. Weaver, *RELAP5/MOD3 Code Manual*, NUREG/CR-5535, EGG-2596, June 1990.
11. L. Sachs, *Applied Statistics: A Handbook of Techniques*, 2nd edition, *Springer Series in Statistics*, Springer-Verlag, 1984.
12. H. Tran, V. E. Schrock, "Decay Power Evaluation for Licensing Analysis," *ANS Transactions*, 54, 1987, pp. 246-247.
13. ANSI/ANS-5.1-1979, "American National Standard for Decay Power in Light Water Reactors," American National Standards Institute/American Nuclear Society.
14. P. A. Roth and R. Schultz, *Analysis of Reduced Primary And Secondary Coolant Level Experiments In The Bethsy Facility Using RELAP5/MOD3*, EGG-EAST-9251, July 1991.

## **Appendix A**

### **RELAP5/MOD3 Assessment Using MIST**

## Appendix A

### RELAP5/MOD3 Assessment Using MIST

Prof. Yassin Hassan  
Texas A&M

#### INTRODUCTION

The Multiloop Integral System Test (MIST) facility is a scale model of a Babcock & Wilcox Company (B&W) nuclear power plant. This facility is designed to experimentally investigate the transient occurring after reactor trip and primary pump coastdown. The facility is located at Alliance, Ohio. Data generated from the MIST facility is used to resolve current plant licensing issues and analyze computer code behavior.

The objective of this report is to assess the capability of the RELAP5/MOD3 thermal hydraulic code by comparing the code related results with those obtained experimentally for Test 3109AA. This test, called the nominal case, was a scaled, 10-cm<sup>2</sup>, cold leg pump discharge break located on the bottom of the pipe several inches downstream the high pressure injection (HPI) nozzle. A complete test description is given in the MIST Group 31 report.<sup>a</sup> A brief test description is given in the next section. By comparing the experimental data with the results obtained from the code, one can determine the effectiveness of the models and correlations used in the code. One can also gain an understanding of the physical phenomena involved in the experiment.

The reasons the experimental data differed at times from the code-generated results can be attributed primarily to the impossibility of representing a three-dimensional plant in a one dimensional model. Numerical inconsistencies also cause departure from the experimental data. The third reason of departure is inaccurate or incomplete knowledge of the test facility itself, which

then have to made up by approximations or guesses. However, the overall RELAP5/MOD3 predictions of Test 3109AA are in an excellent agreement with the data.

#### Test Description

The Test 3109AA is the as-run nominal test for the MIST program. It is a small-break loss-of-coolant accident (SBLOCA) and also exhibited major post-SBLOCA phenomena. This phenomena include interrupted loop flow, depressurization to saturation, boiler-condenser mode (BCM) cooling, refill among others.

The break modeled was a 10-cm<sup>2</sup> (0.01076-ft<sup>2</sup>) break in the B1 cold leg pump discharge. HPI and auxiliary feedwater flow were available. Reactor coolant pumps were not available. The reactor vessel vent valves (RVVVs) were automatically controlled on differential pressure throughout the transient. Guard heaters and steam generator (SG) secondary liquid levels were automatically controlled and the SG secondary side levels were maintained constant level after refill.

The primary system was initialized in a single-phase natural circulation. The transient was initiated from this natural circulation steady-state with hot and cold leg average thermocouple readings of 584.4 K (592.3°F) and 561.4 K (550.9°F), respectively. Primary pressure was 11.9 MPa. During the steady state, the guard heaters were under automatic operation and the RVVVs were manually closed. The core power was 3.9% of the scaled full power. The pressurizer level was 1.57 m (5.2 ft) above the bottom of the pressurizer, and the A and B steam generators secondary pressures and levels were 6.991 MPa (1,014 psia) and 6.998 MPa (1,015 psia) and 1.42 m (4.65 ft) and 1.44 m (4.74 ft), respectively. Steady-state

<sup>a</sup>. Babcock & Wilcox Company proprietary information, 1986.

## Appendix A

conditions and code calculations are given in Table A-1.

The test was initiated with a 10-cm<sup>2</sup> (0.01076-ft<sup>2</sup>) leak in the cold leg pump discharge piping. The steady-state control functions were preserved until the pressurizer liquid level decreased to 0.305 m (1 ft). Then the following actions were taken:

1. Change the SG secondary level control setpoint to 9.63 m (31.6 ft).
2. Activate the full HPI flow.
3. Start the core power decay.
4. Transfer the RVVV control from manual to automatic/independent with open/close points of 862 Pa (0.125 psi) and 276 Pa (0.04 psi).
5. Begin the abnormal transient operator guidelines (ATOG) based SG secondary pressure control.

These transient conditions are listed in the Table A-2.

The SG secondary pressure was automatically controlled during the test with a control based on the ATOG. The ATOG-based setpoint pressure was determined from the core exit temperatures and the two saturation temperatures corresponding to the SG secondary pressures. The ATOG-based setpoint pressure was determined automatically during Test 3109AA and applied to both the SGs.

Manual controls were also specified depending on the system conditions. The manual control actions included:

1. Opening the power-operated relief valve (PORV) if the system pressure reached 16.2 MPa (3500 psia)
2. Isolating the core flood tank (CFT), depending on the core exit subcooling

3. Opening the high point isolation vents, depending on system conditions or time
4. Throttling the HPI flow according to the pressurizer level and core exit subcooling if the PORV was closed.

**Test Phenomena (Observed).** The test was initiated at time zero by a scaled 10 cm<sup>2</sup> (0.01076 ft<sup>2</sup>) in Cold Leg B1. At this time, the primary was full of liquid and the coolant was driven by natural circulation. As the pressurizer level fell below 0.305 m (1 ft) at 126 seconds, the core power decay was started: the RVVV automatic control was initiated, allowing the RVVVs to open. The SG secondaries also started refilling as the level setpoint was changed from 1.52 m (5 ft) to 9.63 m (31.6 ft).

Saturation first occurred at 185 seconds in the intact loop hot leg. Liquid from the pressurizer warmed the liquid in the intact loop hot leg so that flashing first occurred in the intact loop U-bend. Natural circulation in the intact loop ended at 240 seconds as the liquid level in the hot leg dropped too low for spillovers to occur. This removed the intact loop SG as a heat sink.

As the SG secondaries were refilled by auxiliary feedwater, the liquid levels in the intact loop SG primary dropped so that the condensing surface was exposed to the tubes cooled by auxiliary feedwater (AFW). This resulted in intermittent BCM heat transfer from about 480 to 1000 seconds as the intact loop SG secondary liquid level reached the high setpoint and some AFW was required as the liquid level settled in on the set point. This had an impact on the early course of the transient.

The condensation in the intact loop SG reduced the pressure in the intact loop U-bend, raising the liquid level in that SG. This shifting of the primary inventory contributed to the voiding in the broken loop U-bend. Starting at 900 seconds, the broken loop flow decreased rapidly and reached a minimum at 1,020 seconds.

With this decrease in broken loop flow, the primary to secondary heat transfer reduced. This



**Table A-1.** Calculated and measured steady-state conditions.

	RELAP	MIST data
Primary pressure (psia)	1708	1739
SG A secondary pressure (psia)	1010	1014
SG B secondary pressure (psia)	1010	1015
SG A collapsed liquid level (ft)	4.53	4.65
SG B collapsed liquid level (ft)	4.53	4.74
Hot leg subcooling (°F)	26.3	23.9
Pressurizer collapsed level (ft)	22.7	23.17
Core power into the fluid (%FP)	3.8	3.9
SG primary exit temperatures (°F)	547.2	550.0
Core exit temperatures (°F)	587.6	592.4
Core total mass flow rate (lb/s)	2.06	1.9
Uncompensated heat losses (%FP)	0.4	0.5

**Table A-2.** Sequence of events comparisons.

	RELAP (min)	MIST data (min)
Break opening	0.0	0.0
Pressurizer level to 1.0 ft	2.3	2.1
Hot leg A flow interruption	4.2	3.8
SG A high elevation BCM started	7.9	8.0
SG secondary level to 31.6 ft	9.6	9.8
Hot leg B flow interruption	15.5	17.0
Complete loss of natural circulation	19.5	26.0
Feed cycle BCM started	62.5	65.0
Primary system refill start	63.0	66.0
Termination of transient	80.0	—

caused the system to pressurize at about 1,000 seconds. Voiding in the upper head of the reactor vessel pushed more liquid into the hot legs, causing the broken loop flow rate to increase. At 1,150 seconds, the RVVVs closed as different draining rates in the vessel and the downcomer exposed the RVVV nozzles. Reopening of the RVVVs allowed steam to flow from the vessel to the downcomer. Flow over the broken loop U-bend ended because the core generated steam was not forcing any more liquid up the hot legs. Repressurization ended because the cold HPI liquid condensed a part of this core generated steam in the downcomer.

The system then entered a relatively inactive period during which the system slowly cooled and depressurized. SG secondary pressures remained nearly constant until the setpoint decreased to the actual pressures.

The ATOG set points were reached at 3,600 seconds. The level in the intact loop SG primary was well below the AFW elevation so that a large surface area was available for condensation when AFW was started. The BCM heat transfer caused a significant increase in the depressurization rate. Primary pressure was reduced sufficiently so that HPI flow exceeded the break flow rate. The liquid level in the reactor vessel remained near the hot leg elevation and did not approach the top of the core during the transient.

Condensation in the intact loop SG reduced the pressure in the U-bend so that the level rose in the intact loop SG and the hot leg. This caused the level in the broken loop SG to drop. This level dropped below the AFW nozzle elevation of 15.48 m (50.8 ft) and the BCM heat transfer then occurred in the broken loop SG as the level changed. This caused a large depressurization rate, which increased the refill rate. A primary repressurization started at about 5,500 seconds because the primary system inventory had increased so that the SG levels were sufficiently high to preclude BCM heat transfer. The repressurization ended at 9,000 seconds. During this period, the leak flow rate increased to near the HPI flow rate, resulting in a near equilibrium

condition lasting for about three hours. Five spillover events also occurred at around 17,000 seconds due to the raised liquid level in one of the hot legs to the U-bend. At 25,000 seconds, refill was sufficient to restart continuous natural circulation in the B loop. The primary pressure then stabilized around 1.4 MPa. The test was terminated after 12 hours on the maximum time criteria.

## Code Description

The calculations described were performed with the RELAP5/MOD3 version 7J (beta testing stage) thermal hydraulic code. This code is a best estimate transient simulation code.<sup>1</sup> It has the capability to model both large and small-break LOCAs and operational transients such as loss of offsite power. RELAP5/MOD3 is a nonhomogeneous, nonequilibrium, one-dimensional, two-phase flow code. The fluid in the system can be a mixture of steam, liquid water, one noncondensable specie, and one nonvolatile source. The system simulation capabilities include the primary system, the secondary system, feedwater train, system controls and core neutronics. RELAP5 is used for analysis of system component interactions as opposed to detailed simulations of fluid flow within the individual components.

The code uses six field equations: two phasic continuity equations, two phasic momentum equations, and two phasic energy equations. Numerical solutions of these equations which are partially implicit with respect to time. The reactor kinetics equations are ordinary differential equations and are solved using the Runge-Kutta technique.

The RELAP5/MCD3 is an improved version of the MOD2 version. The specific areas of improvement are as follows:

1. Modification of the calculation of the interphase drag between the liquid and vapor phases. This was accomplished by changing the computation from volume based to junction based, using the donor upstream volume conditions to determine the junction interphase drag for concurrent flow and

void fraction weighing between the two volume for countercurrent flow.<sup>2</sup>

2. The Biasi-Zuber correlation<sup>3</sup> utilized in the MOD2 version was replaced by the 1986 AECL-UO Critical Heat Flux Lookup Table developed by Groeneveld.<sup>4</sup> This table has tube data but has factors which can be used to modify the values to account for rod bundles, grid spacers, axial power distribution, bundle inlet boundary layer effects.
3. A general CCFL model was implemented that allows the user to select the Wallis form,<sup>5</sup> the Kutateladze form, or a form between these forms. The user must specify the form of the flooding correlation, the gas intercept used in the CCFL correlation and the slope used in the CCFL correlation.<sup>6</sup>
4. The critical flow model was improved by smoothing the transition from the subcooled choking model and correcting a coding error in the computation of throat mixing internal energy.<sup>7</sup>
5. A new input component, ECCMIX, was created, which is modeled as a branching of the coolant loop piping near the emergency core cooling system injection point. The model is based on determining the flow regime in the existing in the area of injection and then invoking the interphase heat transfer correlations appropriate to that flow regime.

The above is only a list of some of the modifications contained in the RELAP5/MOD3 V7J and is not an all inclusive list.

**RELAP5/MOD3 Nodalization.** The nodalization is shown in the Figure A-1. RELAP5 uses two types of models: generic component models and special process models. Generic component models include pipes, pumps, valves, heat structures, electric heaters, turbines, separators, accumulators and control system components. Special process models include those of form loss, flow at

an abrupt area change, branching, choked flow, boron tracking, and noncondensable gas.

For the present simulation, a MOD2 version input deck written for MIST Test 3202 was modified to the MOD3 version with the changes necessary for the test conditions.

The heated region of the core was modeled by Pipe Component 350. The reactor vessel downcomer was modeled by Component 300. The once-through steam generators were modeled using a series of pipe and branch components. The AFW spray was simulated using a time-dependent volume and junctions. The rest of the facility was modeled using various components. Control components were added to perform the necessary control functions such as opening valves, adjusting the liquid levels, and maintaining the core power levels.

The input deck for the steady-state initialization and the transient is included in the appendix.

## COMPARISON OF THE EXPERIMENTAL RESULTS WITH THE CODE CALCULATIONS

The RELAP5/mod3 V7J thermal hydraulic code was used for posttest analysis of the MIST Test 3109AA. The steady-state and the transient calculations are discussed below. The discrepancies between the experimental data and the code calculated results are also described below.

### Steady-State Initialization

Before proceeding with the transient calculations it was necessary to calculate the steady-state results. The calculated steady-state results are compared with the experimental data and summarized in Table A-1. The primary pressure as calculated was 1,708 psia compared to 1,739 psia (experimental). The SG secondary pressures, the collapsed levels, the hot leg subcooling, and the pressurizer collapsed level were all accurately predicted. Good agreement between the experimental and the calculated

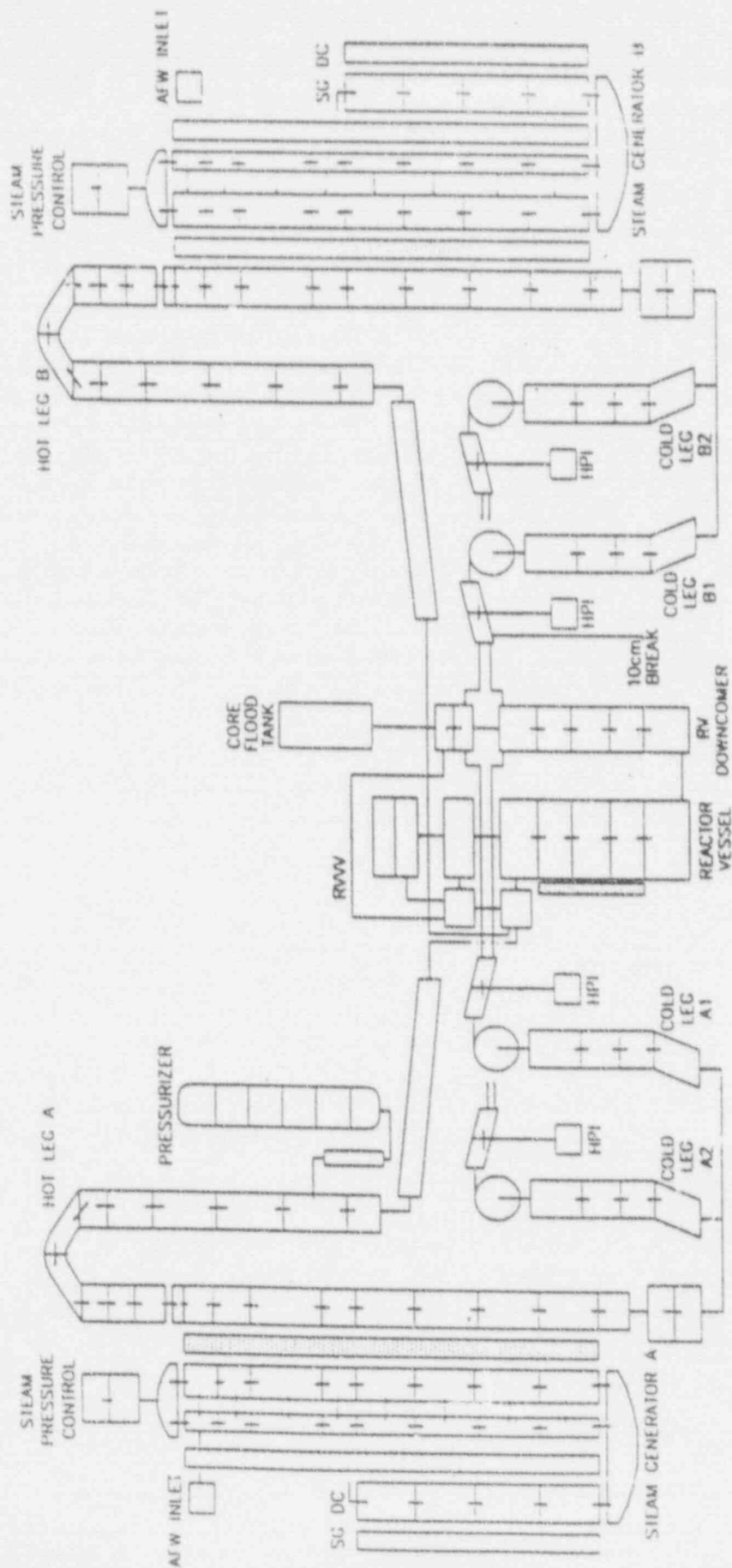


Figure A-1. MIST nodalization.



results were observed and these values were within the uncertainties of the measure values.

## Transient Calculation Results

The primary parameters of interest in this study are pressure, loop flows, hot/cold leg temperatures, secondary liquid levels, break flow, reactor vessel coolant level, primary mass inventory, emergency feedwater flow, and SG power. In the discussion to follow, the experimental data and the code calculated results are compared and any discrepancies between them are pointed out.

The sequence of events as predicted by the code are compared with the experimental data in Table A-2. The transient was initiated by a 10-cm<sup>2</sup> (0.0107-ft<sup>2</sup>) opening in the cold leg at 0.0 seconds. The transient was run for 4,800 seconds. There are basically four transient phases, which are in turn described below. Phase 1 involved subcooled decompression covering the period from the start of the transient to 185 seconds into the transient. Phase 2 covers the period from the 185 to 1,560 seconds, when there is complete loss of natural circulation. This period is characterized by intermittent flow in the loops. Phase 3 starts at 1,560 seconds till 3,960 seconds, when primary system refill starts and is a period of loop stagnation. Phase 4 extends from the start of primary system refill till the termination of the transient at 4,500 seconds.

**Phase 1.** The primary pressure is shown in Figure A-2. The primary pressure drops continuously from 1,700 to 500 psia in 4,800 seconds. The drop is rapid in the first 450 seconds, after which the drop is relatively slower till about 3,600 seconds, after which the pressure again drops rapidly. Saturation began at about 185 seconds into the test in the calculations. Prior to saturation, the fluid in the system was subcooled liquid and the primary system pressure decreased rapidly because of liquid expansion owing to the leak flow. At the beginning of the transient, the entire primary system was in single-phase, steady-state circulation. This natural circulation was driven by the difference in temperatures and hence densities between the liq-

uid in the hot legs and the cold legs. This decrease in pressure is accompanied by a decrease in pressurizer level. The level in the pressurizer dropped to 0.305 m (1 ft) in about 126 seconds in the test and 138 seconds in the calculation. At this point, core power decay was started and the HPI flow was started. The liquid in the pressurizer was near saturation temperature, and as this liquid was discharged into the intact loop hot leg, it mixed with the hot leg fluid. This resulted in a higher fluid temperature in the intact loop hot leg, relative to the broken loop hot leg. This caused an increase in natural in the intact loop at the beginning of the transient.

The effect of the core power decay after the pressurizer low-level trip was to increase in the calculated and the measured primary depressurization rates. This depressurization rate is quite high because the primary fluid was subcooled and expanding due to the leak. At the time of the low-level trip, the RVVVs were switched from manually closed to automatic control. The vent valves opened immediately, causing a reduction in the loop flows. This reduction was followed by an increase in loop flows with the sharpest increase in the intact loop flows.

At 185 seconds into the transient, the hot leg flow increase was terminated in the experiment. At this time the system pressure had decreased to the temperature of the intact loop hot leg, which caused a vapor bubble in the intact loop U-bend and interrupted the natural circulation in the intact loop hot leg. Subsequent depressurization in the hot leg was then prevented by the flashing of the liquid in the intact loop hot leg. This marked the end of Phase 1.

**Phase 2.** The point of saturation was followed by a period of intermittent circulation and the level of liquid in the hot leg happened to determine the extent of natural circulation in each loop. During this phase, the control procedures initiated in Phase 1 affected the SG AFW flows and the steam flows. At the beginning of this phase, the SG AFW flows were on as the secondary levels increased to 9.63 m (31.6 ft). As the hot leg liquid level receded, the U-bend was uncovered and the loop flow terminated. This stage



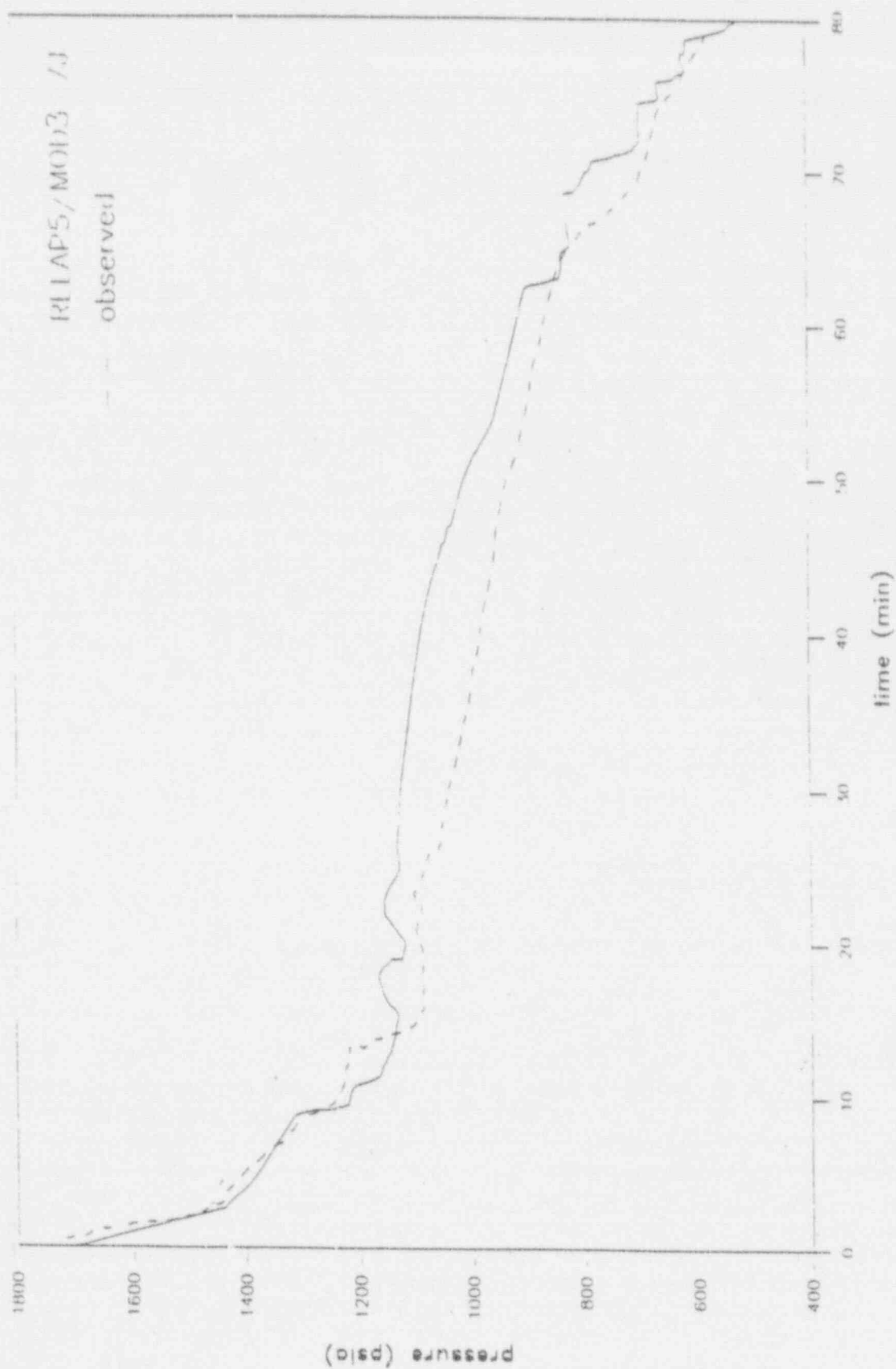


Figure A-2. Primary pressure.

extends to about 1,560 seconds in the test and 1,200 seconds in the calculation.

After saturation in the intact loop hot leg, the intact loop hot leg liquid level decreased rapidly (Figure A-3). This happened because of flashing caused by decreased pressure. As a result, the hot leg flow interruption occurred at 228 seconds into the transient. This was predicted by the code to occur at 252 seconds. This loss of natural circulation from the intact loop caused a decrease in heat transfer from the primary, and the SG secondary pressure decreased. This decrease, caused by the AFW flow (Figure A-4) into the intact loop continued until the SG level (Figure A-5) reached a level of 9.63 m (31.6 ft) at 582 seconds into the transient in the experiment and 576 seconds in the calculation. The AFW flow decreased as shown in Figures A-4 and A-6 for SGs A and B, respectively. With continuing natural circulation, flow in the broken loop SG caused a gradual secondary depressurization. The steam flow in the intact loop secondary SG terminated after the loop SG secondary fell below the ATOG setpoint. Steam flow was terminated in the broken loop SG secondary by the pressure controller but restarted shortly after at 2,100 seconds in the calculation and 2,700 seconds in the test (Figure A-7).

The intact loop SG secondary was refilled to 9.63 m (31.6 ft) in the experiment, and the AFW controller was switched to the constant level mode. The AFW refilled the intact loop SG til 582 seconds in the experiment and 576 seconds in the calculations (Figure A-4). Thereafter the AFW was briefly terminated till about 800 seconds, when the flow resumed again. When the AFW was restarted in the intact loop SG, there was vapor present in the primary side of the tubes at the AFW elevation of 50.8 m (15.48 ft), resulting in condensation heat transfer. This BCM heat transfer occurred at 480 seconds into the test and 474 seconds in the calculations. This condensation stopped when the primary level in the intact loop SG reached the AFW elevation. In the absence of the steam flow, the AFW was not required to maintain the SG secondary level in the intact loop 9.63 m (31.6 ft), and the AFW flow was completely terminated at

1,500 seconds both in the test and in the calculation.

In the broken loop, similar loop behavior was observed though at different timings owing to a cooler hot leg fluid temperature in the broken leg as compared to the intact leg. The broken loop hot leg was maintained liquid til 1,200 seconds as the liquid level in the intact loop hot leg receded due to local flashing. The broken loop hot leg level (Figure A-3) rapidly decreased after 1,200 seconds and the natural circulation in the broken loop correspondingly decreased. This caused a decrease in the heat transfer in the broken loop, resulting in an increase in the primary pressure at 1,200 seconds. This was accompanied by a corresponding decrease in secondary pressure in the broken loop. The core outlet flows was diverted through the RVVVs. The repressurization caused a retardation in the flashing in both the loops. However, increased flashing occurred in the uphead because of increased diverted core outlet flow. As a result, the intact loop levels increased after 1,200 seconds.

Thereafter, the loop hot leg liquid levels increased, accompanied by a corresponding decrease in the core collapsed liquid level, as shown in Figure A-8. The primary system continued to drain and the natural circulation in the broken loop began to decrease. The hot leg flow in the broken loop was interrupted at 930 seconds in the calculation and 1,020 seconds in the test. The natural circulation was completely interrupted at 1,560 seconds into the test. This marked the end of Phase 2. At the end of Phase 2, the primary system continued depressurizing, the broken loop SG secondary pressure was controlled to the decreasing ATOG setpoint, while the AFW was controlling the SG level in the broken loop. The intact loop SG was inactive in this phase because the pressure was well below the ATOG-based setpoint.

**Phase 3.** Loop stagnation was observed, resulting in stagnation of natural circulation flow loops. This stagnation lasted til refilling began at the times mentioned below. During this period, the primary was cooled by the HPI and by the broken loop SG AFW. The primary system

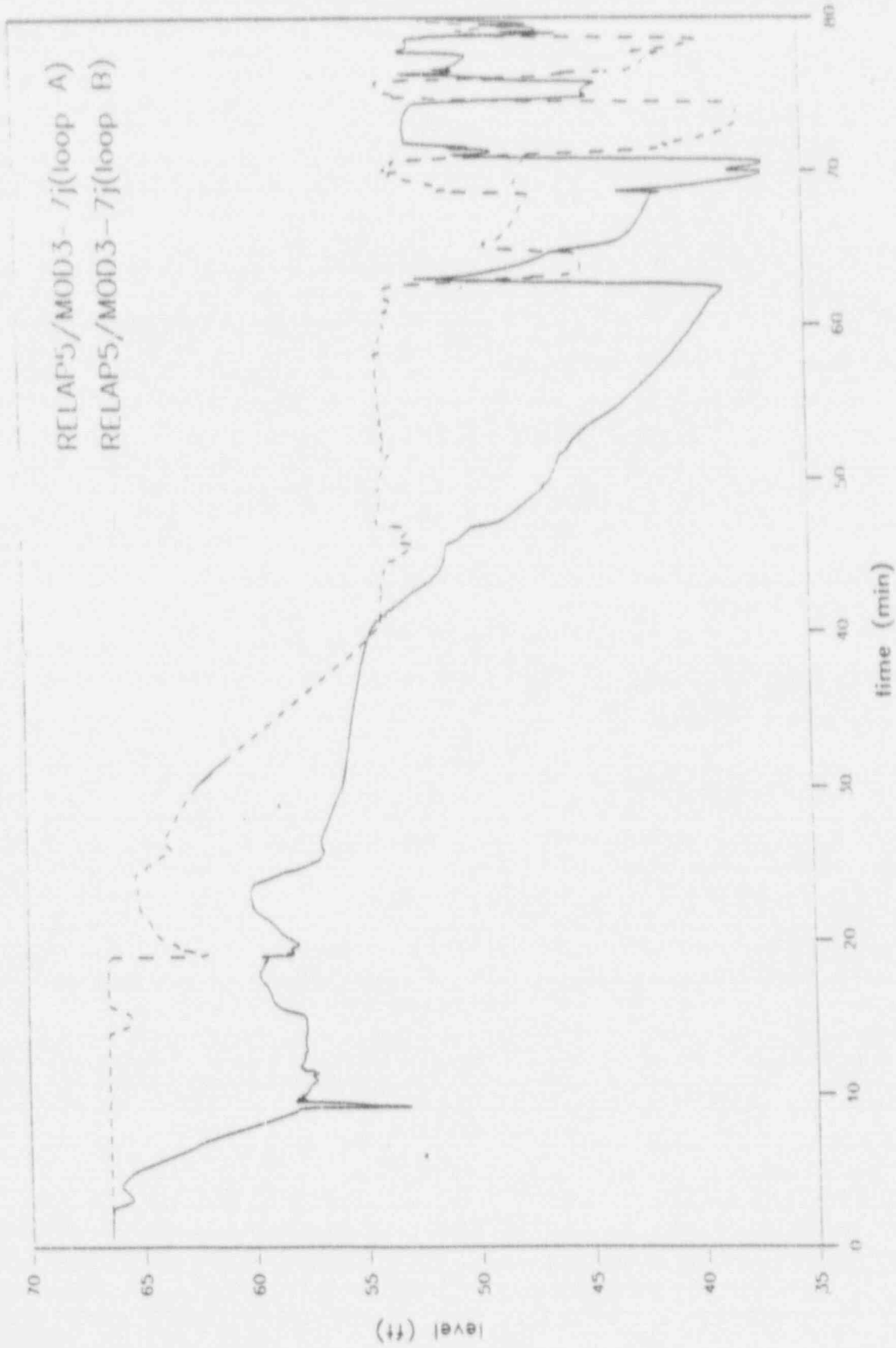


Figure A-3. Hot leg collapsed liquid level.

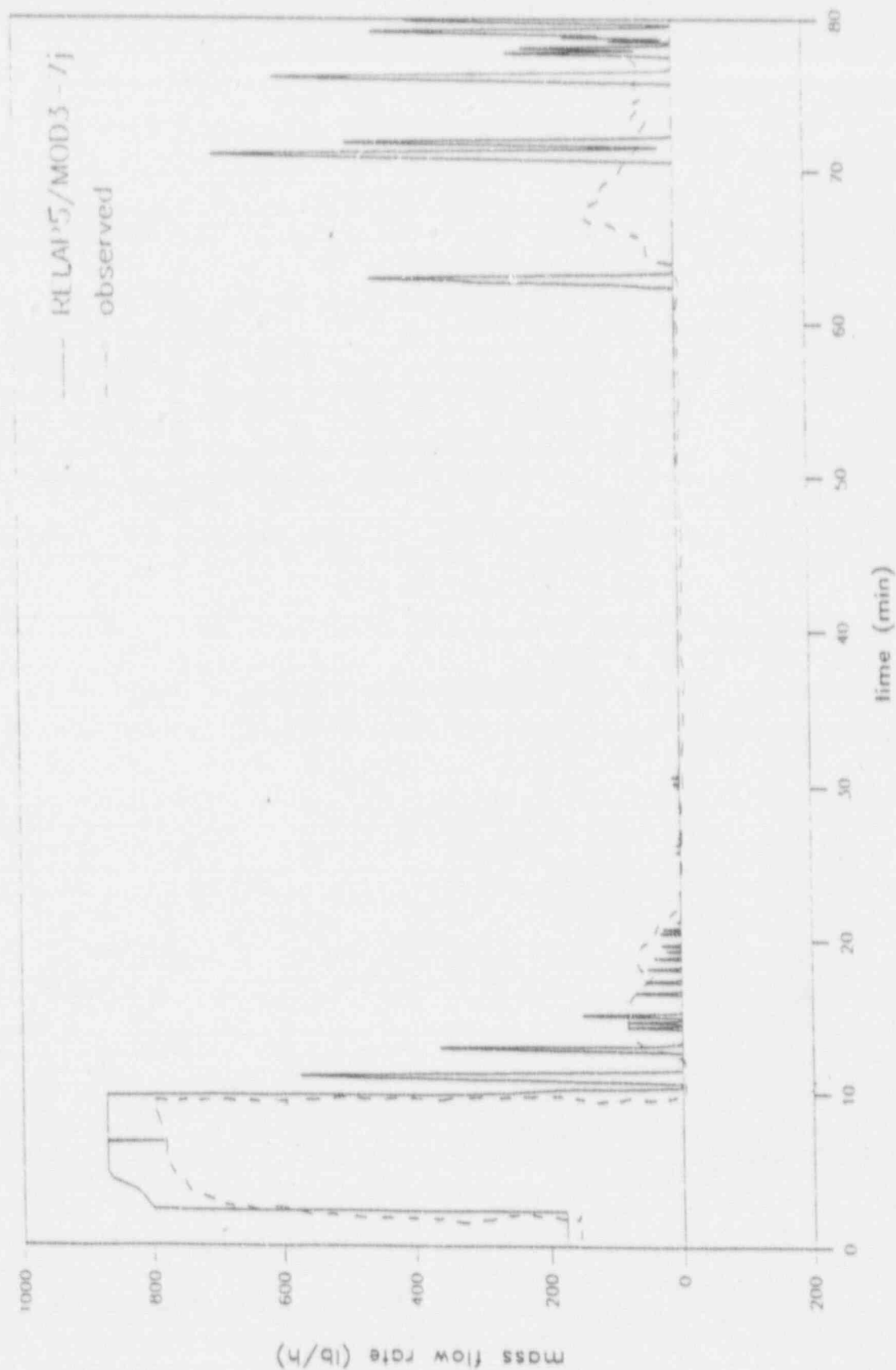


Figure A-4. Feedwater flow rate.

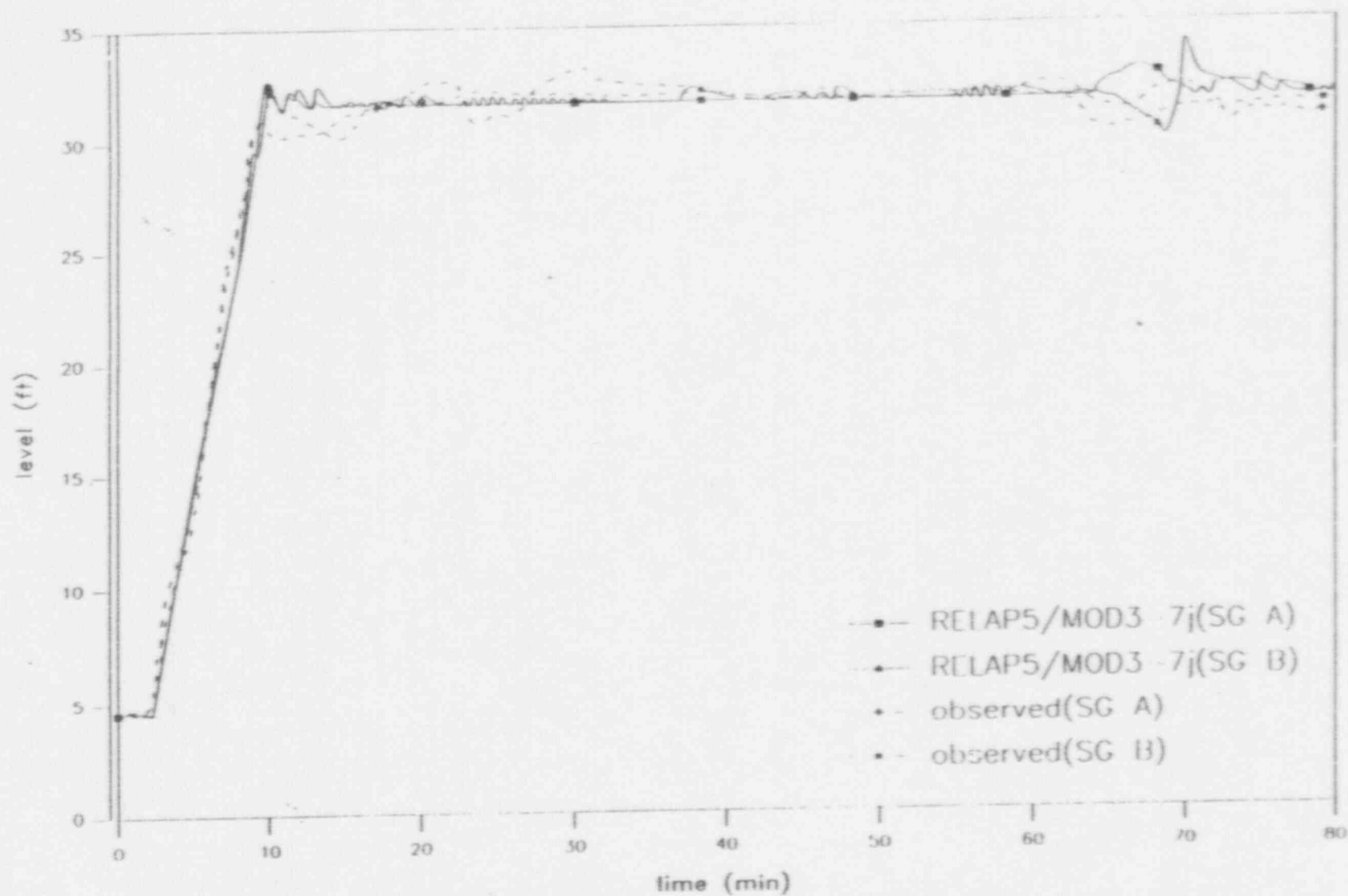


Figure A-5. Steam generator collapsed liquid level.



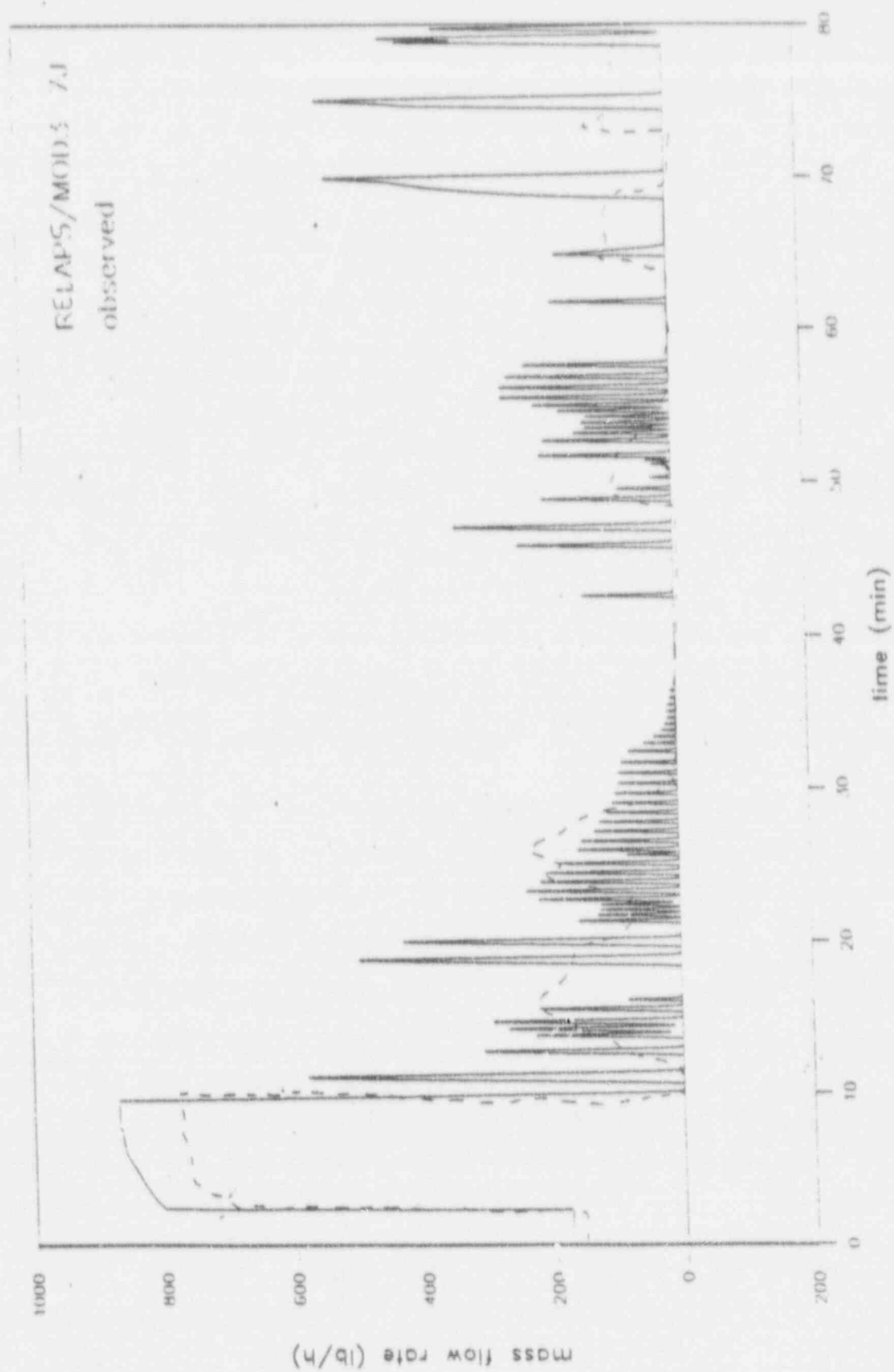


Figure A-6. Feedwater flow rate.

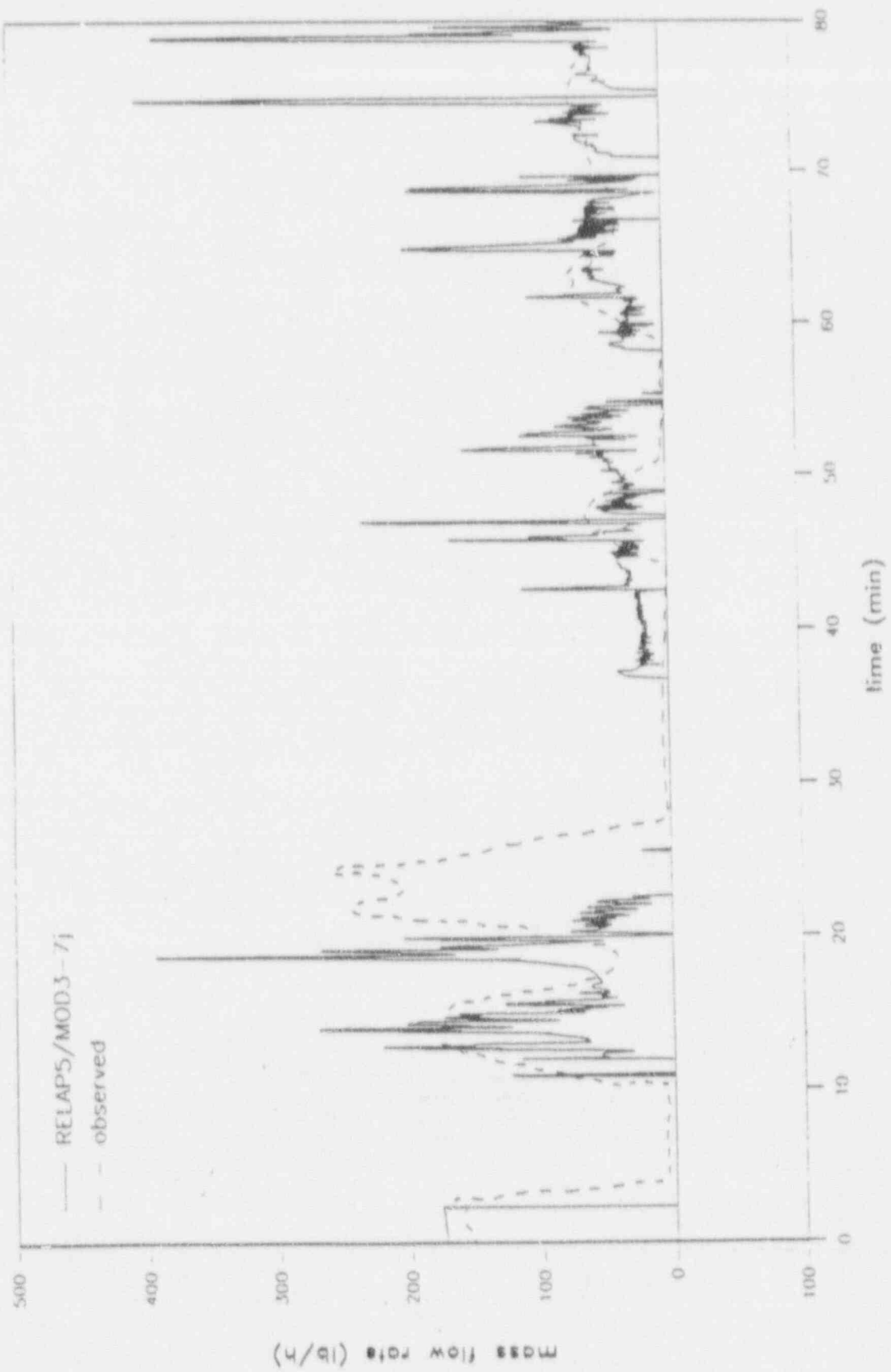


Figure A-7. Steam flow rate.

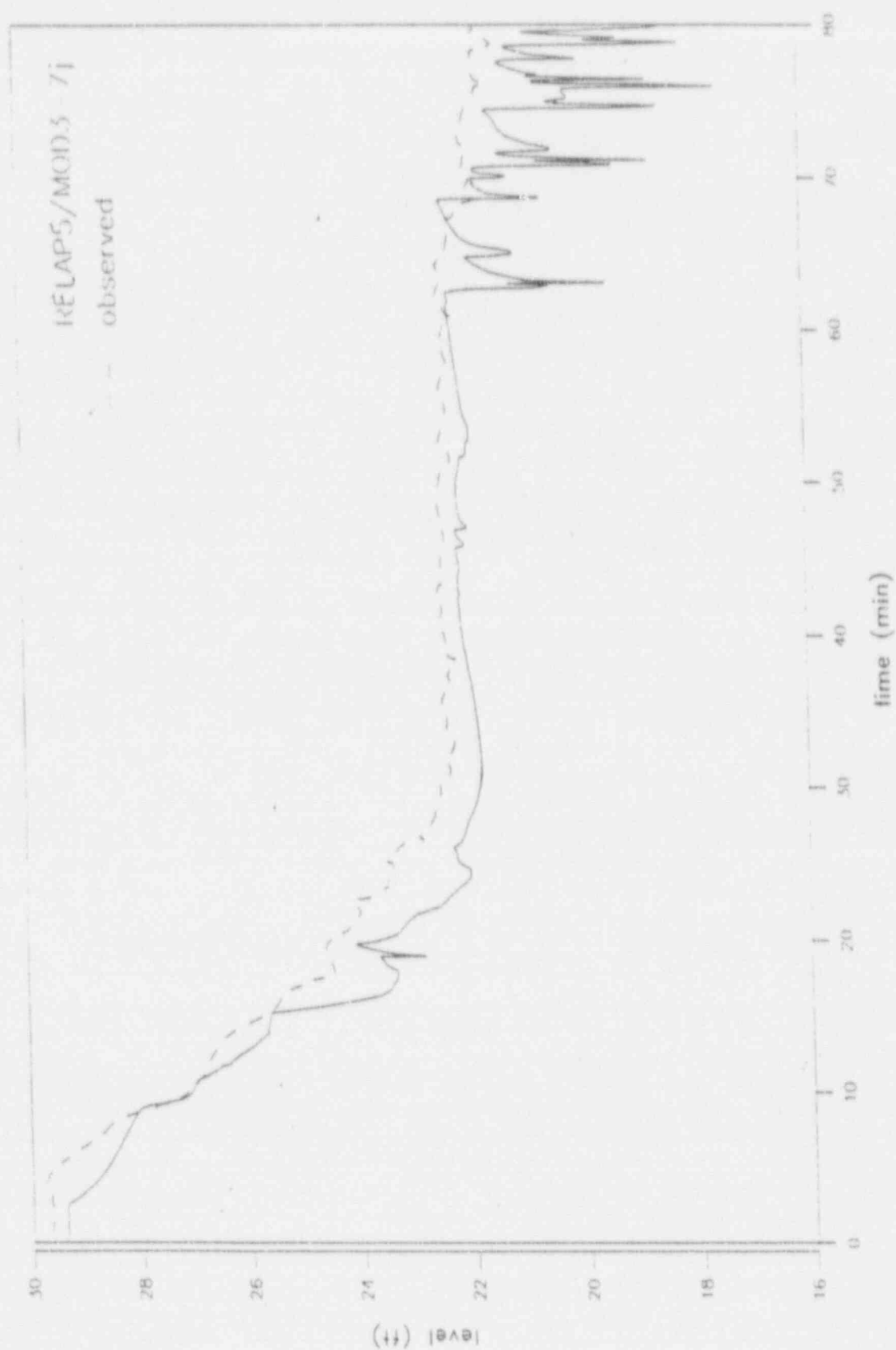


Figure A-8. Core collapsed liquid level.

pressure decreased in this stage due to the decay of core power.

The SG secondary pressure control affects the AFW flow in each SG. The AFW flow depends on the pressure control and is used to maintain the SG secondary liquid levels as illustrated in Figure A-6. During this stage, the broken loop AFW was on most of the time during both the test and the calculation. The intact loop AFW, as shown in Figure A-4 between transient time about 26 and 66 min, was off, but since the intact loop SG secondary pressure was well below the ATOG setpoint, the intact loop steam flow (Figure A-9) was zero at this stage.

The intact loop SG pressure remained constant at this stage, as illustrated in Figure A-10, when the AFW and the steam flows were off. The beginning of the AFW flow at 3,960 seconds marked the end of this stage and the beginning of the refill stage explained below.

**Phase 4.** Primary system refilling started at 3,960 seconds. The code calculated this event to occur at 3,780 seconds. At the end of Phase 3, the ATOG base setpoint pressure decreased to the intact loop SG secondary pressure, causing the AFW flow to be resumed. This caused condensation heat transfer, resulting in the increase in the primary to secondary heat transfer and a depressurization of the primary side, as shown in Figure A-2. This caused the HPI flow to exceed the leak flow. Because of this condensation, the liquid level in the intact loop hot leg, rose while it fell in the broken loop hot leg, as illustrated in Figure A-3. After refilling started, the levels in the loops increased. The primary system continued to depressurize rapidly in both the test and the calculation. After the start of the refill, the levels in the intact loop and the broken loops increased. The primary system continued to depressurize until the SG primaries were filled above the tube sheets. The transient was terminated at

4,800 seconds as in the experiment. See also Figures A-11 to A-14.

When the overall results are compared as depicted in Table A-2, it is observed that the RELAP5/MOD3 calculations for the Test 3109 AA are comparable to the experimental values and are reasonably calculated within the margin of error of the experimental values.

## ADDITIONAL OBSERVATIONS AND CONCLUSIONS

It was found that the primary mass inventory was highly dependent on the SBLOCA mass flow rate. This mass flow rate was in turn dependent on the coefficient of discharge used for the break flow. The results obtained by varying the coefficient of discharge of the break flow are included in Figure A-15. It was observed that with a Cd of 0.8, close agreement was obtained between the calculated mass flow rate through the leak and the observed flow rate. This indicates that accurate system modeling is required at the system boundaries.

Problems were also faced with the time step, in particular with the AFW spray insertions. It was found that very small time steps were necessary for reasonably accurate calculations. During the modeling phase, there was some difficulty experienced in the complex controller function required for the AFW. Since the AFW spray enters from the top of the SG and 2D effects of the spray could be modeled accurately. It was therefore necessary to renodalize the secondary side to simulate the spray insertion into the shell outer radius.

In conclusion, it can be inferred from Table A-2 and calculations that the RELAP5/MOD3 code performed well and predicted the major events and phenomena reasonably well. We believe that this code can be used for similar analysis and predictions.

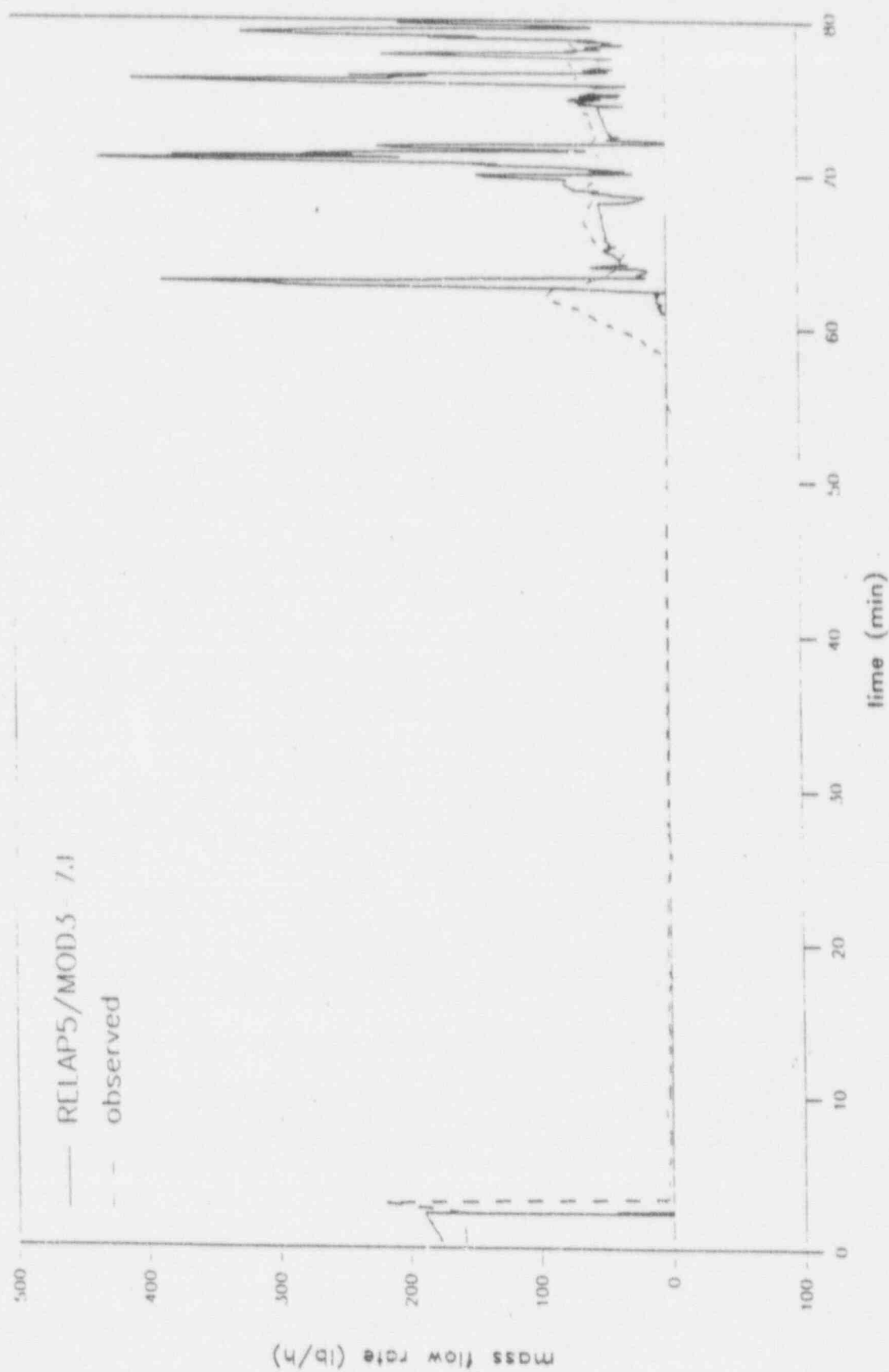


Figure A-9. Steam flow rate.



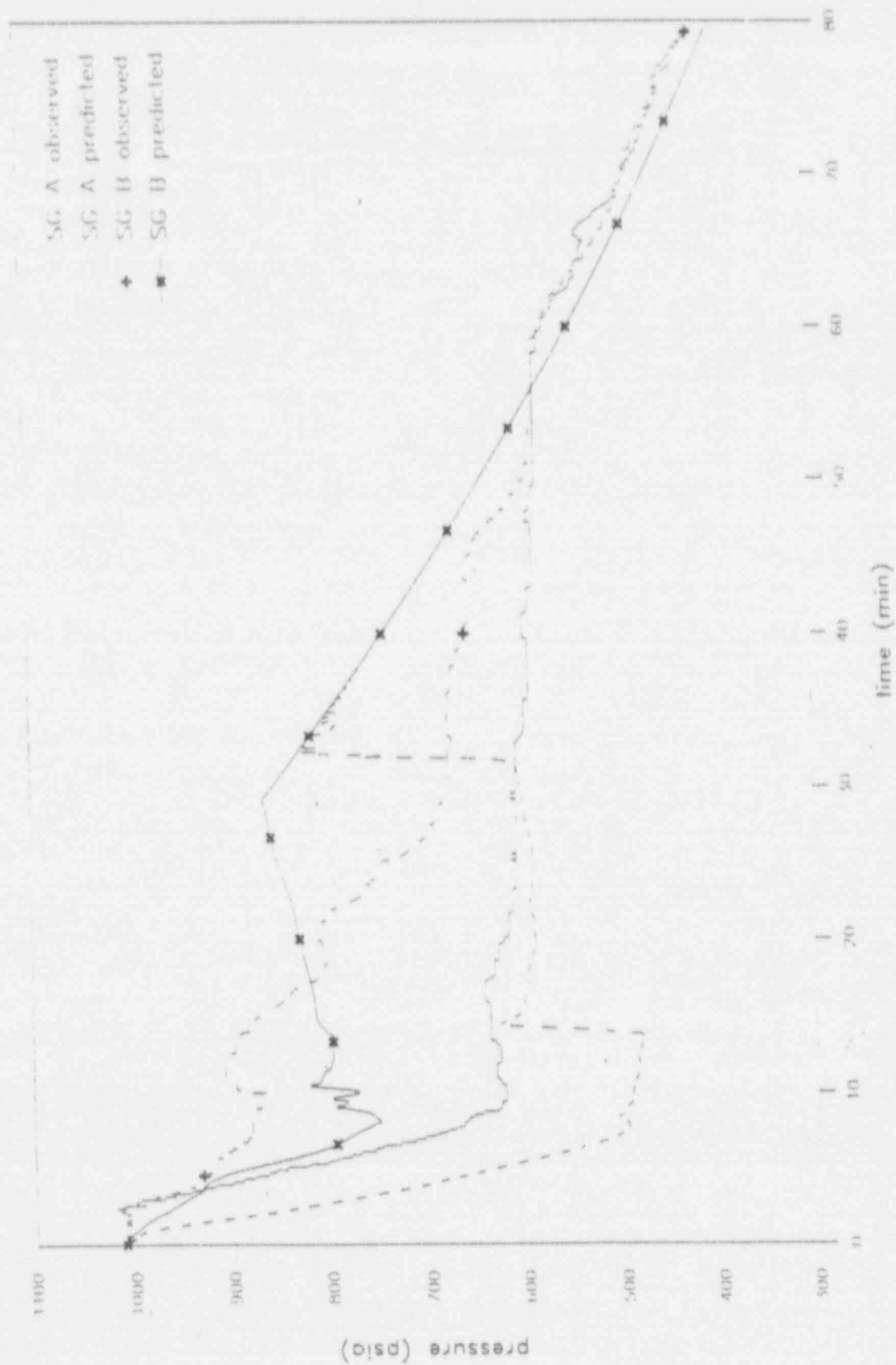


Figure A-10. Secondary system pressure.

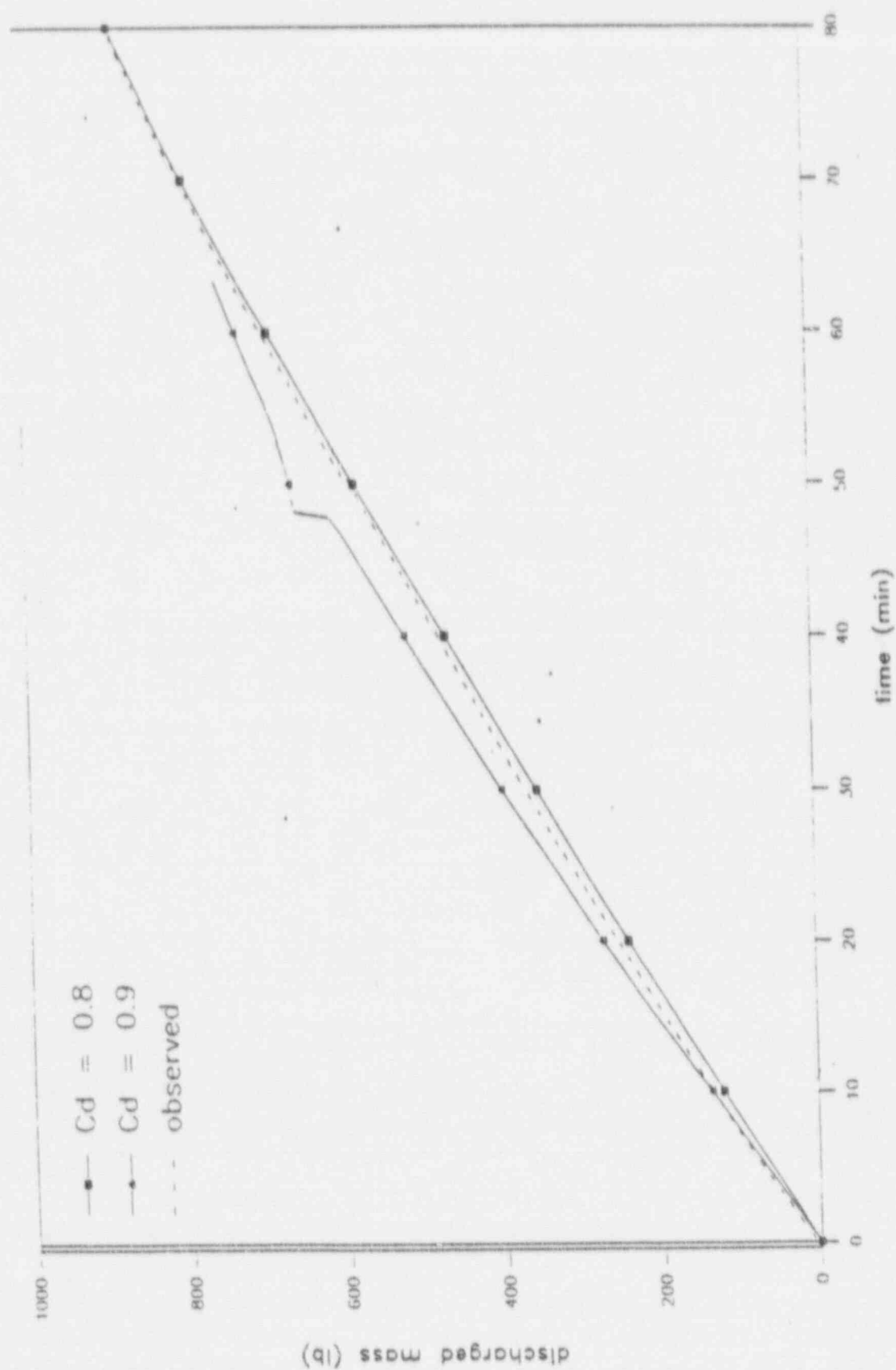


Figure A-11. Steam generator power.

NUREG/CR-5818

A-22

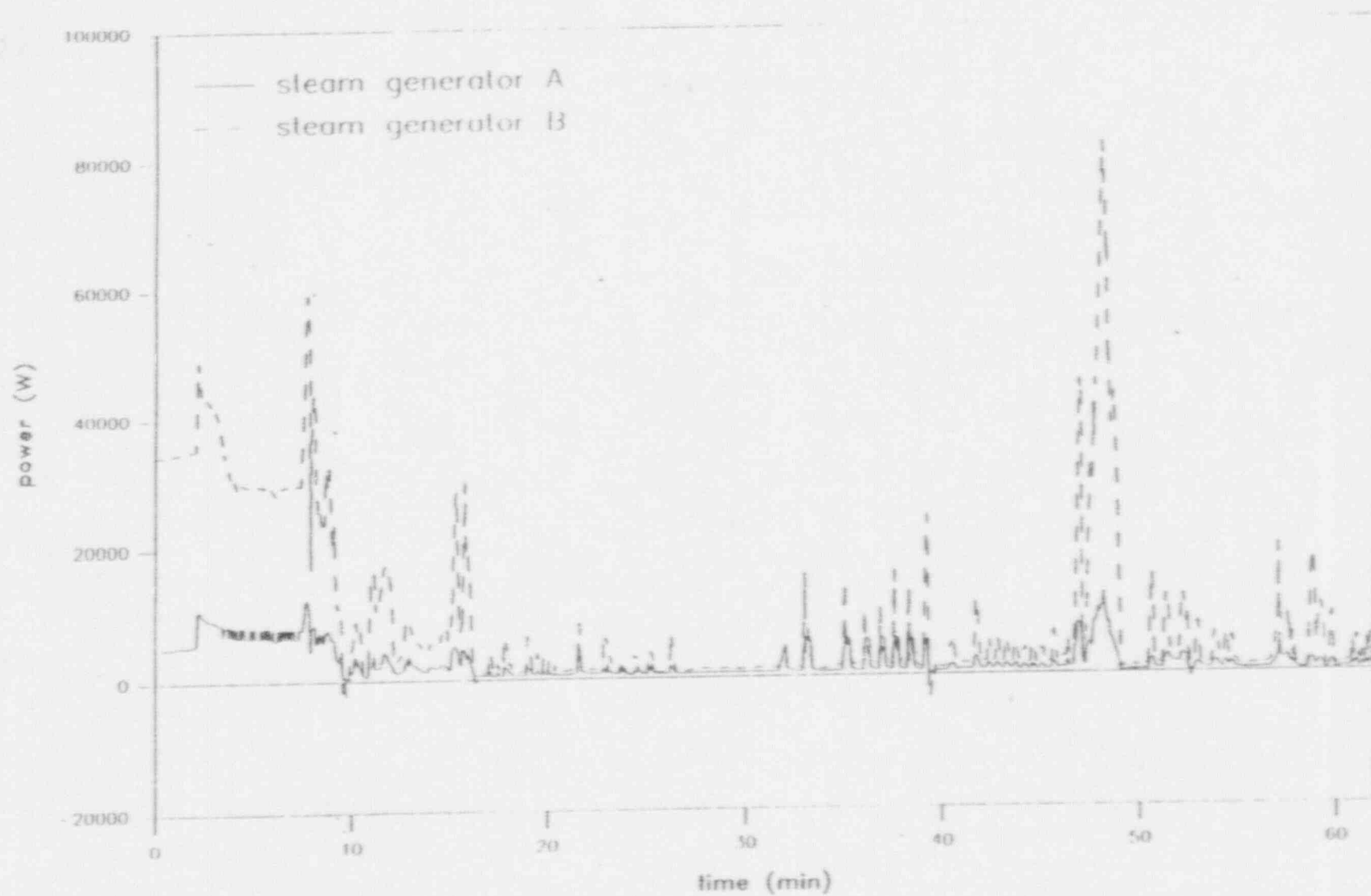


Figure A-12. Primary system mass inventory.

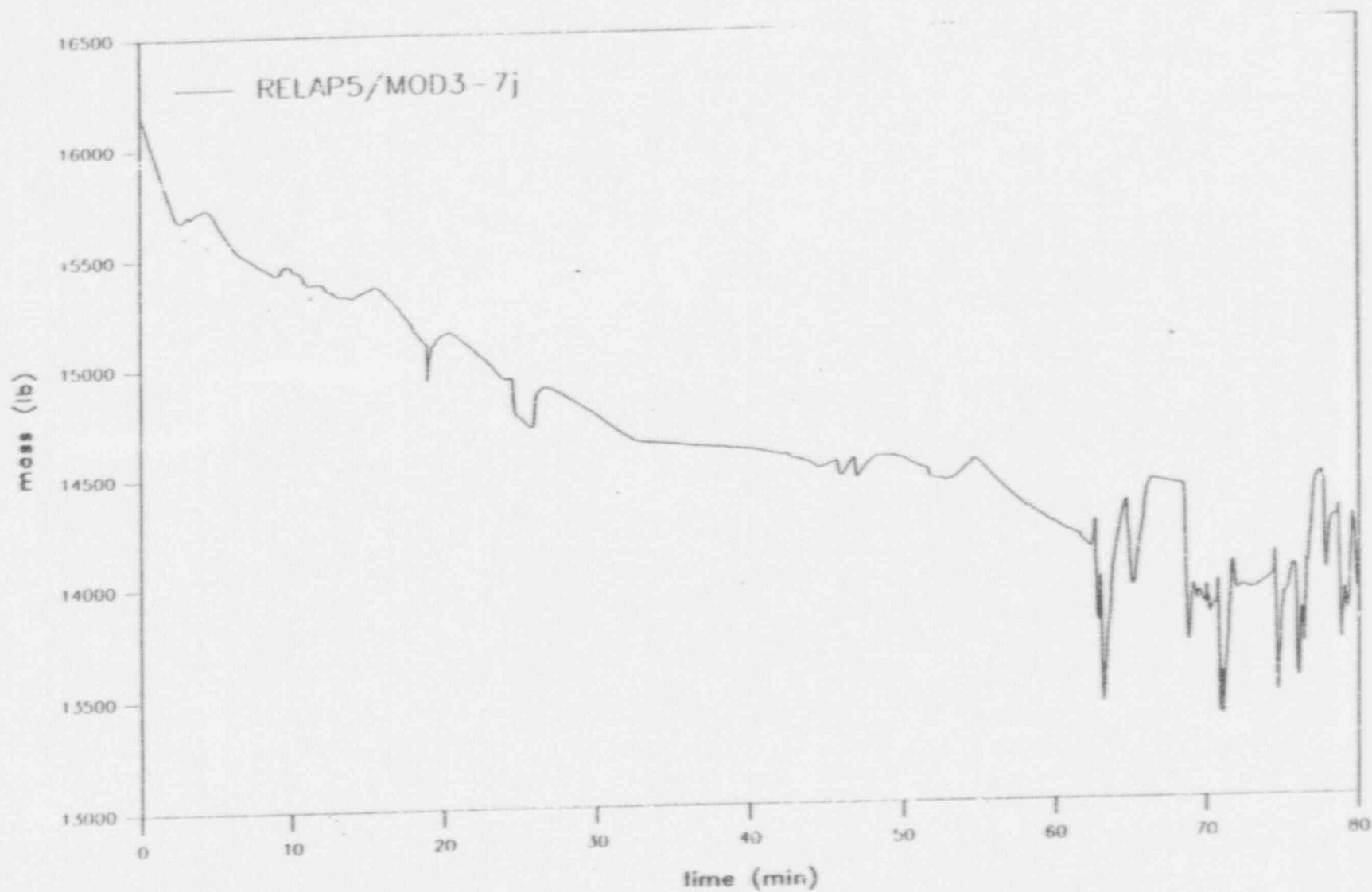


Figure A-13. Core exit temperature.

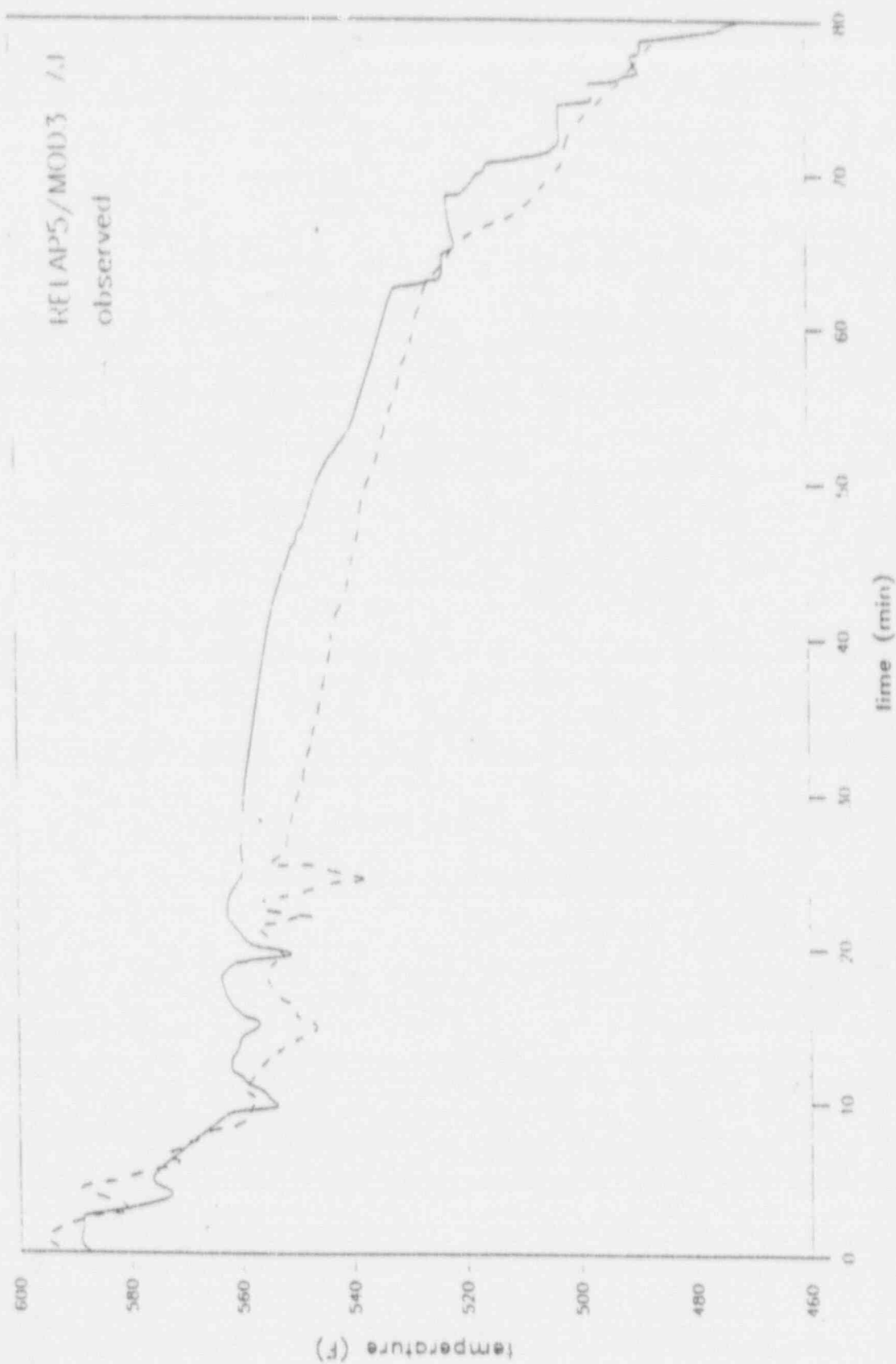


Figure A-14. Break mass flow rate.



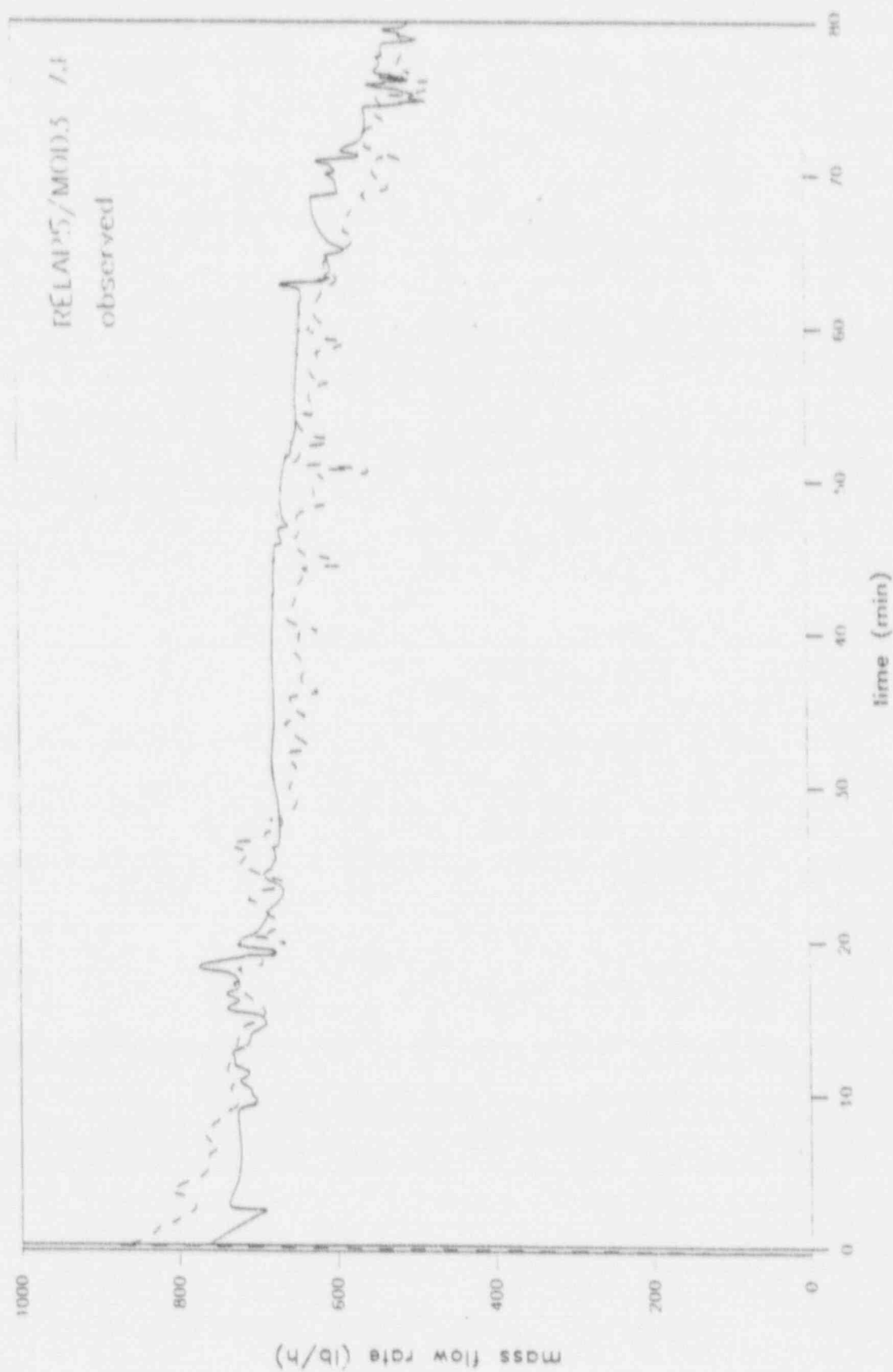


Figure A-15. Integrated break flow.

## REFERENCES

1. K. E. Carlson, R. A. Riemke, S. Z. Rouhani, R. W. Shumway, W. L. Weaver, *RELAP5/MOD3 Code Manual*, EGG-2596, June 1990.
2. R. A. Riemke, *Junction Based Interphase Drag and Vertical Stratification Modifications for RELAP5/MOD3*, EGG-EAST-8580, June 1989.
3. R. A. Dimena, J. R. Larson, R. W. Johnson, T. K. Larson, C. S. Miller, J. E. Streit, R. G. Hanson, and D. M. Kiser, *RELAP5/MOD2 Models and Correlations*, EGG-2531, August 1988.
4. D. C. Groeneveld, S. C. Cheng, and T. Doan, "1986 AECL-UO Critical Heat Flux Lookup Table," *Heat Transfer Engineering*, 7, 1-2, 1986.
5. G. B. Wallis, *One-Dimensional Two-Phase Flow*, New York: McGraw-Hill, 1969.
6. R. A. Riemke, *Report on CCFL and Interphase Drag Models for RELAP5/MOD3*, EGG-TFM-8012, February 1988.
7. W. L. Weaver, *Improvements to the RELAP5/MOD3 Choking Model*, EGG-EAST-8822, December 1989.

**Appendix B**  
**The Analytic Hierarchy Process**

## Appendix B

### The Analytic Hierarchy Process

The Analytical Hierarchy Process (AHP) is a tool used to accurately determine the relative importance of a group of selections with respect to some prescribed criteria. The process is explained and demonstrated here by applying it to the situation of interest to this report.

In this case, the objective is to establish the relative importance of the plant components relative to the primary safety criteria, for each phase of the transient. To illustrate the application of AHP, we chose Phase 2 of the transient (two-phase natural circulation), for which only six plant components were considered. These are

1. The upper vessel: upper plenum, hot leg, and U-bend
2. Steam generator (SG)
3. Break
4. Cold side: cold leg, vent valve, and downcomer
5. Lower vessel: lower plenum and core
6. High-pressure injection (HPI).

The primary safety criteria were: (a) peak clad temperature (PCT) and (b) core liquid inventory.

Let's assume that, in the context of the primary safety criteria chosen, the components listed above have the absolute rankings *a*, *b*, *c*, *d*, *e*, and *f*, which correspond to the way in which they are listed and are unknown at this point.

The panel of experts was asked to rank these phenomena in pair-wise fashion (importance of component *i* only with respect to component *j* only), according to their knowledge and experience, and with respect to the primary safety criteria. The scale chosen to quantify this importance was ranged from 1 to 5. If the phenomena *i* was much more important than *j*, then it was given a relative rank of 5; if *i* was only slightly more important than *j* it was given a relative rank of 3; and for equal importance the rank was 1. If on the other hand, *i* was much less important than *j*, the rank was 1/5; if *i* was only slightly less important than *j*, it was given a 1/3.

A ranking matrix was established and the experts were asked to rank by rows, comparing row element *i* versus column element *j*. Only the upper half of the matrix, above the diagonal, (*i* vs *j*) needed to be filled in; the bottom half (*j* vs *i*) was entered accordingly. The results are shown in Table B-1.

If one could evaluate absolute values of importance, and in these case those values were *a*, *b*, *c*, *d*, *e*, and *f*, what the experts are doing is estimating the following matrix, in which we use the absolute rankings.

**Table B-1.** Two-phase natural circulation phase.

$\Phi 2$	Upper vessel	SG	Break	Cold side	Lower vessel	HPI
Upper vessel	1	3	1/3	3	5	1
SG	1/3	1	1/3	3	1	1/3
Break	3	3	1	3	5	1
Cold side	1/3	1/3	1/3	1	3	1/3
Lower vessel	1/5	1	1/5	1/3	1	1/3
HPI	1	3	1	3	3	1

Sum the elements of each column and define the following variables:

COLUMN SUM	S/a	S/b	S/c	S/d	S/e	S/f
------------	-----	-----	-----	-----	-----	-----

where  $S = a + b + c + d + e + f$ .

Notice that this last row already summarizes an inverse relative ranking of all components. However, because of likely inconsistencies in the ranking, we continue to process further to include more of the information in the final result. Note that inconsistencies do not disqualify the expert opinion. An important source of inconsistency is the ranking scale itself, which is limited to a discrete set of values. If we divide each element of each column by the corresponding column sum, we then have:

If the original estimates are exact, this matrix has identical columns. In such an unlikely event, we need not proceed any further. In our case however, we need a few more steps to refine the answer.

The next step is to generate a new column by averaging the elements in each corresponding row and finally normalize with respect to the greatest value. In theory this corresponds to the following results:

The final rankings are then obtained from the normalized rankings by scaling them according to the scale of choice. For instance, if one wants the final ranks to be from 1 to 9, the lowest normalized rank is assigned a 1, the largest a 9, and everything in between is ranked proportionally.

If the hierarchy has one more level, as it is in our case, then the normalized rankings are kept as weighing factors to be used later. The items in the next level, the phenomena in each component, are ranked the same way as the components have been ranked. The process is conducted to rank the phenomena in the context of each component. The final ranking of each phenomenon in each phase of the transient is then a composite of these rankings.

The application of AHP used in this report deviates somewhat from Saaty's original scheme.

To demonstrate both the orthodox application and the modified version, let's consider only one phase of the transient and a generic set of components and phenomena.

In which all rankings indicated are normalized (0-1), as results from the matrix operation described earlier.

The unmodified procedure defines the final phenomena rankings as follows:

1. All rankings are re-normalized so that their sum in each component adds up to 1. The sum of the component rankings will also add up to unity.
2. For each phenomenon a composite rank is developed adding the contributions of its normalized rank in all components:

$$r1 = a \cdot A1 + b \cdot B1 + c \cdot C1$$

$$r2 = a \cdot A2 + b \cdot B2 + c \cdot C2$$

$$r3 = a \cdot A3 + b \cdot B3 + c \cdot C3$$

$$r4 = a \cdot A4 + b \cdot B4 + c \cdot C4$$

$$r5 = a \cdot A5 + b \cdot B5 + c \cdot C5$$

3. The final results are scaled to the scale of choice (i.e., 1 to 9) as described earlier.

**The Modified Procedure.** In our application, this approach is not always appropriate. Not all phenomena are present in all components; thus, if one component has many phenomena and another component has only one phenomenon, the resulting rankings may be unfairly biased. Also, if a phenomenon occurs throughout the plant, its final ranking may be unreasonably higher than that of a phenomenon that, although important, is localized in specific components (i.e., wall heat transfer vs. ECCS flow). To eliminate these source of bias, the procedure was modified (by R. Dimenna of Savannah River Laboratory) as follows:



1. All rankings are renormalized with respect to the highest rank. This is done at the component level, and at the phenomenon level for each component. Thus, the sums of the rankings no longer equal one.
2. The compound rankings are evaluated in each component, without adding the contributions from other components; thus:

$$\begin{aligned}\text{In A} \quad r1 &= a \cdot A1 \\ r2 &= a \cdot A2 \\ &\dots\end{aligned}$$

$$\begin{aligned}\text{In B} \quad r1 &= b \cdot B1 \\ r2 &= b \cdot B2 \\ &\dots\end{aligned}$$

$$\begin{aligned}\text{In C} \quad r1 &= c \cdot C1 \\ r2 &= c \cdot C2 \\ &\dots\end{aligned}$$

3. The final rank of each phenomenon is the maximum rank for that phenomenon found among all components. These ranks are then scaled to the final integer scale of 1 to 9.

The results that each expert panel obtained (Appendix II of this report) were obtained through this modified procedure. The final phenomena rankings in the resolution section of the report did not have component rankings as an intermediate step.

**The Measurement Of Consistency.** As noted in the previous section, if the matrix representing the experts opinion is truly consistent, the rank of all components can be identified in every column and every row. However, two sources of inconsistency affect this result:

1. As mentioned before, the discrete set of values chosen to indicate the pair-wise rankings are not necessarily accurate enough to include all values of  $i/j$ . This will result in some inconsistencies between the rankings in different rows or columns. It is likely, as is evident in the chosen example, that in some rows (or columns) some items are

ranked equally while in other rows (or columns) a difference is indicated.

2. The experts perception of importance in a pair-wise comparison, does not have to adjust to the entire set of choices and therefore remain consistent throughout the process. That is, the experts may remember or become aware of additional pertinent information about the items being ranked, which may affect the way they view comparisons later in the process.

Thus, the final ranking that results in the described process, includes a systematic average of all the information presented by the panel of experts. Despite the limitations of the process, it is still our objective to determine a consistent ranking. Therefore a measurement of consistency needs to be implemented to define our level of tolerance in the results. The following method is proposed by Saaty.<sup>1</sup>

Let's consider the matrix of pair-wise comparisons  $A$ , and the vector of absolute rankings  $w$ . The product

$$A \cdot w = (n \cdot a, n \cdot b, n \cdot c, \dots) = n \cdot w \quad (1)$$

where  $n$  is the order of the square matrix  $A$ .

It follows that:

$$A \cdot w - n \cdot w = 0$$

$$\text{or} \quad (A - n \cdot I) w = 0$$

where  $I$  is the identity matrix.

Thus, for a perfectly consistent matrix,  $w$  is the matrix eigenvector and  $n$ , the order, is the matrix eigenvalue.

Since we don't have a perfectly consistent matrix, we will find eigenvalues different from  $n$ . Our measurement of inconsistency can then be examined by the "approximate" eigenvalues departure from  $n$ . This can be estimated by using our matrix  $A$  (experts opinion) and the estimated eigenvector  $w$  (which we obtained through our manipulation of the information) and solve for an average  $n$  in Equation (1).

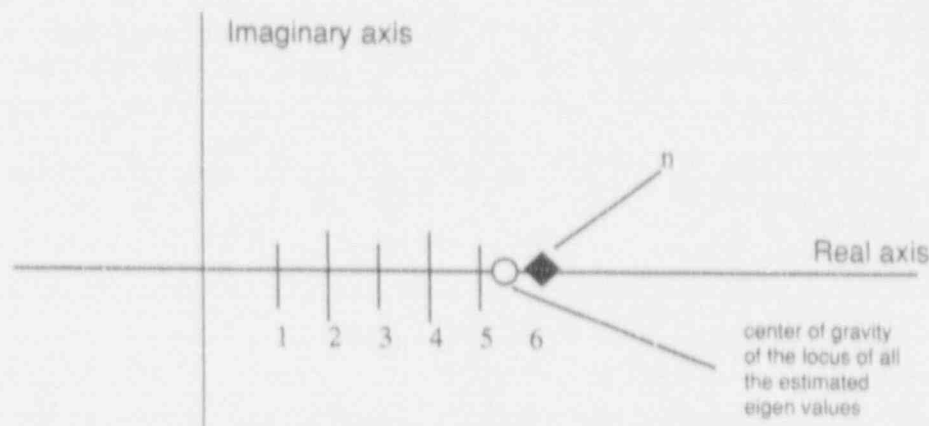
## Appendix B

$$A \cdot w = n \cdot w$$

1	3	1/3	3	5	1		1.292		5.268
1/3	1	1/3	3	1	1/3		0.613		5.034
3	3	1	3	5	1	×	1.841	=	6.556
1/3	1/3	1/3	1	3	1/3		0.515		6.25
1/5	1	1/5	1/3	1	1/3		0.349		6.467
1	3	1	3	3	1		1.389		5.865

$$n = 35.44/6 = 5.906$$

Graphically, in the complex plane, what we have done can be described as follows:



Saaty<sup>1</sup> defines a consistency index,  $CI$ , as follows:

$$CI = \frac{\text{deviation from } n \text{ per unique weighting ratio}}{(n - n_{\max})/(n-1)}$$

which in our case translates into:  $(6 - 6.556)/5 = 0.1112 = CI$ .

Furthermore, Saaty defines a consistency ratio, which compares the deviation at hand, using  $CI$ , with the deviation that a randomly generated

matrix of comparisons would have. It is implied that a randomly generated matrix has the largest departure from consistency. For a random matrix of order 6 the  $CI$  is 1.24. Thus,

$$CR = 0.1112/1.24 = 0.0897.$$

Saaty recommends that a  $CR$  of less than 0.1 is an acceptable measure of consistency. However, we have found that for large matrices this criterion is hard to fulfill. Other researchers have reported similar results.<sup>2</sup> We recommend that the best validation of the final result is the expert's agreement that the relative rankings are satisfactory.

## REFERENCES

1. T. L. Saaty, *Decision Making for Leaders*, Celmont, CA: Lifetime Learning Publications, 1982.
2. B. L. Golden, E. A. Wasil, P. T. Harker (editors), *The Analytic Hierarchy Process: Application and Studies*, New York: Springer-Verlag, 1989.

## **Appendix C**

### **Probabilistic Analysis of Small-Break LOCA Level in a B&W Reactor**

## Appendix C

### Probabilistic Analysis of Small-Break LOCA Level in a B&W Reactor

Gerald S. Lellouche  
TDA, Inc.

The series of 33 RELAP5MOD3 calculations listed in Table 8-2 provided 16 two-sided sensitivity results for the variation of the eight parameters considered of importance as well as 16 double and triple variations. These results were examined and a regression analysis was performed to establish the most appropriate surface to fit through the data. A Monte Carlo analysis was then used to prepare a probability distribution function for the random realization of the eight parameters given their presumed statistical behavior.

The results of the sensitivity studies when plotted showed a very linear behavior with the one exception of the interphase drag coefficient variation, which seemed quadratic. We begin the regression analysis with a linear surface and proceed upwards to a quadratic and then add cross terms. The results of this regression study are found in Table C-1. It can be seen that varying the number of terms from 9 to 25 has relatively little effect on the RMS error. With only 33 total data points available, it was recognized that further

small increases in the number of unknowns in the algebraic surface could bring the RMS error down to zero; hence the RMS error could not be used as a decision maker. Indeed, the RMS error was never less than 0.010, while the average deviation from the nominal was 0.0556; hence, the RMS error indicates a rather poor fit for all the surfaces considered. Alternatively, since the nominal value is unity and the maximum and minimum values calculated were 1.0701 and 0.9664, the RMS error can also be looked at as being hardly more than a one percent error. In either case, the RMS error is not appropriate to use as the sole deciding factor. As a result of this decision, we moved on to a Monte Carlo assessment.

Although Table 7-2 shows that the underlying probability distributions are a mix of normal and uniform, it was decided to examine the effect of normality by considering two separate cases:

- All underlying distributions are uniform
- Distributions are as specified in Table 7-2.

**Table C-1.** Regression results.

Model number	Model type	Number of terms	RMS error
1	Linear + constant term	9	0.013247
2	Type 1 + squared terms	17	0.014240
3	Type 1 + cross term (1,2)	10	0.013388
4	Type 2 + cross term (1,2)	18	0.014210
5	Type 1 + cubic cross terms (1,2; $\chi$ : $\chi = 2 - 8$ )	16	0.011264
6	Type 2 + cubic cross terms (1,2; $\chi$ : $\chi = 1 - 8$ )	25	0.010559



We interpret the  $\pm 2s$  values of the normal distributions as the end points of uniform distributions and proceed with our analysis.

Table C-2 shows a preliminary Monte Carlo assessment of these six surfaces using 2,000 histories and the assumption of uniform distributions for the parameters. One will observe that the maximum difference in the mean values between the models is hardly different from the RMS error of the model with respect to the data. This indicates to us that these models are all essentially the same statistically and that there is little reason to choose between them. As a result, we choose to examine the two models with the smallest and largest standard deviations. These will be referred to as the "best" (most optimistic) and "worst" (most conservative) models because we expect that the larger the standard deviation the broader the distribution and the lower the possible vessel water level (hence, most conservative or "worst"), and vice versa. Hence the regression models we consider are Models 3 and 6.

Table C-3 shows the 100,000 history results for the two models. Although we do not show them,

the maximum change in the mean and standard deviations for both models is less than one in the third significant figure as we vary the number of histories from 25,000 to 100,000, while the probability (level  $< 0.85$  of nominal) is never greater (in the "worst" model) than  $4 \times 10^{-5}$  (at 25,000 histories). Because even at 105 histories there is only one hit below a level of 0.85 of nominal, this number has a relatively large uncertainty; none the less, it is unlikely to reach higher than the  $4 \times 10^{-5}$  value found at 25,000 histories where there was also only one hit below 0.85.

Figures C-1 and C-2 show the normalized frequency distributions which we interpret as probability distribution functions (pdf). Figures C-3 and C-4 show the respective cumulative distribution functions. It is noted that there is a lack of smoothness in the pdf and this is a result of the fact that we have used 200 bins in the interval 0.75 - 1.2. In Figure C-5, for example, we repeat the binning process with 100 bins and find a much smoother result. It is likely that a more refined bin distribution would remove the residual oscillations. The following Monte Carlo studies all use 100 bins.

**Table C-2.** All uniform parameter distributions preliminary Monte Carlo assessment using 2,000 histories.

Model number	Mean	Standard deviation
1	0.9891	0.0286
2	0.9942	0.0315
3	0.9893	0.0272
4	0.9963	0.0327
5	0.9895	0.0387
6	0.9972	0.0405

**Table C-3.** 100,000 history Monte Carlo study of Models 3 and 6.

Model number	Mean value	Standard deviation	Probability (level $< 0.85$ of nominal)
3	0.9895	0.0280	0.0
6	0.9961	0.0408	$1 \times 10^{-5}$

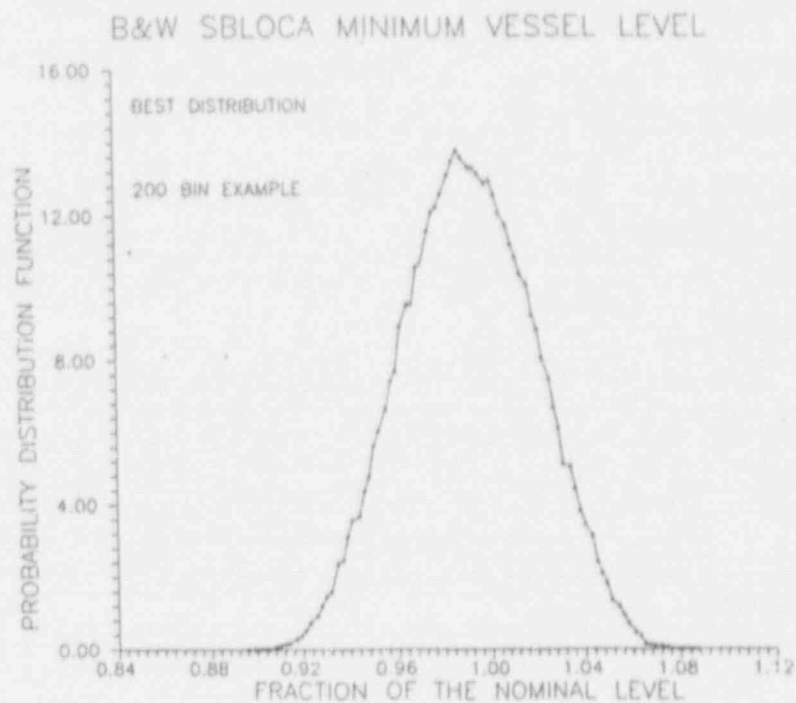


**Figure C-1.** B&W SBLOCA minimum vessel, probability distribution function of 200-bin example: best distribution.

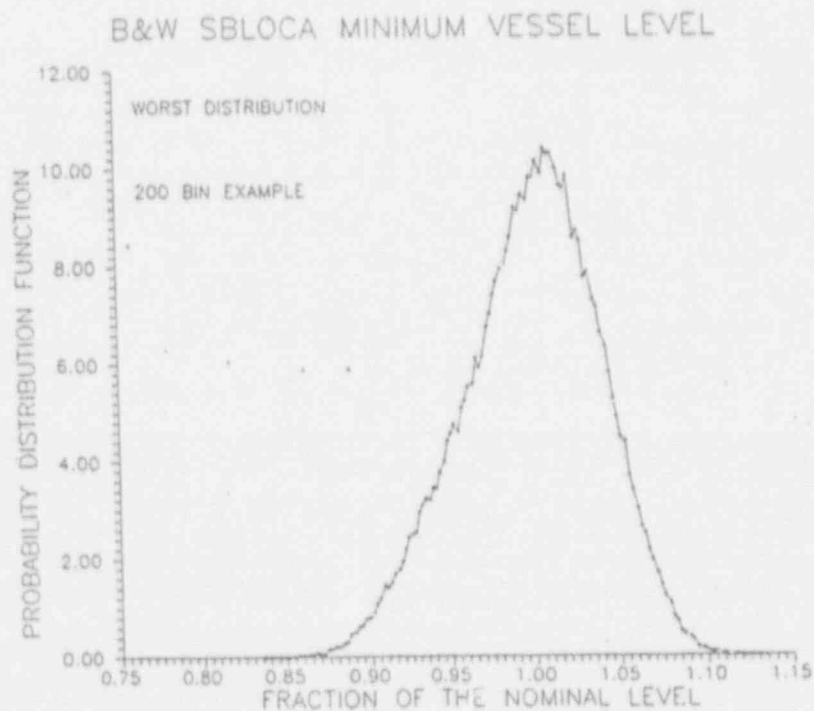


**Figure C-2.** B&W SBLOCA minimum vessel, probability distribution function of 200-bin example: worst distribution.

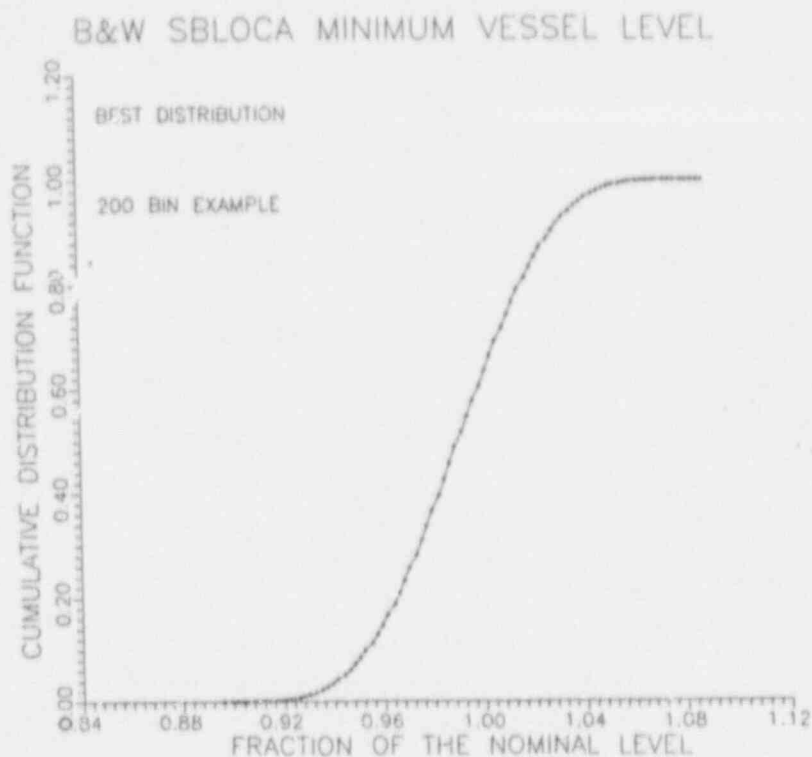


**Figure C-3.** B&W SBLOCA minimum vessel, cumulative distribution function of 200-bin example: best distribution.

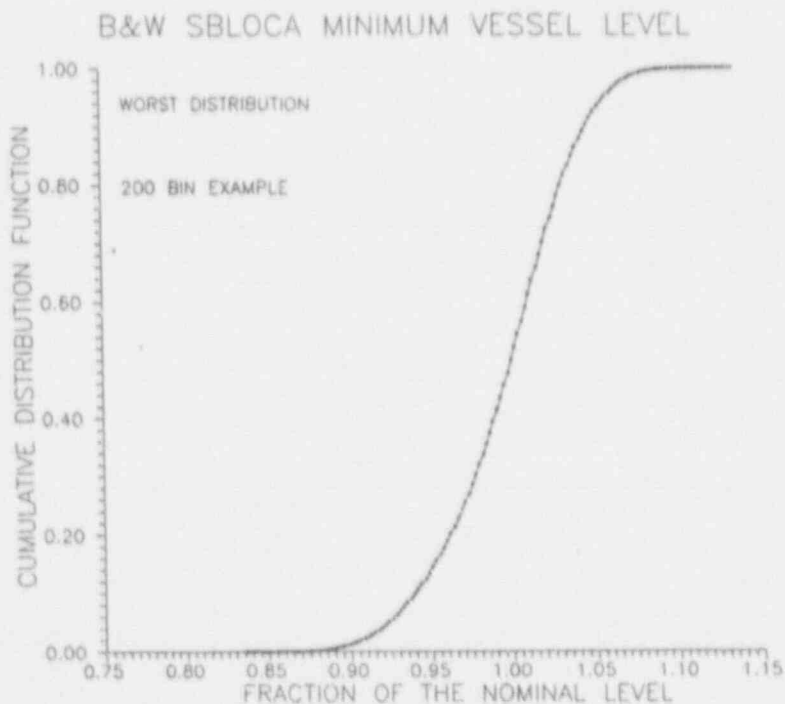


**Figure C-4.** B&W SBLOCA minimum vessel, cumulative distribution function of 200-bin example: worst distribution.

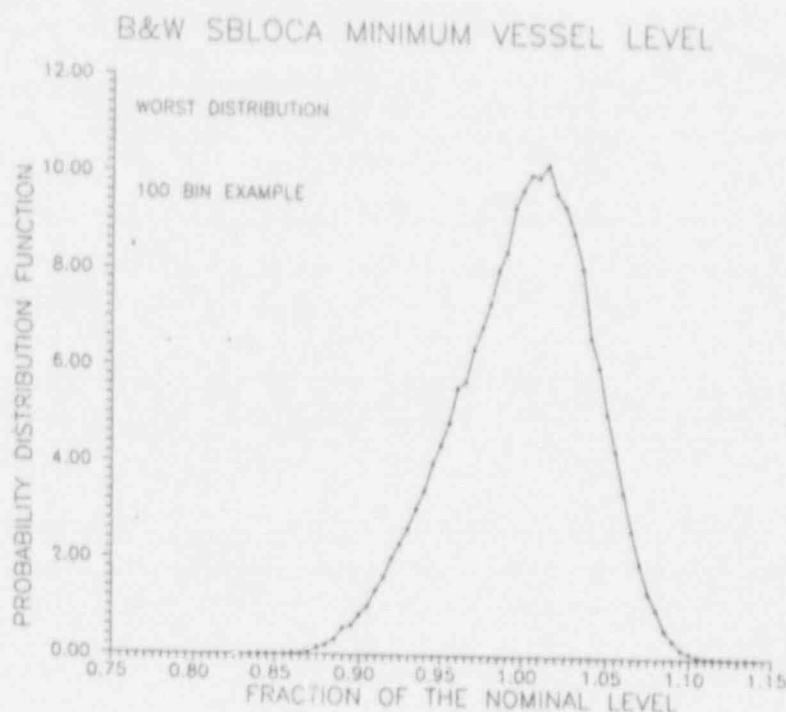


**Figure C-5.** B&W SBLOCA minimum vessel, probability distribution function of 100-bin example; worst distribution.

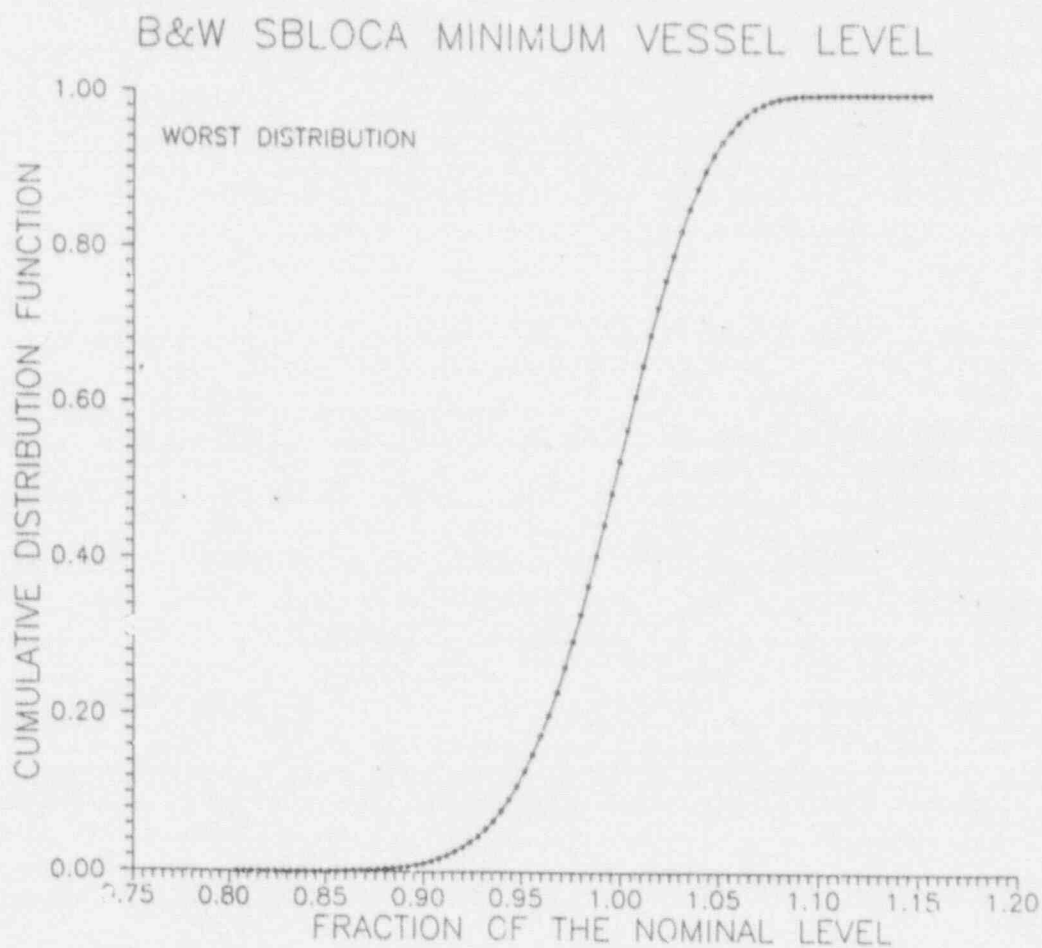
We move on now to a repetition of these tables and figures for the mixed normal/uniform case. In Table C-4, we repeat the sample Monte Carlo study used to produce Table C-2. The results are nearly identical in determining which model has the largest and smallest standard deviation. There are no important differences found here. Figures C-6 and C-7 show the cumulative distribution functions for the best and worst cases, while Figures C-8 and C-9 show the underlying pdfs. It will be noted that the jagged results of the earlier studies are much less apparent here because the centralizing probabilities are much higher due to the normal distributions. Table C-5 shows the same statistical characteristics seen in Table C-3. However, the probability of the level lying below 0.85 of nominal is  $4.5 \times 10^{-4}$ , many times larger than in the uniform case.

The reason for the larger low end behavior is undoubtedly due to the larger tails of the normal distributions and the fact that these particular parameters dominate the cross terms. One may conclude then that tail probabilities will be impacted by the choice of tail behavior in the underlying parameters (a fairly obvious conclusion). However, it is fairly clear that in this case the gross statistical behaviors—mean, standard deviation, etc.—are hardly affected.

The conclusions of this study are fairly clear. Within the expected range of the parameters found to be significant to this SBLOCA in this B&W reactor representation, there is no meaningful likelihood of core uncover.

**Table C-4.** All uniform parameter distributions preliminary Monte Carlo assessment using 2,000 histories.

Model number	Mean	Standard deviation
1	0.9890	0.027
2	0.9924	0.029
3	0.9889	0.027
4	0.9946	0.03
5	0.9861	0.037
6	0.9944	0.038

**Figure C-6.** B&W SBLOCA minimum vessel, cumulative distribution function of 100-bin example: worst distribution.



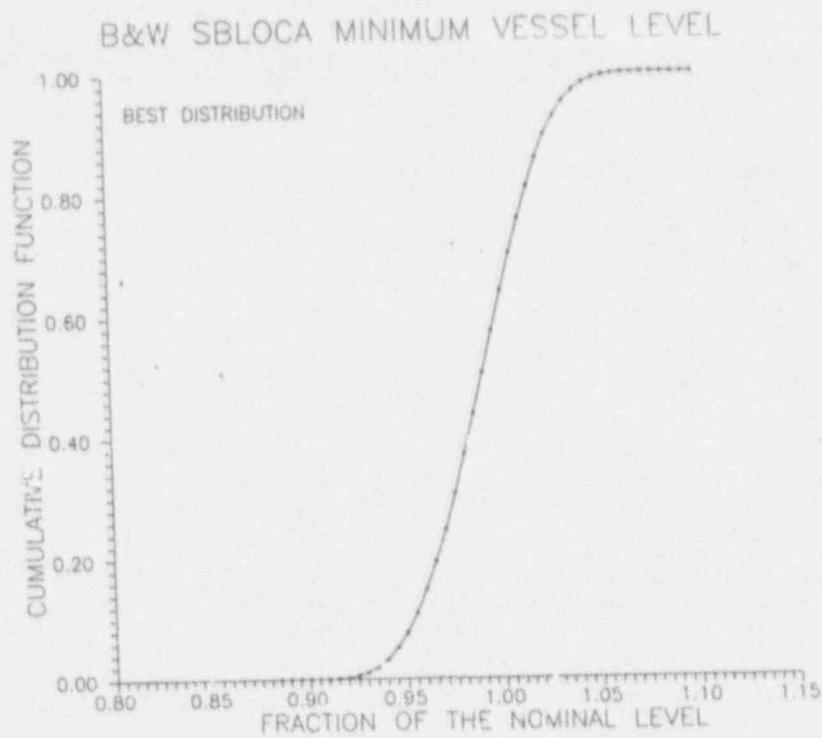


**Figure C-7.** B&W SBLOCA minimum vessel, cumulative distribution function of 100-bin example: best distribution.

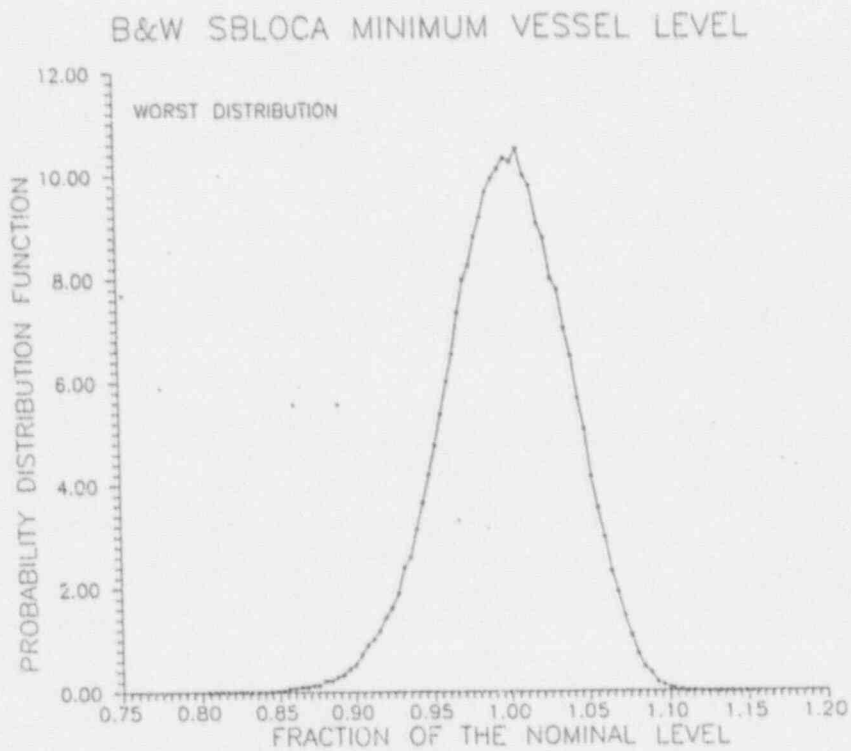


**Figure C-8.** B&W SBLOCA minimum vessel, probability distribution function of 100-bin example: worst distribution.

## B&amp;W SBLOCA MINIMUM VESSEL LEVEL

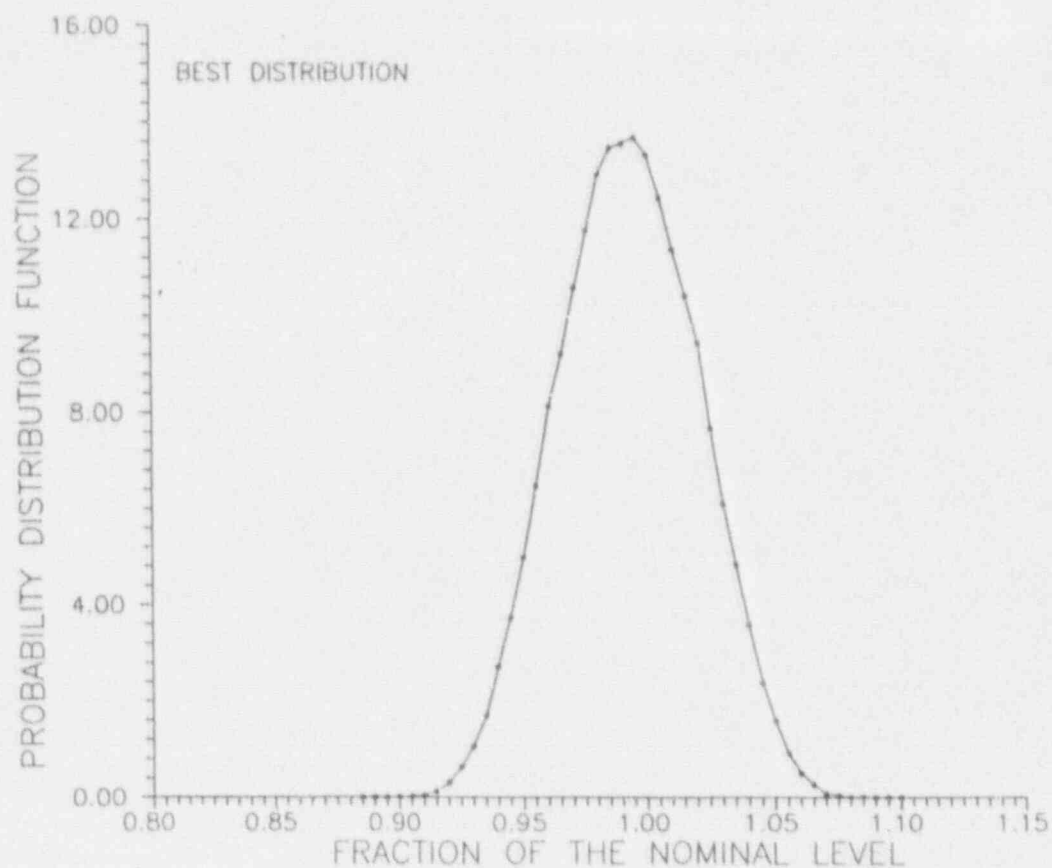


**Figure C-9.** B&W SBLOCA minimum vessel, probability distribution function of 100-bin example: best distribution.

**Table C-5.** 100,000 history Monte Carlo study of Models 3 and 6.

Model number	Mean value	Standard deviation	Probability (level <0.85 of nominal)
3	0.9895	0.0273	0.0
6	0.9955	0.0384	$4.5 \times 10^{-4}$

**BIBLIOGRAPHIC DATA SHEET**

(See instructions on the reverse.)

1. REPORT NUMBER  
(Assigned by NRC. Add Vol., Supp., Rev., and Addendum Numbers, if any.)

NUREG/CR-5818  
EGG-2665

2. TITLE AND SUBTITLE

Uncertainty Analysis of Minimum Vessel Liquid Inventory During a Small-Break LOCA in a B&W Plant—An Application of the CSAU Methodology Using the RELAP5/MOD3 Computer Code

3. DATE REPORT PUBLISHED

MONTH YEAR

December 1992

4. FUNDING OR GRANT NUMBER

11111

5. AUTHOR(S)

\*A. G. Ortiz, L. S. Ghan

6. TYPE OF REPORT

Technical

7. PERIOD COVERED (Inclusive Dates)

8. PERFORMING ORGANIZATION — NAME AND ADDRESS (If NRC, provide Division, Office or Region, U.S. Nuclear Regulatory Commission, and mailing address; if contractor, provide name and mailing address.)

Idaho National Engineering Laboratory  
EG&G Idaho, Inc.  
Idaho Falls, ID 83415

9. SPONSORING ORGANIZATION — NAME AND ADDRESS (If NRC, type "Same as above." If contractor, provide NRC Division, Office or Region, U.S. Nuclear Regulatory Commission, and mailing address.)

Division of Systems Research  
Office of Nuclear Regulatory Research  
U.S. Nuclear Regulatory Commission  
Washington, D.C. 20555

10. SUPPLEMENTARY NOTES

11. ABSTRACT (200 words or less)

The Nuclear Regulatory Commission (NRC) revised the emergency core cooling system licensing rule to allow the use of best estimate computer codes, provided the uncertainty of the calculations are quantified and used in the licensing and regulation process. The NRC developed a generic methodology called Code Scaling, Applicability, and Uncertainty (CSAU) to evaluate best estimate code uncertainties. The objective of this work was to adapt and demonstrate the CSAU methodology for a small-break loss-of-coolant accident (SBLOCA) in a Pressurized Water Reactor of Babcock & Wilcox Company lowered loop design using RELAP5/MOD3 as the simulation tool. The CSAU methodology was successfully demonstrated for the new set of variants defined in this project (scenario, plant design, code). However, the robustness of the reactor design to this SBLOCA scenario limits the applicability of the specific results to other plants or scenarios. Several aspects of the code were not exercised because the conditions of the transient never reached enough severity. The plant operator proved to be a determining factor in the course of the transient scenario, and steps were taken to include the operator in the model, simulation, and analyses.

12. KEY WORDS/DESCRIPTORS (List words or phrases that will assist researchers in locating the report.)

Uncertainty analysis  
SBLOCA  
LBLOCA  
RELAP5  
operator  
ECCS  
best estimate  
CSAU  
PIRT

13. AVAILABILITY STATEMENT

Unlimited

14. SECURITY CLASSIFICATION

(This Page)

Unclassified

(This Report)

Unclassified

15. NUMBER OF PAGES

16. PRICE



Federal Recycling Program

UNITED STATES  
NUCLEAR REGULATORY COMMISSION  
WASHINGTON, D.C. 20555-0001

OFFICIAL BUSINESS  
PENALTY FOR PRIVATE USE, \$300

100558189511 JAN 1993  
US NRC-DADM  
DIV FOIA & REPLICATIONS SVCS  
TCC-PDR-NUREG  
D-211  
WASHINGTON DC 20555

SPECIAL FOURTH CLASS RATE  
POSTAGE AND FEES PAID  
USNRC  
PERMIT NO. G-87